UNIVERSIDAD AUTÓNOMA DE MADRID

Facultad de Ciencias

Departamento de Biología Molecular

Tesis Doctoral

NEW ONCOGENIC NETWORKS REGULATED BY THE RNA BINDING FACTOR CUGBP1 IN MELANOMA

METEHAN ÇİFDALÖZ

Madrid, 2016

AUTONOMOUS UNIVERSITY OF MADRID

Faculty of Science

Department of Molecular Biology

Doctoral Thesis

NEW ONCOGENIC NETWORKS REGULATED BY THE RNA BINDING FACTOR CUGBP1 IN MELANOMA

METEHAN ÇİFDALÖZ

Thesis Director

Dr. María S. Soengas

Spanish National Cancer Research Center

Madrid, 2016

Dr. María S. Soengas, Head of the Melanoma Group at Molecular Oncology program of the Spanish National Cancer Research Center (CNIO)

CERTIFIES:

That the Doctoral Thesis **"New oncogenic networks regulated by the RNA binding factor CUGBP1 in melanoma"** developed by **Metehan Çifdalöz** meets the necessary requirements to obtain the **PhD Degree** and, to this purpose, will be presented at the Universidad Auntónoma de Madrid. The thesis has been carried out under my direction and hereby I authorize its defense to a specific PhD Committee assembled for this purpose.

I hereby issue this certification in Madrid on May 13th 2016.

María S. Soengas

PhD, Thesis Director

ACKNOWLEDGEMENTS

AGRADECIMIENTOS

After a challenging five and a half years, finally I have reached the end of my PhD thesis. It has been a period of intensive learning, working and developing for me, not only in the scientific level, but also on personal level. Throughout this period, directly or indirectly, I have received help, support and assistance from many people who deserve my sincere gratitude.

Foremost, **Marisol**, thank you very much for your confidence in me and thank you one more time for giving me the opportunity to conduct this research as being part of your lab and for the critical reading of this thesis. Your continuous supervision, guidance and support made it possible for me to finish my research and my thesis. Thank you very much for all the things I have learned from you and for being there when I needed.

Besides my mentor, I would like to thank the rest of my thesis committee: **Dr. Manuel Serrano**, **Dr. Daniel Lietha** and especially **Dr. Juan Valcárcel** for their insightful comments, feedback and encouragement during my committee meetings. Also, I would like to thank my thesis jury members **Dr. Hector Peinado**, **Dr. Raúl Mendez**, **Dr. Fátima Gebauer**, **Dr. José Luis Rodríguez**, **Dr. Jose Esteban**, **Dr. Pablo Luis Ortiz** and one more time **Dr. Juan Valcárcel** for accepting being in part of my thesis evaluation jury and also for their questions and comments in our occasional meetings which definitely helped me to improve my research. Also, I would like to thank my tutor at the Universidad de Autonoma, **Encarnación Martinez Salas**, for her advices and for helping me with the registration bureaucracy.

Now, coming to the people who have been absolute parts of this thesis: it is only my name on the cover, but it was only possible thanks to my lab mates. I want to express my most sincere gratefulness to all of them.

When I first came to the lab for the short stay in May 2010, I was really impressed by the atmosphere here. I left 3 months later, but I always felt that I would come back. And when Marisol offered me the opportunity for coming back, you guys, by far, had the most influential effect on my positive decision. Thank you very much for being my family here. Couple of years ago, I didn't feel like I belonged somewhere. After these years, now I feel Madrid as home and this is absolutely thanks to you all. Of course, all of you helped me in this work with your intellectual input and technical help. I am very very VERY grateful for all of these, but this is not what I want to talk about. During these five and a half years, I have felt collapsed many times, and I have always seen hands of yours around me to support me and raise me back onto my feet. THANK YOU!

The lists go alphabetically in each section. I couldn't order them in any other way. So, blame your parents, not me, if you are not the first one :)

Cristina, first of all, thanks for choosing to be part of this lab, twice. It was been a real pleasure knowing and working with you. I hope you will never ever lose the joy you have. The thesis in front of you will be tough, but a laugh can cure everything. Keep on being positive and enjoyable. **Daniela**, I will remember you with your immense knowledge on all the CD proteins and immunology, with your knowledge of weird things and your nice sense of humor. I hope you will never lose the science passion inside of you. You and science fit very well. **David**, the senior. I would like to thank you for several things but first of all for our trip in Grand Canyon. That breathtaking view deserved a mention here. Your comments and different approaches to problems helped to make this thesis better. You are born for science. **Estela**, the ultimate lab manager, thank you for being always there. I really cannot think any lab manager better than you. Always in control, always helpful, always ready to seek solutions and give advice. Thank you very much for all the help you have offered even without asking. You are a heroine. **Raul**, el niño. Not only your height but also your heart is very big. Thank you for offering your help whenever I needed. And thanks for inviting over for the Christmas dinner back in 2014. That really meant a lot to me. I will never forget that. I tell you again, consider the fish shop, hehe. **Takis**, tio. You are a machine. I have met very few people in my life that works as hard as you do with multiple tasks. I would like to thank you for sharing enjoyable moments with me and always giving hand whenever I felt miserable and helpless. Thanks tio. Maybe you can try to be little, just a little bit more optimistic, hehe. **Tonan**, the master technician. I remember how you were smiling when we have seen the 'how we see each other in the lab' comic which shows everyone as babies from the eyes of a technician. That's so true. You have been looking after all the lab all the time without a complaint. Thank you for being such a good person and technician.

Besides all current members of the lab, I had the great pleasure to work with many people during these years.

Agi, thank you very much for showing me the official welcome to the lab, the incubator cleaning. It is by far the worst duty to do in the lab, but you feel part of the lab when you finish, and you feel that are the person to be proud for no contamination there. Such a nice (!) feeling. **Alicia**, thank you for all the constructive comments you have given during these years. It was a pleasure to know you. **Ana**, hum... ummm... hmmm... mmm… hehe. After a week so, it was obvious that you were part of this lab from the beginning. Thanks for the happiness you have brought to the lab and for being trustworthy and very accurate and perfectionist in explaining the details. **Angel,** the joy. It took you only few days to change the atmosphere of the lab. With your energy (not the physical one) you turn everything into better and more enjoyable. Thanks for all the nice moments spent together. **David Saenz**, thank you very much for your patient and calm explanation of things in detail and for your never disappearing smile. **Direna**, to be honest, several times I've thought your

brain would explode one day in front of us. You have such a beautiful mind. I know you will be someone important and I will show you to my kids and be proud. Thanks for all the comments and the Christmas dinner in your grandma's place, it was my first Christmas dinner, hehe. **Erica,** thanks for all your help in biopsy samples and for all the nice and encouraging words when I needed to hear them. Always, smile. **Eva,** la *Flash*. It was not easy to catch your speed in these years. Cannot believe how fast you eat, how punctual you are. I want to become an "Evito" one day, hehe. Joking aside, I miss you a lot in the lab. Expect me in DC, one day I will knock the door. Thanks for being on my side at any time I needed someone to talk to. And thanks for the New Year's invitation and the grapes; and also taking me to the hospital when I've injured my ribcage and taking care of me. **Hannelore,** the speed you adapted to the lab was impressive. It was thanks to your friendly smile and nature. For the same reason, everyone expects to see you back in here soon. **Lisa**, you absolutely deserve a special mention. I really feel fortunate for knowing you. You are a great person. You helped me so much when I started and always continued to do so. I want to thank you for all the things you have done and for the enjoyable moments we have spent together outside of the lab and also in USA. You are the best. **Maria,** the super mom. Thanks for being the living proof for the possibility of woman scientist with children. I admire the balance you have established between two worlds. I hope you never stop laughing loud, hehe. And finally, I want to thank everyone who joined the lab for short stays and with whom I have spent time and received help and support during their stays: **Albano, Carol, Elena, Jesus, Lucía** (my sweetie, un besito)**, Miguel Angel, Napala, Renata, Sandra, Sara, Silvia and Yesim**.

Also, one of the best sides of CNIO, I want to thank the people in the units. This thesis is based on many high-throughput screenings which without the invaluable contributions of these wonderful people wouldn't be possible: **Diego, Manu and Ximo** from confocal microscopy core unit, **Javier** and **Pilar** from proteomics core unit, **Orlando** from genomics core unit and **Gonzalo** from bioinformatics unit. Thank you all hundreds of times. I would like to thank **Osvaldo** from bioinformatics unit, separately. He deserves an extra emphasis as he analyzed several data over and over again and taught me many analysis techniques. I am very grateful for all your help, thank you.

I would like to thank people from our neighbor lab, Epithelial Carcinogenesis Group. First, I would like to thank **Paco**, for his constructive comments in our joint lab meeting. And to the people in his lab for their continuous support: **Cristina, Eleonora, Francesc, Isidoro, Jarek, José, Laia, Luis, Marta, Miriam, Victor, Xavi**. Thank you guys!

Also for all the friends at CNIO who didn't withhold their smiles, "hola"s and all kinds of chats. Thank you very much guys!

GO CNIO GO!!!

Bu kadar yabancı dil yeter bence. İnsan duygularını ifade edemiyor gönlünce.

Her şeyden önce, önüme ellerindeki bütün imkanları sermekten imtina etmeyen, hasret çekmek pahasına bana hep destek olan **anneme** ve **babama,** bana hür olmayı ve kendi kararlarımı korkusuzca kendim vermemi sağladıkları için çok ama çok teşekkür ederim. Her şey sizin sayenizde mümkün oldu ve oluyor. Daha sonra ailemin diğer bireylerine, **abilerim** ve **kardeşlerime** bana ihtiyacım olduğu her an yardım ettikleri için çok teşekkür ederim. Hepinizi çok seviyorum.

Aileden ve Türkiye'den uzak olmanın manevi yükünü bir sözle, bir sohbetle, bir gülüşle hafifleten Madrid'deki arkadaşlarım **Erdener**'e, **Ezgi**'ye ve **Kürşat**'a, "*arkadaşların yanında olsa Madrid dünyanın en güzel yeri*" tezimi ispatladıkları için; haftasonlarının değişmez mekanı "Cem's"teki arkadaşlarım **Cem**, **Hakan**, **Rafet** ve **Yılmaz**'a, bütün eğlenceli ve derin muhabbetli anlar için; çok sevdiğim dostlarım **Emre**, **Engin**, **Evren**, **Furkan**, **Hulusi**, **Melih**, **Özgür**, **Sıtkı** ve **Tolga**'ya, bana her konuda hep destek oldukları ve fırsat oldukça beni ziyaret ve konuk ettikleri için çok teşekkür ederim. Umarım beklentilerinizi boşa çıkarmamışımdır. Son olarak da makalelere erişimde bana yardımcı olan bütün ekşisözlük yazarlarına çok teşekkür ederim.

Once again, I would like to thank you all from the bottom of my heart for everything you have done. All of you are wonderful, generous and thoughtful people.

KEEP BEING YOURSELVES. THAT WILL BE ENOUGH.

CONTENTS

ÍNDICE

LIST OF FIGURES

LIST OF TABLES

LIST OF SUPPLEMENTARY TABLES

I. ABBREVIATIONS

ABREVIATURAS

ActD	Actinomycin D
ADAR	Adenosine deaminase acting on RNA
AKT3	v-AKT murine thymoma viral oncogene homolog 3
ALM	Acral lentigious melanoma
ANK2	Ankyrin 2, neuronal
AP-2α	Activator protein 2 alpha
AR	Androgen receptor
ARE	AU-rich element
ARID	AT rich interactive domain
AURK	Aurora kinase
BAP1	BRCA1-associated protein 1
BCL2	B-cell lymphoma 2
BCL2A1	Bcl-2-related protein A1
Bcl-x	BCL2-Like
BIN1	Bridging integrator 1
BIRC	Baculoviral IAP repeat containing
BRAF	v-RAF murine sarcoma viral oncogene homolog B
BrdU	5-bromo-2'-deoxyuridine
BRUNOL	Bruno-Like
BSA	Bovine serum albumin
BUB1	Budding uninhibited by benzimidazoles 1
C/EBP	Cytosine-cytosine-adenosine-adenosine-thymidine enhancer binding protein
Capzb	Capping protein (actin filament) muscle z-line, beta
CBP	CREB-binding protein
CCNB1	Cyclin B1
CCND1	Cyclin D1
CDC25A	Cell division cycle 25A
CDK	Cyclin-dependent kinase

CDKNA2	Cyclin-dependent kinase inhibitor 2A
cDNA	Complementary deoxyribonucleic acid
CDX1	Caudal type homeobox 1
CELF	CUG repeat binding protein, Elav-like family
CK2	Casein kinase 2
Clcn1	Chloride channel, voltage-sensitive 1
CNIO	Centro Nacional de Investigaciones Oncológicas
COX-2	Cyclooxygenase 2
CPEB	Cytoplasmic polyadenylation element binding proteins
CREB	Camp-response element binding protein
CRT	Calreticulin
CTLA-4	Anti-cytotoxic T-lymphocyte-associated protein 4
cTNT	Troponin T Type 2, cardiac
CTSB	Cathepsin B
CUGBP	CUG repeat binding protein
Cypher	Protein cypher
DAPI	4',6-diamidino-2-phenylindole
Daxx	Death-domain associated protein
DEK	DEK proto-oncoprotein
DM1	Myotonic dystrophy type I
DMEM	Dulbecco's modified Eagle's medium
DMPK	Dystrophia myotonica protein kinase
DNA	Deoxyribonucleic acid
E2F	E2 factor
E-box3	Enhancer Box 3
EDTA	Ethylenediaminetetraacetic acid
EGTA	Ethylene glycol tetraacetic acid
eIF2	Eukaryotic initiation factor 2

EMT	Epithelial-to-mesenchymal
ERBB	Erb-B2 receptor tyrosine kinase
ERK1/2	Extracellular signal-related kinase 1/2
ERα	Estrogen receptor alpha
ESPL1	Extra spindle pole bodies Like 1
ESR1	Estrogen receptor 1
ETR	ELAV-type RNA-binding
ETV1	Ets variant 1
EZH2	Enhancer of zeste 2 polycomb repressive complex 2 subunit
FACS	Fluorescence-activated cell sorting
FAM188A	Family with sequence similarity 188, member A
FBS	Fetal bovine serum
FDA	United States Food and Drug Administration
FDR	False discovery rate
FGF-2	Fibroblast growth factor-2
FITC	Fluorescein isothiocyanate
FXR1	Fragile X mental retardation, autosomal homolog 1
G1 phase	Growth 1/Gap 1 phase
G2 phase	Growth 2/Gap 2 phase
GABT4	GABA-A transporter 4
GAPDH	Glyceraldehyde 3-phosphate dehydrogenase
Gfat	Glutamine fructose-6-phosphate amidotransferase
GFP	Green fluorescent protein
GNAQ	Guanine nucleotide binding protein (G Protein), Q Polypeptide
GO	Gene ontology
GRE	GU-rich element
GSEA	Gene set enrichment analysis
H2afy	H2A histone family, member Y

HIV	Human immunodeficiency virus
HJAY	Human junction array
HKGS	Human keratinocyte growth supplement
HMGS	Human melanocyte growth supplement
hnRNP-h	Heterogeneous nuclear ribonucleoprotein H1
HPRT	Hypoxanthine guanine phosphoribosyl transferase
HPV-E6	Human papillomavirus E6 oncoprotein
HRAS	Harvey rat sarcoma viral oncogene homolog
HuR	Hu antigen R
IDH1	Isocitrate dehydrogenase 1
IEC	Intestinal crypt cell line
IFNβ	Interferon beta
IgG	Immunoglobulin G
IF	Immunofluorescence
IHC	Immunohistochemistry
IL-2	Interleukin-2
iMSRC	Intelligent matrix screening remote control
INSR	Insulin receptor
IR	Insulin receptor
IRES	Internal ribosome entry site
ITGA3	Integrin, alpha 3
ITGB1	Integrin, beta 1
iTRAQ	Isobaric tags for relative and absolute quantitation
kDa	Kilodalton
Ki67	Marker of proliferation Ki-67
KIT	v-KIT Hardy-Zuckerman 4 feline sarcoma viral oncogene homolog
KSRP	K Homology splicing regulatory protein
LAP	Liver-enriched activator protein

LIP	Liver-enriched inhibitory protein
LMM	Lentigo malignant melanoma
Luzp4	Leucine zipper protein 4
MAPK	Mitogen-activated protein kinase
MAX	MYC associated factor X
MBNL1	Muscleblind-like splicing regulator 1
MC1R	Melanocortin 1 receptor
MCL-1	Myeloid cell leukemia-1
MCM	Minichromosome maintenance complex component
MDM	Mouse double minute human homolog
MEF	Mouse embryonic fibroblasts
MEF2A	Myocyte enhancer factor 2A
MEK1/2	Mitogen-activated protein/extracellular signal-regulated kinase kinase 1/2
Mfn2	Mitofusin 2
miR-/miRNA	micro RNA
MITF	Microphthalmia-associated transcription factor
MLLT3	Myeloid/lymphoid or mixed-lineage leukemia; translocated to, 3
MM	Malignant melanoma
mRNA	Messenger RNA
MS/MS	Mass spectrometry / mass spectrometry
MSH	Melanocyte-stimulating hormone
Mtmr	Myotubularin related protein
NAB50	Nuclear polyadenylated RNA-binding protein, 50-KD
NAPOR	Nuclear polyadenylated RNA-Binding protein
NEDD9	Neural precursor cell expressed, developmentally down-regulated 9
NF1	Neurofibromin 1
NFY	Nuclear transcription factor Y
NF-κB	Nuclear factor kappa beta

NM	Nodular melanoma
NMDAR-1	N-methyl-D-aspartate receptor subunit NR1
NMR	Nuclear magnetic resonance
NRAS	Neuroblastoma RAS viral oncogene homolog
NSCLC	Non-small cell lung carcinoma
OIS	Oncogene induced senescence
p	Probability values
PARN	Poly(A)-specific ribonuclease
PCAF	P300/CBP-associated factor
PCR	Polymerase chain reaction
PD-1	Programmed cell death protein 1
PD-L1	Programmed death-ligand 1
PI3K	Phosphatidylinositol-4,5-bisphosphate 3-kinase
PKC	Protein kinase C
poly(A) tail	Poly-adenosine tail
PPFIBP1	PTPRF interacting protein, binding protein 1
PPP6C	Protein phosphatase 6, catalytic subunit
PTB	Polypyrimidine-tract-binding protein
PTEN	Phosphatase and tensin homolog
qPCR	Quantitative polymerase chain reaction
RAB27A	RAS-related protein Rab-27A
RAC1	RAS-related C3 botulinum toxin substrate 1
RAS	Rat sarcoma
Rb	Retinablastoma
RBM47	RNA binding motif protein 47
RBP	RNA binding protein
RCF3	K homology (KH) domain-containing nuclear-localized putative RNA-binding protein 3
RGP	Radial growth phase

Rho	Rhodopsin
RIP-SEQ	RNA immunoprecipitation - sequencing
RNA	Ribonucleic acid
RRM	RNA recognition motif
RT	Room temperature
RyR1	Ryanodine receptor 1
S phase	Synthesis phase
SA-β-Gal	Senescence-associated beta-galactosidase
SDS-PAGE	Sodium dodecyl sulfate polyacrylamide gel electrophoresis
SEER	Surveillance, epidemiology, and end results
Serca1	Sarcoplasmic/endoplasmic reticulum calcium atpase 1
SHMT1	Serine hydroxymethyltransferase 1
shRNA	Short-hairpin RNA
siRNA	Short interfering RNA
SMARCA4	SWI/SNF related, matrix associated, actin dependent regulator of chromatin, subfamily A, member 4
snRNA	Small nuclear RNA
Sorbs1	Sorbin and SH3 domain containing 1
SSM	Superficial spreading melanoma
SWI/SNF	Switch/Sucrose Non-Fermentable
TBX2	T-Box protein 2
TCF3	Transcription factor 3
TCGA	The Cancer Genome Atlas
TERT	Telomerase reverse transcriptase
TIA-1	T-cell internal antigen 1
TITF1	Thyroid transcription factor 1
TMA	Tissue Microarrays
TNF-α	Tumor necrosis factor alpha
TNM	Tumor-Node-Metastasis

TNRC	Trinucleotide pepeat containing
TP53	Tumor protein 53
TRP2	Tyrosinase-related protein 2
TYR	Tyrosinase
TYRP1	Tyrosinase-related protein 1
U2AF	U2 small nuclear RNA auxiliary factor
UAP56	DEAD-box protein UAP56
UM	Uveal melanoma
UTR	Untranslated Region
UV	Ultraviolet
VEGF	Vascular endothelial growth factor
VGP	Vertical growth phase
WB	Western blotting
WHO	World Health Organization

II.

SUMMARY

PRESENTACIÓN

SUMMARY

Melanoma is a prime example of an aggressive tumor that accumulates a plethora of changes in the transcriptome and the proteome. Consequently, distinguishing drivers from inconsequential passenger events has been a main challenge in this disease. Consequently, and despite great progress in identifying (epi)genetic defects accumulated during melanoma progression, the molecular bases underlying the aggressive behavior of this tumor type are not completely understood.

RNA binding proteins remain largely unexplored in melanoma. We considered this lack of information of prime relevance as transcripts of nearly all known oncogenes and tumor suppressors may be regulated by alternative splicing and/or controlled by various mechanisms that define mRNA stability and ultimately, competency for translation. Here we show that a screen for all reported mRNA binding proteins (mRBPs) suggested that these genes are not prime targets of mutation or copy number variation. Instead, a customized microarray revealed a series of RBPs overexpressed in melanoma cells when compared to normal melanocytes. Of those factors, we found particularly attractive the CUGBP1/CELF1 protein. First, CUGBP1 is a multifunctional mRBP with a broad spectrum of functions, ranging from the modulation of alternative splicing to modulation of mRNA decay. Secondly, there is little information on comprehensive genome-wide analyses for CUGBP1 in cancer cells, with no previous report in skin cancer. Therefore this PhD thesis was set to address the following unknown aspects of CUGBP1 in melanoma: (*i*) expression, (*ii*) functional requirement, and (*iii*) mechanism of action.

In brief, CUGBP1 was found overexpressed in human melanoma cells and tissue specimens. Targeted gene depletion demonstrated that CUGBP1 is required to sustain melanoma cell proliferation. Mechanistically, genome wide human junction arrays, RNA immunoprecipitation followed by sequencing and iTRAQ-MS/MS proteomics assays were utilized and identified novel and direct targets of CUGBP1. Together, these high throughput approaches (to our knowledge the first in class for this gene) uncovered a coordinated network of tumor-associated cell cycle regulators and chromatin remodelers as CUGBP1 targets. Central in this CUGBP1 regulated networks was the oncogene DEK, a feature we validated by targeted gene depletion, cDNA arrays and histological validation in clinical datasets. Mechanistically, CUGBP1 was found to bind to the 3'UTR of DEK stabilizing its mRNA levels and ultimately allowing for an efficient cell proliferation.

These results illustrate the power of comprehensive analyses of RNA regulators in the identification of novel malignant features of cancer cells.

PRESENTACIÓN

El melanoma es un tipo de tumor muy agresivo que acumula una gran cantidad de aberraciones en su transcriptoma y proteoma, por todo esto, la identificación de genes esenciales para el desarrollo de esta neoplasia es uno de los grandes retos pendientes. Pese a los grandes avances en la identificación de alteraciones genéticas y epigenéticas que ocurren durante la progresión del melanoma, las bases moleculares que explican el comportamiento tan agresivo de este tumor no se han descrito en profundidad.

Las proteínas de unión a ARN no han sido caracterizadas en detalle en este tipo de tumor. Consideramos que esta falta de información es de gran relevancia ya que los transcritos de casi todos los oncogenes y supresores tumorales conocidos pueden estar regulados por procesos de splicing alternativo y/o diversos mecanismos que definen la estabilidad del ARNm, y por último, la competencia para su traducción. En una búsqueda de todas las proteínas de unión a ARNm (mRBPs) previamente descritas, hemos observado que estos genes no son los principales objetivos de mutaciones o alteraciones en el número de copias. En cambio, un microarray personalizado para este tipo de proteínas ha revelado numerosas mRBPs sobreexpresadas en células de melanoma en comparación con melanocitos primarios. De esos factores, hemos encontramos particularmente atractiva la proteína CUGBP1/CELF1. En primer lugar, CUGBP1 es una mRBP multifuncional con un amplio espectro de funciones que van desde la modulación del splicing alternativo hasta la regulación del deterioro del ARNm. En segundo lugar, existe poca información del papel de CUGBP1 en análisis exhaustivos de todo el genoma realizados en líneas celulares tumorales, sin reportes previos en cáncer de piel. Por todo lo anterior, esta tesis doctoral se estableció para abordar los siguientes aspectos desconocidos de CUGBP1 en melanoma : *(i)* su expresión , *(ii)* requisitos funcionales, y *(iii)* mecanismo de acción .

En breve, CUGBP1 está sobre expresado en líneas celulares de melanoma y biopsias clínicas humanas. La depleción de CUGBP1 demostró que este gen es requerido para el mantenimiento y la proliferación del melanoma. Mecanísticamente, estudios de asociación de uniones en el genoma humano, inmunoprecipitación de ARN seguida de secuenciación y espectrometría de masas fueron empleados para identificar nuevas dianas de CUGBP1. Juntos, estos enfoques alto rendimientos (a nuestro conocimiento la primera vez que sea realiza para este gen) han descubierto una red de reguladores del ciclo celular asociados a tumores y remodeladores de la cromatina como dianas de CUGBP1. En estas redes, el oncogén DEK tiene un papel central. Estos resultados fueron validados mediante la depleción del gen, arrays de ADNc y validación histológica en biopsias clínicas. Mecanísticamente, CUGBP1 se une a la región 3'UTR de DEK para estabilizar sus niveles de ARNm logrando así una proliferación celular eficiente.

Estos resultados demuestran el potencial de los análisis a gran escala de reguladores de ARN en la identificación de nuevas características de células tumorales.

III.

INTRODUCTION

INTRODUCCIÓN

1. MELANOMA

Melanoma is a cancer type that arises from melanocytes, neural crest-derived melanin-producing cells[1], which reside mainly in basal layer of the skin[2], and also in the hair follicles[3], the inner ear[4], meninges[5], uvea[6], connective tissues[7] and heart[8]. This tumor is clinically relevant for its increasing incidence and mortality (responsible for 80% of skin cancer related deaths) due to high aggressive capacity to metastasize[9-12].

1.1. INCIDENCE, MORTALITY, DIAGNOSIS AND RISK FACTORS

During the last four decades, melanoma incidence has been increasing worldwide, mainly in the developed countries. According to the latest surveillance, epidemiology, and end results (SEER) program reports, in the United States, the incidence rate has increased 4-folds since 1975[13]. It is the fifth and seventh most frequent cancer type in United States among males and females, respectively[14]. Approximately 79000 new melanoma cases and more than 10000 melanoma-related deaths are expected as year of 2016[15]. In Spain, incidence rate is 13.11/100000 in population and this number is estimated to increase to 13.64 by 2022[16].

The most important environmental risk factor for melanoma development is natural and artificial ultraviolet-exposure[17,18]. Other contributing risk factors can be listed as: family history (genetic disposition)[19-21], number of nevi[22], bearing dysplastic nevi, eye/hair color[23], suppressed immune system due to organ transplantation[24,25] or HIV infection[26,27].

In addition to its complex genetic and histopathological background[28,29], its ability to develop chemoresistance hardens the struggle against finding cure to melanoma[30,31]. Since the major risk is a preventable factor (UV-exposure), and its observability in the skin is relatively easy compared to other cancer types, early detection and prevention campaigns to raise awareness of this disease in the society is important. Over the last years, these campaigns have helped to improve the survival rates of melanoma patients in high incidence countries. Early detection is particularly important[32-34]. 5-year survival rates fall to 17% if the disease is at its later stages, such as distant metastasis[15]. This rate is reversely correlated by the depth of the malignant lesion, the Breslow depth (named after pathologist Alexander Breslow in 1970)[35]. In addition to Breslow depth, staging criteria include metastasis, mitotic rate, and ulceration[36]. The correct staging is important for patient management for the correct treatment regimen of patient.

However, Breslow depth method is limited to physical examination of the lesion(s) and evidently prone to human errors[37,38]. Therefore, search for better diagnostic markers is a hot topic in melanoma field (reviewed in refs[39,40]).

1.2. MELANOCYTIC LESIONS

Melanocytes, precursors of melanocytic lesions including melanoma, as described above, are of neural crest origin and melanoblasts migrate during embryonic development mostly to the normal skin, where melanocyte:keratinocyte number ratio is typically of 1:10[1,2]. Melanocytes are specialized in melanin production, transferring the melanin to keratinocytes in the epidermis, hence the pigmentation of skin and hair (also feather and fur, in other animals) in order to provide protection against the damaging effects of UV radiation by forming a photo barrier[41]. In more detail, UV-radiation causes elevated expression of tumor protein 53 (TP53) in keratinocytes which increases the transcription of melanocyte-stimulating hormone (MSH)[42]. Secreted MSH binds and activates melanocortin 1 receptors (MC1R) on melanocyte surface, which activates adenylate cyclase cascade and the CREB pathway, ending in the activation of microphthalmia-associated transcription factor (MITF)[43]. MITF promotes melanin synthesis and the skin gets darker as a result of accumulated melanin in keratinocytes. Any defect in melanocytes may lead to pigmentation disorders, benign melanocytic neoplasms (nevi or moles) or can go further and lead to formation of malignant tumors (melanomas)[28,44]. These melanocytic lesions have characteristic clinical, histopathological and molecular features[28,45,46].

1.2.1. Benign Melanocytic Lesions: Nevi

Nevus, also generally known as mole, is the medical term used for clearly bounded chronic lesions of the melanocytes[45]. Despite the lack a universal classification consensus, nevi are typically classified based on their time of onset (congenital or acquired) and histological structure (junctional, compound, dermal or dysplastic)[47,48].

Congenital nevi appear at birth or within the six months after birth[49], whereas acquired nevi are described to appear after more than six months of age[44]. Although the chances of malignant transformation of congenital and acquired nevi are low, high number of nevi is one of the risk factors for developing melanoma[22,50]. Congenital and acquired nevi can be further sub-classified into junctional, dermal, compound or dysplastic nevi according to their histological location within the skin[45,51,52]. Recently, dysplastic nevi has been shown to be an intermediate lesion for developing melanoma[53] and patients with dysplastic nevi syndrome have high risk of developing melanoma[54]. Nevertheless, the question to which extent nevi can transform into melanoma cells still stands[55].

Time of onset, histological location and mutation status of the lesions form the basis for the current benign nevi classification (classes such as common acquired, congenital, Spitz and blue nevi etc.) by World Health Organization (WHO)[45,56-59].

Some mutations observed in nevi (i.e. BRAF, NRAS etc.) are also frequently observed in melanoma lesions; and in addition, histological similarities between benign and malignant lesions lead to misdiagnosis[37,38]. Indeed, errors in diagnosis of melanoma is one of the major issues for cancer malpractice[60].

1.2.2. Malignant Melanocytic Lesions: Cutaneous Melanoma

Classically, malignant melanomas were classified according to their physical properties such as anatomical location, histopathological features and sun damage level[28,44,45]. The cutaneous melanoma was subdivided into 4 categories: superficial spreading melanoma (SSM), nodular melanoma (NM), lentigo malignant melanoma (LMM) and acral lentigious melanoma (ALM). Now, we know that each melanoma type has its characteristic mutational status as summarized in Figure 1[61]. SSMs grow horizontally on the skin[62] and mostly observed at intermittent sun exposed body parts of the body. NMs, considered the most aggressive and invasive type, grow quickly and deeper in the intermittent and accumulated sun exposed body parts[44,62]. LMMs are rarer, grow slowly and observed more in elder people and more on skin frequently exposed to the sun[63,64]. ALMs are typically observed on the palms on the hands, on the soles of the feet, and is the most common form of melanoma seen among black and Asian ethnic groups[63]. Also other rare forms of melanoma, uveal melanoma (UM) and mucosal melanoma (MM) exist and together make up the non-cutaneous melanomas[64]. UMs, which make up about 3% of all melanoma cases, occur in the iris, ciliary body and choroid of the eye[28,65,66]. MMs, on the other hand, may arise from melanocytes located in mucosal membranes lining several organs such as nasal cavity, oral cavity etc.[67].

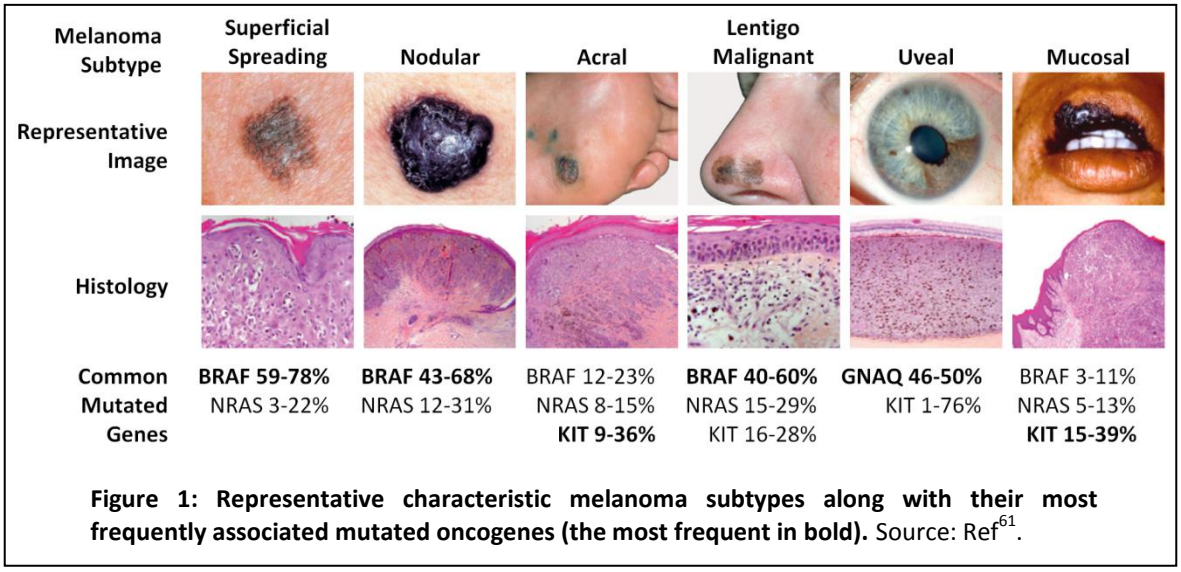

Figure 1: Representative characteristic melanoma subtypes along with their most frequently associated mutated oncogenes (the most frequent in bold). Source: Ref[61].

According to the WHO classification[45] there are also other very rare types of melanoma which differ in their specific clinical and/or histological presentation such as desmoplastic melanoma[68], blue naevus originated melanoma[69], naevoid melanoma[70], persistent melanoma[71], congenital nevi originated melanoma[72], and melanoma of the childhood[73]. While ALM and other rare melanomas make up about 10% of all melanoma cases, SSM, LMM and NM constitute the majority of the cases with 90%.

1.3. MELANOMA PROGRESSION MODEL

In 1984, based on histological classification, Clark and colleagues have proposed a linear evolution model for melanoma progression in five consecutive stages[74-76]: acquired and congenital nevi formation; transformation into dysplastic nevi with structural and architectural atypia; radial-growth phase (RGP) melanoma; vertical-growth phase (VGP) melanoma; and metastatic melanoma.

In contrast to this initial five consecutive step model, most of the melanoma patients don't have intermediate stages between normal melanocytes and melanoma lesions[77-82] suggesting *de novo* formation of melanoma lesions from melanocytes directly[83] (Figure 2).

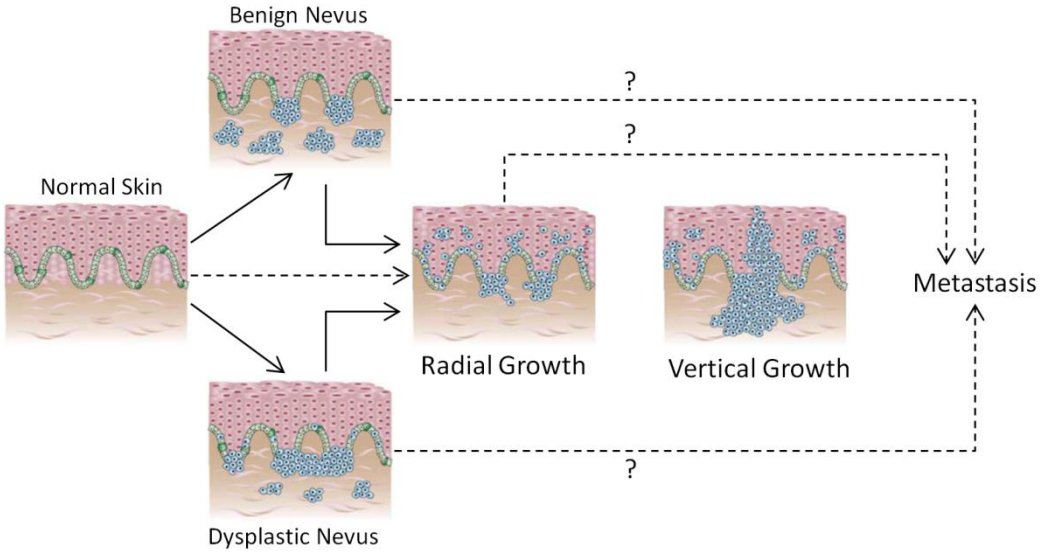

Figure 2: Model for melanoma progression. Adapted from ref[84].

In these models, generally first phenotypic change in melanocytes is the development of benign nevi or dysplastic nevi.

In benign nevi, frequently observed mutations in mitogen-activated protein kinase (MAPK) pathway activating oncogenes (BRAF, NRAS or HRAS) are not enough for malignant transformation of the melanocytes[85]. This phenomenon is known as oncogene-induces senescence (OIS), a tumor

suppression mechanism that detain the progression of benign tumors into malignant tumors by acting as a potent barrier to oncogenic transformation[55,86-88]. By these mechanisms a nevus can be growth-arrested for decades. Tumor suppressor pathways, $p19^{ARF}$-p53 or $p16^{INK4A}$-Rb, play critical roles in execution of OIS (reviewed in refs[89,90]). OIS-related phenotype, such as multinucleated giant cells and positive SA-β-Gal; and expression of OIS markers, such as high levels of $p16^{INK4A}$ and decreased levels of Ki67, are observed in benign melanocytic lesions[87,91-98]. However, these features cannot be used as specific markers of benign melanocytic tumors since malignant melanoma cells may also exert similar phenotypic and molecular signatures[99-103].

Less understood is the formation of dysplastic nevi, abnormal growth of melanocytes in a pre-existing nevus or new location resulting in a pre-malignant lesion with random cytologic atypia[74]. Major genetic changes in the transition from benign lesions into dysplastic nevi are the deletion of cyclin-dependent kinase inhibitor 2A (CDKNA2), phosphatase and tensin homolog (PTEN) loci and mutations in the telomerase reverse transcriptase (TERT) promoter[10,51,53].

Radial growth phase is defined as the horizontal proliferation of melanoma cells intra-epidermally, as a result of bypassing OIS barrier and accumulating genetic alterations such as loss of tumor suppressor genes, mainly CDKN2A[104], PTEN[105,106], TP53[107,108], retinoblastoma 1 (RB1)[108] or neurofibromin 1 (NF1)[109]; and the activation of additional oncogenes, such as v-akt murine thymoma viral oncogene homolog 3 (AKT3)[110] and MITF[111]. At this stage, melanoma cells are not capable of invasion and their survival still depends upon the continuous signaling from keratinocytes[10,112,113].

At vertical growth phase, melanoma cells acquire the ability to survive without signaling through keratinocytes, resulting in the competency to invade into the dermal layer, thus the capacity to metastasize through circulation or lymphatic system. They promote angio- and lymphangiogenesis by secreting factors such as vascular endothelial growth factors (VEGFs) and fibroblast growth factor-2 (FGF-2)[114]. Downregulation of differentiation[115] and proapoptotic genes[116], or abnormal expression of miRNAs[117,118] have been credited to this phenotype switch. In addition, deregulation of cell adhesion and matrix remodeling factors, such as E-cadherin, N-cadherin, matrix metalloproteinase-2 (MMP-2) and cathepsins have shown to be partially involved in this process[119-121]. Secretion of soluble factors and extracellular matrix proteins enable melanoma cells to interact and communicate with their microenvironment cells such as fibroblasts, macrophages, mast cells, and endothelial cells[122,123]. Melanoma cells also promote progression by blocking the anti-tumor response of immune cells residing in or recruited to the tumor microenvironment[124,125]. Over the last two decades, with the advances in sequencing technology, several transcriptomic data have been produced comparing different stages of melanoma progression. One of the main outcomes of

these studies is that the transition from RGP to VGP entails the highest level of molecular changes compared to other steps required[126-129]. These studies helped scientists to identify the players and underlined the importance of epithelial-to-mesenchymal (EMT) transition in melanoma progression[129,130].

At the metastatic phase, melanoma cells are capable of surviving in the circulation and colonizing distant organs upon arrival[131]. Skin, lymph nodes, brain, liver, bone and intestine are the sites that are most frequently colonized by metastatic melanoma cells[83]. Also in the last decade, studies from several groups showed that melanoma cells start sending out signals from the very early stages of progression; and these signals prepare (or so to say educate) the organs[132] to be metastasized for the colonization of melanoma cells to come (for this theory, the term "seed-and-soil" had been first coined by Stephen Paget in 1889[133]). These factors can be sent soluble such as VEGFC[134,135], or in vesicle enclosed form (exosomes) for distant metastasis[136,137]. Nevertheless, still there are no molecular markers in order to distinguish these steps with high accuracy.

1.4. GENETIC ASPECTS OF MELANOMA

To date, numerous genes have been implicated in melanoma development and progression. The majority of these genes are involved and have impact on MAPK and phosphatidylinositol-4,5-bisphosphate 3-kinase (PI3K) pathways as well as cell cycle check-points.

The v-raf murine sarcoma viral oncogene homolog B (BRAF) is the most frequently mutated oncogene among melanoma patients with 50%[138,139] (as well as in other cancers[66]). BRAF, upon stimuli from extracellular matrix, such as growth factors, activates downstream MAPK kinases (MEK1/2) via phosphorylation which activates downstream extracellular signal-regulated kinases (ERK1/2) also via phosphorylation (MAPK pathway), which in turn regulates cell cycle genes (such as upregulation cyclin D1 and downregulation of cyclin-dependent kinase inhibitor 1B, $p27^{Kip1}$), altogether leads to hyperphosphorylation of Rb protein and derepression of E2 factor (E2F) transcription factor and finally progression through the G1/S phase of cell cycle[140,141]. A point mutation in BRAF gene (predominantly V600E, but also V600K and K601E) causes constitutive activation of this gene, resulting in the activation of downstream MAPK pathway without extracellular signals, and the promotion of the cell cycle progression continuously[140].

Rat sarcoma (RAS) family proteins act upstream of RAF genes including BRAF, and activate them via phosphorylation. In addition, they also activate PI3K/Akt pathway, thus inducing cell proliferation and survival. In melanoma, neuroblastoma RAS viral oncogene homolog (NRAS) gene is the most frequently mutated member of the RAS family[138]. BRAF and NRAS mutations appear to be mutually exclusive and both lead to activation of the MAPK pathway with the resulting induction of proliferation and survival[142]. Capable of activating both MAPK and PI3K/Akt pathways,

NRAS has broader effects on melanoma progression, however the mutation rate of NRAS is lower than that of BRAF, around 20%. And as mentioned earlier, mutations in these two oncogenes are also found in benign melanocytic lesions: $BRAF^{V600E}$ in 82% of common nevi[58] and NRAS in 56% of congenital nevi[30]. As a result of OIS, the overexpression of such oncogenes in cultured melanocytes triggers a nonproliferative state[91,97], thus other mutations or genetic abnormalities are required to develop melanoma.

Another frequent event (50-60%) observed in melanoma patients is the loss of PTEN. PTEN inhibits the activation of PI3K/Akt by inhibiting Akt phosphorylation, thus acts a negative regulator of cell cycle[143]. Loss of PTEN contributes to the promotion of cell cycle in melanoma cells[144].

Another gene that is frequently inactivated in melanoma is CDKN2A: 20-40% of familial melanomas harbor germline mutations in this gene. CDKN2A codes for two proteins, $p14^{ARF}$ and $p16^{INK4A}$, both of which have cell cycle inhibitory actions. $p14^{ARF}$, stabilizes p53 by binding to mouse double minute 2 homolog (MDM2) and inhibiting its function, which is to target p53 for proteasomal degradation[145]. $p16^{INK4A}$, on the other hand, binds to cyclin-dependent kinase 4/6 (CDK4/6), inhibits its binding to cyclin D1, thus preventing the phosphorylation of Rb protein. So, mutations in the CDKN2A gene results in degradation of p53 and hyperphosphorylation of retinoblastoma at the same time and promote cell proliferation.

During the last decade, many genome-wide sequencing studies on melanoma samples have been performed and these studies contributed to the identification of other genes mutated or deregulated in this disease; such as cell cycle regulators, CCND1, CDK4, TP53, RB, MDM2/4; chromatin remodeling genes, ARID1A-B, ARID2, SMARCA4, IDH1, and EZH2 or BAP1 in uveal melanoma; MAPK, PI3K pathways regulators, cKIT, GNAQ, ERBB4, AKT3; and also cell-cell interaction and cell adhesion proteins, NEDD9 and RAC1 (see Table 1 for a summary of driver and additional genetic alterations observed in cutaneous melanoma). However, underlying mechanisms driving these molecular changes are not completely understood yet[44,59,146-148].

Besides these aberrant activated/deactivated genes which are shared among different types of cancer, there are also some genes which are specific to particular cancer types. These oncogenes are known as lineage-specific oncogenes, such as thyroid transcription factor 1 (TITF1) in lung cancer[149], caudal type homeobox 1 (CDX1) in colorectal cancer[150], androgen receptor (AR) in prostate cancer[151], and estrogen receptor 1 (ESR1) breast[152] (reviewed in refs[153,154]). In melanoma, MITF is the best characterized lineage specific gene[111]. It has been identified to be amplified in more than 20% of the cases[111]. MITF is the master regulator of melanocytic development and function by regulating proliferation (positively CDK2 and TBX2; and negatively $p16^{INK4A}$ and

p21[155,156]), survival (BCL2A1, BCL2 and BIRC7[157,158]) and pigmentation genes (TYR, TYRP1, TRP2 or RAB27A[159,160]).

Table 1: Driver and additional genetic alterations in melanoma development and progression.
Sources: Refs[44,146,147,154,161]

GENE	ALTERATION	FREQUENCY	AFFECTED PATHWAY	FUNCTION
Driver genetic abnormalities				
BRAF	Point Mutation	50%	MAPK	Signaling kinase
NRAS	Point Mutation	20%	MAPK, PI3K	Signaling kinase
KIT	Point Mutation	1% overall[a]	MAPK, PI3K	Tyrosine kinase
GNAQ	Point Mutation	<1% overall[b]	MAPK, PI3K	G protein-coupled receptor
ERBB4	Point Mutation	15-20%	PI3K	Tyrosine kinase
CCND1	Amplification	10-18%	Cell cycle	G1 entry
CDK4	Mutation/Amplification	5-37%	Cell cycle	G1 entry
Additional genetic abnormalities				
MITF	Amplification	20%	Melanocyte lineage	Transcription factor
ETV1	Amplification	15%	MITF, MAPK	Transcription factor
AKT1/3	Mutation/Amplification	25%	PI3K	Signaling kinase
PTEN	Mutation/Deletion	50-60%	PI3K	Tumor suppressor
CDKN2A	Mutation/Deletion	30%	Cell cycle	Tumor suppressor
TP53	Point Mutation	5-19%	Cell cycle	Tumor suppressor
RB	Point Mutation	6-14%	Cell cycle	G1/S transition
MDM2/4	Amplification	3-5%	Cell cycle	S phase
PPP6C	Point Mutation	9%	Cell cycle	Tumor suppressor
NEDD9	Amplification	36%[c]	Focal adhesion	Cell-cell interaction, invasion
RAC1	Point Mutation	5%	Rho	Adhesion/Migration/Invasion
ARID1/2	Point Mutation	13%	SWI/SNF complex	Chromatin remodeling
EZH2	Point Mutation	3%	Histone modification	Chromatin remodeling
DEK	Amplification	6%	Histone modification	Chromatin remodeling

a: 10% acral and 10% mucosal; b: 70-80% uveal; c: metastatic.

1.5. DEK AS A MELANOMA DRIVER ONCOGENE

In addition to the above-indicated genes, alterations in chromosome 6 are observed frequently in melanoma patients[162]. Especially, short arm (p) of chromosome 6 amplification is a common cytogenetic alteration in cutaneous, mucosal, acral and uveal melanomas[163], which is predicted to correlate with the poor survival outcome[164]. Within this amplified area maps the chromatin remodeling oncogene DEK. DEK is a DNA binding protein with functions in transcriptional modulation, apoptosis, cell proliferation, senescence, differentiation and mRNA splicing (see below). Efforts of the Center for Cancer Genomics' (National Cancer Institute) The Cancer Genome Atlas (TCGA)[161] project recently unrevealed that DEK locus is amplified in 6% and DEK mRNA is upregulated in 22.3% of melanoma cases. It is also known to be upregulated in several cancer types, such as colon[165], breast[166], cervical[167], hepatocellular[168,169] and ovarian[170] cancers.

1.5.1. Cellular Functions of DEK Oncogene

DEK has contradictory functions on gene regulation as it can activate or repress transcription of the target gene. DEK promotes the transcription of complement receptor 2 (CR2) and topoisomerase 1 by binding to their promoters in euchromatin[171,172]. DEK also increases the activity of transcription activators activator protein 2 alpha (AP-2α), CCAAT-enhancer-binding protein alpha (C/EBPα) and myeloid/lymphoid or mixed-lineage leukemia; translocated to, 3 (MLLT3)[173-175]. On the other hand, in other settings, DEK is involved in preserving heterochromatin[176]. It has been shown to interact with death-domain associated protein (Daxx) in a transcription repression complex and act antagonistically with nuclear factor kappaB (NF-κB) and tumor necrosis factor alpha (TNF-α)[177,178]. DEK represses the transcription of peroxiredoxin 6 by inhibiting the acetylation of its promoter, most likely through inhibition of p300 and p300/CBP-associated factor (PCAF) histone acetyltransferases[179,180]. Thus, DEK is implicated in gene regulation but its precise role is yet to be elusive.

Interestingly, DEK also has been found to be secreted by macrophages in secretome or in exosomes. Its secretion attracts immune cells such as neutrophils, natural killer cells and T-cells[181]; and its secretion in exosomes, sequential uptake by DEK depleted target cells and translocation to the nucleus has been observed to correct heterochromatin depletion and DNA repair deficits[182].

DEK is overexpressed in highly proliferative cells and its expression decreases with differentiation [183,184]. In melanoma cells, our group has shown that: (*i*) DEK is upregulated in melanoma cells, (*ii*) DEK downregulation results in impaired proliferation and increased senescence, and (*iii*) DEK contributes to chemoresistance of melanoma cells due to upregulation of myeloid cell leukemia-1 (MCL-1) gene[185]. Similarly reduced proliferation was observed in keratinocytes and breast cancer cell lines upon shRNA mediated depletion of DEK (results validated by overexpression as well)[183,184]. Depletion of DEK causes apoptosis in p53-dependent[186] or independent manners (the latter through MCL-1)[186]. DEK also contributes to the chemoresistance against genotoxic agents[186,187], whereas its depletion prevents the activation of DNA damage response[188]. And also, its overexpression in HRAS and HPV-E6 and E7 oncogenes induced keratinocytes led to the increased colony formation in anchor independent medium[189].

Another function of DEK, although the mechanism is not fully clear, is reported to be to interact with splicing factor U2AF and to be essential for intron removal[190,191].

1.5.2. Regulation of DEK Oncogene

At the transcriptional level, DEK has been shown to be regulated by transcription factors E2F1[192], NFY, YY1[193] and ERα[194]. On the posttranslational level, phosphorylation, acetylation and poly(ADP-ribosyl)ation regulates DEK. Casein kinase 2 (CK2) phosphorylates DEK and decreases its DNA

binding affinity and increases its interaction with histones and histone chaperone activity[195,196]. Acetylation of DEK also decreases its DNA binding affinity and allocates DEK to interchromatin granule clusters with RNA processing machinery[197]. Also, miR-489 was shown to suppress DEK expression in muscle stem cells[198] (see Figure 3 for summary). Nonetheless, the intracellular mechanisms underlying DEK regulation, especially at post-transcriptional level are not completely understood, particularly in melanoma.

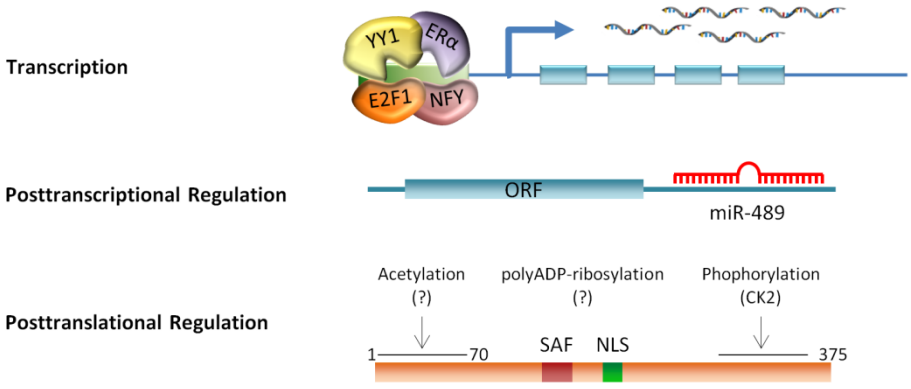

Figure 3: Schematic summary of DEK regulation. SAF: scaffold attachment factor-box, NLS: nuclear localization signal, CK2: Casein kinase 2. Adapted from ref[199].

1.6. CURRENT TREATMENT OPTIONS FOR MELANOMA

Until few years ago the standard treatment for metastatic melanoma was limited with the alkylating agent dacarbazine, which presented very low response rates[200,201]. In 1998, Food and Drug Administration (FDA) approved use of high doses of interleukin-2 (IL-2), but the outcome was still far away from expectations with serious side effects[202,203]. In the last 5 years, therapies targeting MAPK pathway started to emerge. In 2011 and 2013, FDA approved $BRAF^{V600E}$ inhibitors, vemurafenib and dabrafenib; and a MEK inhibitor[204-206]. Nevertheless, these inhibitors were effective only in patients with mutant genes and tumor resistance and relapses appeared in most of patients after initial recession[207]. Other immunotherapeutic approaches approved by FDA are anti-cytotoxic T-lymphocyte-associated protein 4 (CTLA-4) inhibitor, ipilimumab; and programmed cell death protein 1 (PD-1) inhibitors pembrolizumab and nivolumab[208]. CTLA-4 inhibitors bind to CTLA-4 expressed on tumor cell surface and block the inhibitory action of these molecules on T-cells[209,210]. PD-1 inhibitors, on the other hand, bind and block the inhibitory signal from PD-L1 molecules on melanoma cell surface[211-213]. But still, the efficacy of these treatments depends on pre-existing T-cells in the microenvironment and/or PD-L1 expression by melanoma cells, which limits these therapies to a division of patients[214,215]. Currently, many studies are directed to unveil new drug targets to design new strategies in order to improve patient outcome. However, malignant melanoma which is characterized by its high propensity to metastasize and by being the

most lethal form of skin cancer, accumulates a plethora of changes in the transcriptome and the proteome[28,31,216] with approximately 79000 mutations/genome[217]; which makes the search for new targets very intricate.

2. RNA BINDING PROTEINS (RBPs)

RNA binding proteins are one of the most abundant groups of proteins. In a recent study, 1542 manually curated RBPs were identified by bioinformatic analyses and manual curation[218]. Cellular functions controlled by RBPs (described below) range from alternative splicing to RNA decay; from RNA transportation to translational control[219-221] (see Figure 4). Ultimately RNA binding proteins control levels of overall and isoform specific translation, localization and export of mRNAs[222].

2.1. RBPs IN ALTERNATIVE SPLICING

The spliceosome is the largest multiprotein complex, which is composed of 5 uracil rich small nuclear RNAs (snRNA – U1, U2, U4, U5 and U6) and more than 200 highly dynamic proteins[223,224]; and RBPs are main components of this complex. Studies estimate that more than 95% of multiexon genes undergo alternative splicing, which expands the proteomic reservoir[225-227].

2.2. RBPs IN RNA EDITING

RBPs can also function in RNA editing. Adenosine-to-inosine editing by adenosine deaminase acting on RNA (ADAR) proteins change the splicing and the protein outcome of the mRNAs since inosine is interpreted by the spliceosome or translation machinery as guanosine[228,229]. In melanoma cells, ADAR1 expression has been shown to be low, and restoring its expression suppresses melanoma growth and metastasis *in vivo* through editing miR-455-5p and changing the set of gene targets of it[230].

2.3. RBPs IN NUCLEAR AND CYTOPLASMIC POLYADENYLATION

Almost all eukaryotic mRNAs undergo several modifications in the nucleus that include, among others, the addition of a poly-adenosine tail (poly(A)) at the 3' end[231]. This poly(A)-tail contributes not only to mRNA stability and nuclear export, but also to translation initiation, thus expression of the transcript[232,233]. In addition to nuclear polyadenylation, around 20% of transcripts undergo cytoplasmic polyadenylation[234] by cytoplasmic polyadenylation element binding proteins (CPEBs). CPEBs have functions in several biological processes including senescence and tumor formation by altering and regulating stability of their targets (reviewed in ref[235]). In melanoma, it has been shown that the inhibition of CPEB1 by miR-455-5p is required to sustain the metastatic potential of melanoma cells[230].

2.4. RBPs IN mRNA STABILITY AND TRANSLATION

One of the most direct effects of RBPs on gene expression is exerted by their function on mRNA stability and translational regulation. For example, HuR/ElavL1 protein binds to AU-rich elements (ARE) on its targets and stabilize them by protecting them from degradation machinery leading to more translation (by interacting with polysomes) and more protein levels[236]. In docosahexaenoic acid treated melanoma cells, HuR was shown to stabilize COX-2 mRNA and contribute to apoptosis resistance[237]. On the contrary, K homology splicing regulatory protein (KSRP) binds to AU-rich elements and recruit exonucleases as well in order to destabilize the target mRNA, leading to lower protein levels[238].

2.5. RBPs IN mRNA EXPORT AND LOCALIZATION

mRNA export and localization is regulated and operated by RBPs, such as UAP56 and ALY, which would eventually enable the translation of the nascent transcripts[239,240]. Recently, Luzp4, an export adaptor RBP, has been found up-regulated in a wide range of tumors and preferentially in melanoma cells[241]. In this study, it has also been reported that Luzp4 interacts with other RBPs, UAP56 and Nxf1, and that Luzp4 downregulation results in decreased number of colonies formed, suggesting an essential role in melanoma cell growth.

Moreover, many RBPs, such as polypyrimidine-tract-binding protein (PTB), RNA binding motif protein 47 (RBM47), heterogeneous nuclear ribonucleoprotein A1 and members of CUG repeat binding protein, Elav-like family (CELF1/CUGBP1 and CELF2/CUGBP2) bind to multiple targets and operate in diverse processes[242-245]. The functions of these multifunctional proteins are system and cell type dependent and they have been reported to be involved in various cancer types such as breast and oral squamous carcinomas[243,246,247]. Evidently, abnormalities in RBPs expression can lead to different diseases, including cancer[219,248-250].

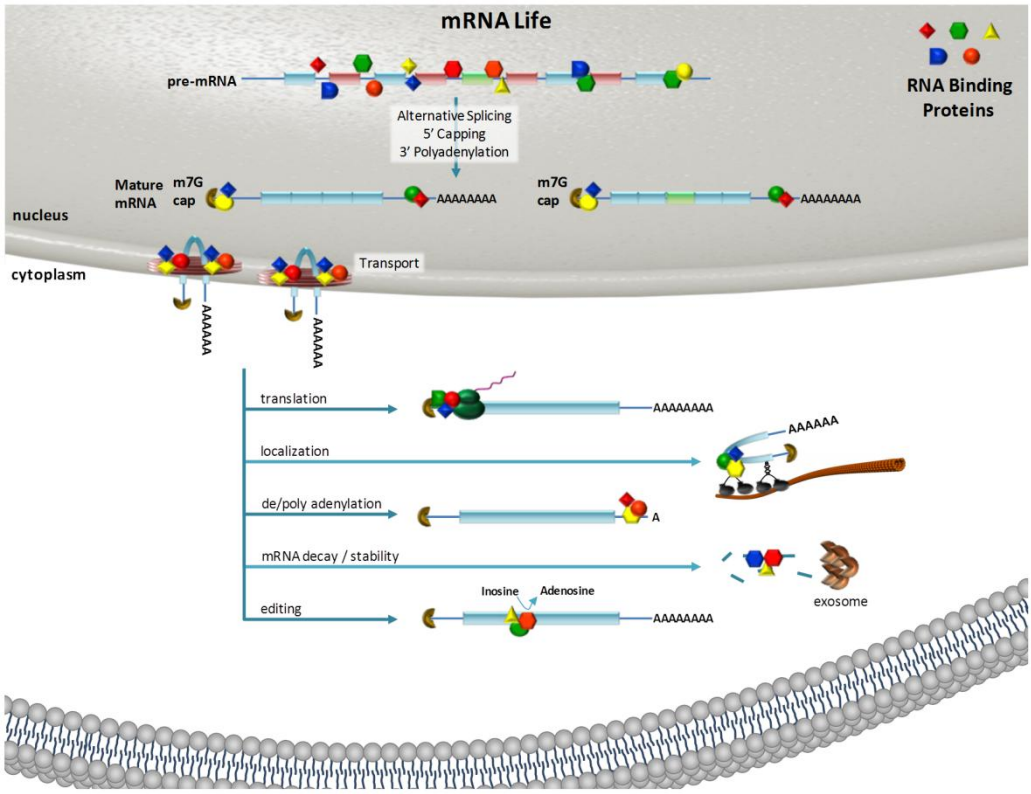

Figure 4: Functions of RNA binding proteins.

3. CUG REPEAT BINDING, ELAV-LIKE FAMILY PROTEINS (CELF/CUGBP)

Several names have been used for the members of this protein family, the most common ones are CELF and CUGBP (see other names in Table 2). Here we will follow the CUGBP nomenclature.

Table 2: Different names of CUGBP family members.

Gene Name	CELF1	CELF2	CELF3	CELF4	CELF5	CELF6
Protein Name	CUGBP1 CUGBP BRUNOL2 NAB50	CUGBP2 BRUNOL3 ETR3 NAPOR	CUGBP3 TNRC4 BRUNOL1 CAGH4	CUGBP4 BRUNOL4	CUGBP5 BRUNOL5	CUGBP6 BRUNOL6

There are 6 members of CUGBP family which are very similar in their domain structure. CUGBPs contain 2 RNA recognition motifs (RRM) in their N-terminal region, and 1 RRM in their C-terminal region connected by a linker region[251]. Based on their sequence similarities, they can be divided into two subfamilies: CUGBP1-2 in one subfamily and CUGBP3-6 in another one (see Figure 5A and 5B). The structure similarities between members of the subfamilies are also reflected in their expression patterns and functions[252].

mRNA and protein expression of *CELF* genes has been shown in various organisms including frogs[253,254], fish[255], birds[256], mice[257,258] and humans[259-261], demonstrating that CUGBP3-6 are largely

restricted to the nervous system in adults, whereas CUGBP1 and CUGBP2 show ubiquitous expression in tissues such as eye, cardiac and skeleton muscle cells as well as nervous system during embryonic development and later on during adulthood[245,256,261,262].

In functional terms, although expression of CUGBP3 is predominantly in the brain, *Celf3* knockout mice display spermatogenesis defects[263]. Moreover, expression level of CUGBP3 deregulates cell proliferation of endoderm-origin organ development in *Xenopus* models[264]. CUGBP4 scarcity has been shown to give rise to eye defects and seizure lesions in the brain both in human patients and mouse models[265-267]. Also, studies with *Cugbp6* knockout mouse model have showed autism-related behaviors[268].

CUGBP2 has been most intensively studied in the brain[269-274], muscle cells[275] and recently in few cancer models[276-279]; and its apoptosis related roles have been shown following irradiation of cancer cells[272,280-282]. Moreover, its genomic deletion has been implicated in cardiac and thymus defects[260].

The most studied member of this protein family has been CUGBP1 and its characteristics are discussed below in detail.

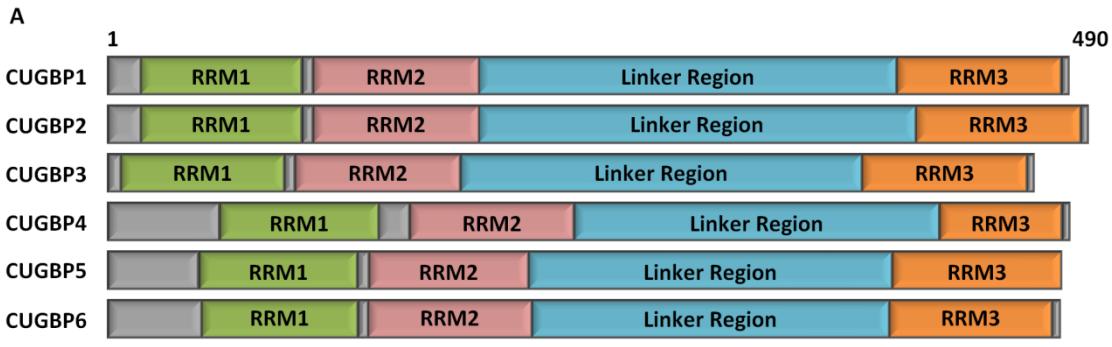

B

	RRM1						RRM2						Linker						RRM3					
	1	2	3	4	5	6	1	2	3	4	5	6	1	2	3	4	5	6	1	2	3	4	5	6
CUGBP1	100	90	53	55	55	54	100	91	59	62	58	56	100	29	ns	ns	ns	ns	100	95	76	61	77	76
CUGBP2		100	53	57	55	55		100	60	64	62	58		100	ns	ns	ns	ns		100	80	61	78	75
CUGBP3			100	84	89	87			100	78	79	78			100	46	34	43			100	68	84	86
CUGBP4				100	86	89				100	86	78				100	28	39				100	69	72
CUGBP5					100	87					100	81					100	42					100	83
CUGBP6						100						100						100						100

Figure 5: A, Domain structures of CUGBP family members. Source: Ref[251]. **B,** Domain sequence similarities (as percentage) amongst CUGBP family members. Source: Ref[252].

4. CUG-REPEAT BINDING PROTEIN 1 (CUGBP1)

CUGBP1 is a multifunctional RBP that confers post-transcriptional functions on pre-mRNAs by regulating alternative splicing, and also on mature mRNAs by regulating translation and modulating stability[283-285]. CUGBP1 was identified in a search for RBPs that bind to a transcript generated from CTG repeat expansion in dystrophia myotonica protein kinase (DMPK) gene[286]. DMPK is the genetic cause of myotonic dystrophy type I disease (DM1 or Steinert disease) with symptoms such as wasting of muscles, heart conduction defects and myotonia[286]. In DM1, available CUGBP1 levels are reduced (due to the sequestration onto the expanded CUG repeats in DMPK mRNA). This alters the balance of CUGBP1 functions, such as alternative splicing of several mRNAs (explained below)[286].

4.1. CONSERVED BINDING SEQUENCES OF CUGBP1

Initially, CUGBP1 was found to bind to CUG repeats, a feature supported by electron microscopy[287]. Subsequently, yeast two hybrid studies revealed UG repeats as CUGBP1 targets[288], and most recently, the binding sequence of CUGBP1 has been defined as GU-rich elements (GREs), the most accepted being the 11-mers UGUUUGUUUGU and UGUGUGUGUGU[284,289]. From a mechanistic perspective, spectroscopic nuclear magnetic resonance (NMR) and crystallography revealed recognition sites for the RRM1 and RRM2 domains[290,291]: CUG for RRM1, and UGUU for RRM2. Other studies point instead to RRM3 as the more relevant RNA recognition motif[292,293]. In addition, the divergent domain connecting RRM1 and RRM2 to RRM3 has also been reported as relevant, most likely via exerting conformational changes in CUGBP1[288]. Overall, these studies show the binding preferences of different RRMs of CUGBP1 for different sequences with the indispensable contribution of the linker domain. In all scenarios, most known CUGBP1 sequences are GREs, although whether this is the case in melanoma is unclear, and addressing this question is a main objective of this PhD Thesis.

4.2. CUGBP1 REGULATION

At the transcriptional level, studies in normal and differentiated myoblasts have identified several transcriptional modulators of CUGBP1: myogenin as a key one, acting through a E-box3 in the *CUGBP1* promoter[294]. In addition, three micro-RNAs have been show to regulate CUGBP1 at posttranscriptional level[295,296]. Specifically, studies in inducible heart specific dicer knockout mice and in rat intestinal crypt cell lines (IEC-6) have demonstrated that miR-23a/b[295], miR-222[296] and miRNA-503[297] regulate the *CUGBP1* mRNA levels by recruiting it to the processing bodies.

Regarding posttranslational regulation, CUGBP1 stability and cellular functions have been related to phosphorylation at residues S28 and S302[298]. In DM1, this phosphorylation (in part mediated by PKC) promotes CUGBP1 upregulation in muscle cells of affected patients[298]. PKC-mediated

phosphorylation of CUGBP1 was also found relevant in postnatal heart and skeletal muscle differentiation, as defined by PKC inhibitors (Nis-IX and Bis1)[299]. S28 can be modified by AKT, a process that increases CUGBP1 interaction with target mRNAs, modulating its roles on protein translation[300]. In turn, S302 is phosphorylated by cyclin D3/Cdk4-6 in aging mouse liver, increasing the interaction affinity of CUGBP1 with eukaryotic initiation factor 2 (eIF2)[301].

4.3. CELLULAR FUNCTIONS OF CUGBP1

Roles of CUGBP1 in cancer are not completely understood, but are likely to depend on the position of the GREs in the target mRNA, as described in other systems. Thus, (i) GREs at flanking areas of introns can modulate alternative splicing, (ii) at 5'UTR, regulate translation, and (iii) the 3'UTR can affect deadenylation (see Figure 6). However, it is important to note that these three functions are cell type and target dependent. To follow is a more detailed summary of cellular functions of CUGBP1.

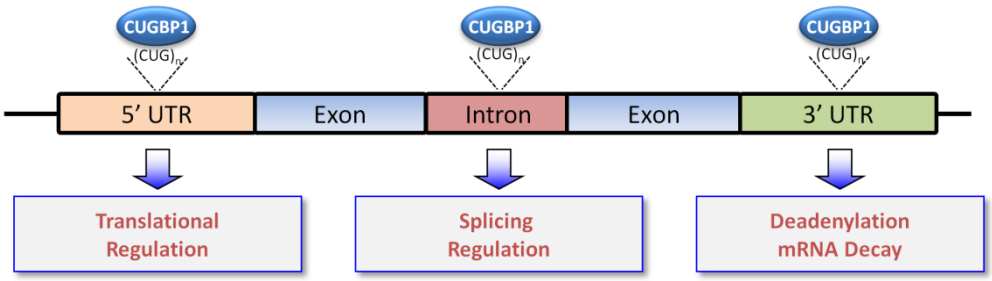

Figure 6: Cellular functions of CUGBP1.

4.3.1. CUGBP1 as an Alternative Splicing Regulator

The role of CUGBP1 as an alternative splicing regulator has been mainly studied in muscle cells, *in vitro* and *in vivo* (see summary and references in Table 3). There, CUGBP1 may favor exon inclusion or exclusion depending on the localization of the GRE that it targets. For example in the C2CL12 mouse myoblast cell line, CUGBP1 can facilitate exon skipping when GREs are located in introns at the 5' flanking site of the exon; instead when the GREs are the 3'flanking intron, exons may be included[283]. Among the alternative splicing events that have been linked to CUGBP1 (summarized in Table 3) one of the best characterized is the insulin receptor (IR) gene[302-304]. *In vitro* and *in vivo* studies using normal and myotonic dystrophy myoblasts, and mouse models demonstrated that CUGBP1 overexpression favors the inclusion of IR exons 5 and 11 as a result of agonistic and antagonistic interactions with two other trans-acting RBPs (hnRNP-h and MBNL1)[302-304]. Other relevant splicing events are exon 22 of SERCA1[305], exon 17 of FXR1[305], exon 5 of FAM188A[305], exon 21 of ANK2[305], exon 20 of ACTN1[306,307], exon 7a of MEF2A[306,307] and exon 9 of PPFIBP1[306,307]. Here we will show that main known CUGBP1 splicing targets are not altered by

depletion of this gene in melanoma cells, pointing to new mechanisms of action of this RNA binding factor.

Table 3: Genes and exons regulated by alternative splicing function of CUGBP1 in different cell lines.
* indicates studies that used cancer cells.

TARGET	SYSTEM	[REF.]
cTNT (e5)	Cardiac and skeletal muscle cells	308
C/EBPb (LIP/LAP)	Mouse liver	309
a-actinin (SM/NM exon)	Muscle cells	307
a-actinin (SM/NM exon)	Mouse fibroblast L cells	310
C/EBPb (LIP/LAP)	Cardiac and skeletal muscle cells	311
C/EBPb (LIP/LAP)	MCF10A (mammary epithelial cell)	312
Mtmr1 (e2.2), MEF2A (e16), ITGB1 (eD), BIN1 (e10)	Cardiac and skeletal muscle cells	306
Tnnt2 (e5), Mtmr1 (e2.2), Clcn1 (e7a), IR (e5), cTNT (e11), Clcn1 (e2)	Cardiac and skeletal muscle cells	303
C/EBPb (LIP/LAP)	Mouse liver	313
C/EBPb (LIP/LAP)	3T3-L1 preadipocytes	314
IR (e11)	Normal and myotonic dystropy myoblasts	304
Clcn1 (e7a), TnnT3	Inducible CTG repeat mouse model	315
C/EBPb (LIP/LAP)	Primary macaque macrophages & U937	316
Clcn1 (e7a), Serca1 (e2.2), Cypher (e11), Ank2 (e21), Capzb (e8), Fxr1 (e15, e16)	Cardiac and skeletal muscle cells	305
NMDAR-1 (e5), GABT4 (e7)	SK-N-SH (Neural (bone marrow metastasis) from human)	317
Clcn1 (e7a), MBNL1	Kennedy Disease mouse model (CAG repeats in AR gene)	318
Ank2 (e21), Cypher (e11), Mtmr1 (e2.2), H2afy (e6b), Capzb (e8), Serca1 (e2.2), Fxr1h (e15), RyR1 (e70), Gfat (e10)	Skeletal muscle	319
Ank2 (e21), Sorbs1 (e6), Mtmr3 (e16), Mfn2 (e3), H2afy (e6)	Heart muscle	295
B-tropomyosin (e6b)	Skeletal muscle	320
Bcl-x	Rat oligodendrocyte progenitors, HeLa & C6 Cells	321*
C/EBPb (LIP/LAP)	HeLa	322*

4.3.2. CUGBP1 as a Translational Regulator

Translational regulation is the least studied and understood function of CUGBP1. In particular, CUGBP1 has been shown to increase p21 protein (but not mRNA levels) during muscle cell differentiation[285]. Other systems where p21 has been modulated by CUGBP1 are mouse embryonic fibroblasts (MEFs) undergoing premature senescence[323].

Another known target of CUGBP1 in translational control is the CCAAT/enhancer-binding protein beta (C/EBPβ) gene, reported in liver[309,322]. C/EBPβ is an intronless gene, coding for several isoforms due to alternative ATG start sites. The ratio between the longer isoform, liver-enriched activator protein (LAP), and the shorter isoform, liver-enriched inhibitory protein (LIP), is an important modulator of cell cycle progression during liver regeneration[324]. After partial hepatectomy in mice, CUGBP1 gets hyperphosphorylated and replaces calreticulin (CRT), which in turn increases LIP/LAP ratio expression[313]. In the same study CUGBP1 was shown to bind to translation initiation factors eIF2a and eIF2b targeting them to the downstream ATG of C/EBPβ ultimately increasing the LIP/LAP ratio. CUGBP1-dependent increase in LIP/LAP ratio has also been

observed in preadipocyte cell lines upon oltipraz treatment which results in blocked adipogenesis[314]; as well as in primary macaque macrophages and human leukemic monocyte lymphoma cell line in which CUGBP1 is shown to be required for interferon beta (IFNβ)-mediated induction of LIP isoform[316].

CUGBP1 has also been shown to be involved in induction of internal ribosome entry sites (IRES), although with distinct effects depending on the gene, namely, favoring the translation of the serine hydroxymethyltransferase 1 (SHMT1)[325] while repressing p27[326] in MCF7 cell line, but the precise mechanisms underlying these opposing effects are unclear. Translation-associated positive or negative effects of CUGBP1 in cancer are not well understood, and addressing this question in melanoma is also a global objective of this PhD Thesis.

4.3.3. CUGBP1 as an mRNA Decay Modulator

Various studies have been performed to assess CUGBP1 roles and targets (see Table 4). For mRNA decay, high throughput studies to identify roles of CUGBP1 as an mRNA decay modulator have been only reported by RNA-immunoprecipitation followed by microarrays in HeLa cells and resting and activated T-cells[284,327]. In these studies, CUGBP1 was shown to be responsible for the destabilization of the target mRNAs by binding to 3'UTR-located GREs, a process weakened if CUGBP1 is phosphorylated[327], supporting results in yeast[289]. A proposed mechanism for mRNA destabilization has been related to the recruitment of the poly(A)-specific ribonuclease (PARN), with the subsequent poly(A) tail shortening and degraded by 3'-to-5' exonucleases[328]. However, emphasizing the complexity of CUGBP1 functions, this protein can also stabilize mRNA transcripts, for example interfering with microRNAs (i.e. as the case for miR-122 in hepatocellular carcinoma)[329]. In summary, CUGBP1 can recognize multiple mRNAs and at multiple sites, but the ultimate impact of this binding may be gene, tissue and context dependent.

Intriguingly, and as we will show in the Figure 12F of the results section, the overlap in the targets whose stability are controlled by CUGBP1 in HeLa[284] and T-cells[327] is minimal (just 1% of common genes).

Table 4: High throughput analyses of CUGBP1. n.d. not determined.

SYSTEM	METHOD	FUNCTION	# TARGETS	VALIDATED TARGETS	REF.
X. tropicalis egg extracts	RIP + Microarray	Binding	162 genes	Lmo4, Cdk1, Cdk2, CPEB, ZMPste24	330
Myelogenous leukemia cell line	RIP-ChIP	Binding	2359 Genes	--	331
Lymphoblastoid cell line	RIP-ChIP	Binding	147 Genes	--	331
Embryonic chicken heart	CLIP	Binding and Splicing	170 genes	MYH7B, HOPX	332
C2C12 mouse muscle cell line	HITS-CLIP	Splicing	n.d.	Sox4, Wtap, MHC, Erbb2ip, Ctage5, Ddr1, Dst, Ktn1, Abi1, Ciz1, Itga6, Mtap4, Ndrg4, Rhot1	283
Heart and muscle specific CUGBP1 overexpressing mice	CLIP	Splicing	540 exons in heart 388 exons in muscle	Clcn1	333
Embryonic chicken cardiomyocytes	RNA-seq upon siCUGBP1	RNA-Seq	8552 transcripts	--	334
C2C12 mouse muscle cell line	RIP + Microarray	mRNA Decay	881 transcripts	cJun, Rnd3, Smad7, Ppp1r15b, Myod1	335
HeLa	RIP + Microarray	mRNA Decay	328 Genes	JunD, TOP1, UBE3A	284
T-Cells	RIP + Microarray	mRNA Decay	1137 Genes	JunB, AKT, EPHA4, NDUFS2, GSN,PPIC	327

5. CUGBP1 AND CANCER

CUGBP1 is emerging as a relevant modulator of tumor cell progression and/or survival, although detailed analyses of the involved targets are still limited (see Table 5 for summary). Initial reports related to non-small cell lung carcinoma (NSCLC) has shown that CUGBP1 was linked to worse postsurgical survival, in part due to enhanced brain metastasis[329]. Moreover, retrospective analyses suggested reduced overall survival in cases with high CUGBP1 expression[336,337]. In addition, studies in hepatocellular[338] and gastric[339] carcinoma cell lines demonstrated that short-hairpin RNA (shRNA) mediated downregulation of CUGBP1 promoted cell cycle arrest. In both cell lines, CUGBP1 depletion led to downregulation of cyclin B1[338,339]. However, cyclin D1, another key factor in cell proliferation, was upregulated by CUGBP1 depletion in hepatocellular carcinoma cell line[338], but downregulated it in the gastric carcinoma cell line[339]. Data in other cancer types relate BIRC5 in esophageal cancer cell lines[340]. On the other hand, CUGBP1 has been shown to destabilize CD9 in HeLa and acute lymphocytic leukemia; and c-Fos in HeLa cell line[341]. Also C/EBPα modulation in non-small cell lung cancer cells[342] has been shown.

Table 5: Cancer related roles of CUGBP1 in different cancer types.

SYSTEM	TARGET/FINDING	REF.
NSCLC patient biopsies and follow-up	Negative correlation with post surgical	337
NSCLC patient biopsies	Positive correlation with brain metastasis	336
HepG2 - hepatocellular carcinoma	CCNB1 downregulation CCND1 upregulation	338
MGC-803 - gastric cancer	CCNB1 downregulation CCND1 downregulation	339
TE7 & TE10 - esophageal cancer	BIRC5 stabilization Protection against apoptosis	340
HeLa - cervical cancer REH - acute lymphocytic leukemia	CD9 destabilization c-Fos	341
A549 - NSCLC	C/EBPα downregulation	342

To date, no published data is available regarding neither the expression nor the function of CUG repeat binding protein family members in melanoma. In addition, identified CUGBP1 targets fail to be consistent in different settings and comprehensive CUGBP1-controlled networks have not been published. With this background, the main purpose of this PhD thesis is to identify the expression levels of RBPs in melanoma; and in particular to understand the function of CUGBP1 in this disease by unraveling the gene networks that it controls.

IV.

OBJECTIVES

OBJETIVOS

Melanoma is a paradigm of histopathologically complex tumors, proceeding with the highest mutational rate known to date, and accumulating a plethora of changes in their transcriptome and proteome. Yet, RNA binding proteins, factors which have the inherently ability to impinge on a broad spectrum of oncogenic and suppressive signaling cascades, remain poorly understood in this disease. A comprehensive mining of all 692 RBPs described to date failed to suggest consistent mutations of copy number alterations in human melanoma specimens. Therefore, we turned to comparative transcriptomic profiles that could reveal differential RBP expression in melanoma cells vs. normal melanocytes. This analysis identified CUGBP1 as a putative novel melanoma-associated factor. The **Specific Aims** of this study were therefore as follows:

1. To perform a histological characterization of CUGBP1 expression in melanoma progression (normal skin, benign nevi and malignant clinical specimens)
2. To define the requirement and functional impact of CUGBP1 in melanoma cells.
3. To dissect the gene networks regulated by CUGBP1, integrating RNA immunoprecipitation, transcriptomic and proteomic analyses.

V. MATERIALS AND METHODS

MATERIALES Y MÉTODOS

1. CELL CULTURE

The human melanoma cell lines SK-Mel-5, SK-Mel-19, SK-Mel-28, SK-Mel-29, SK-Mel-103, SK-Mel-147, G-361, UACC-62, WM-1366 and LU-1205 (see Table 6 for mutation status) and non-melanoma tumor cell lines 639V (bladder cancer), A549 (non-small cell lung cancer), BT549 (breast cancer), HCT116 (colorectal cancer), HeLa (cervical cancer), MiaPaca-2 (pancreatic cancer), U251 (glioma) and 293FT (transformed human embryonic kidney cells) were cultured in Dulbecco's modified Eagle's medium (DMEM, Lonza, cat. no. BE12-604F/U1) supplemented with 10% fetal bovine serum (FBS, Lonza, cat. no. DE14-801F) and 100 µg/mL Penicillin/Streptomycin (Invitrogen, cat. no. 15070-063). Primary human melanocytes, keratinocytes and fibroblasts were isolated as described before[343] from neonatal foreskins obtained from the Hospital Niño Jesús, Madrid, Spain. Melanocytes were cultured in Medium 254 (Invitrogen, cat. no. M-254CF-500) supplemented with 1% melanocyte growth factors (HMGS, Invitrogen, cat. no. S-002-5), 0.2 mM $CaCl_2$ and 100 µg/mL Penicillin/Streptomycin; keratinocytes were cultured in Epilife Medium (Invitrogen, cat. no. M-Epi-500) supplemented with 1% keratinocyte growth factors (HKGS, Invitrogen, cat. no. S-001-5), 0.2 mM $CaCl_2$ and 100 µg/mL Penicillin/Streptomycin and fibroblasts were cultured in DMEM, supplemented with 10% FBS, and 100 µg/mL Penicillin/Streptomycin.

Table 6: Human melanoma cell lines used in this PhD thesis study.
(*: protein levels, WT: wild type, ^{R}: repressed and nd: not determined)

CELL LINE	BRAF	NRAS	PTEN*	TP53	DEK*
SK-Mel-5	V600E	WT	+	WT^{R}	++
SK-Mel-19	V600E	WT	+	WT	++
SK-Mel-28	V600E	WT	+	R273H	++
SK-Mel-29	V600E	WT	-	WT	++
SK-Mel-103	WT	Q61R	+	WT^{R}	+++
SK-Mel-147	WT	Q61R	+	WT^{R}	++
G-361	WT/V600E	WT	-	WT^{R}	+
UACC-62	V600E	WT	-	WT	+
WM-1366	WT	Q61R	nd	nd	+++
LU-1205	V600E	WT	nd	nd	+

2. PROTEIN IMMUNOBLOTTING

Cells were harvested and total cell lysates were obtained using 1X Laemmli buffer (62.5 mM Tris-HCl pH 6.8, 2% SDS, 10% glycerol and 5% β-mercaptoethanol) and boiled at 95°C for 7 minutes. Protein concentrations were determined using the Bio-Rad Protein Assay (Bio-Rad Laboratories) according to manufacturer's protocol. Protein immunoblots were performed by standard SDS-PAGE electrophoresis in 10 or 12% polyacrylamide gels and subsequently transferred to Immobilon-P membranes (Millipore) using Mini Trans-Blot Cell system (Bio-Rad Laboratories). Transfer was performed at 100V during 1 hour at 4°C. Membranes were blocked with 5% milk in tris-buffered saline with 0.05% Tween-20 (TBS-T) for 1 hour at RT. Primary and secondary antibodies were diluted in 5% milk TBS-T incubated overnight at 4°C or 1 hour at RT. Primary antibodies used were: CUGBP1 (Abcam, ab9549), CUGBP2 (Sigma, AV40323), CCND1 (Santa Cruz Biotechnology, 8396), DEK (BD Transduction Laboratories, 610948), and Actin (Sigma-Aldrich, A5441). HRP-conjugated secondary antibodies used were anti-mouse and anti-rabbit (GE Healthcare) or anti-goat (Jackson Immunoresearch). When indicated, image J software was used to quantify protein band intensities.

3. RNA EXTRACTION, PCR and RT-QPCR

Total RNA was extracted and purified from cell pellets using RNeasy Mini-Kit (QIAGEN) following the manufacturer's instructions. RNA concentration was determined by NanoDrop Spectrophotometer ND-100 (NanoDrop Biotechnologies). 1-2µg total RNA was reverse-transcribed into cDNA using the high capacity cDNA reverse transcriptase kit (Applied Biosystems), according to manufacturer´s protocol. 20 ng of the total cDNA were subjected to real-time quantitative polymerase chain reaction (RT-qPCR - 60°C annealing temperature) using Power SYBR® Green PCR Master Mix (Applied Biosystems). Assays were run in triplicates on the 7900HT Fast Real-Time PCR system (Applied Biosystems) or QuantStudio™ 6 Flex Real-Time PCR System (Applied Biosystems). The primer sequences and annealing temperatures listed on Table 7. HPRT and GAPDH were used as loading control to normalize mRNA expression.

Table 7: List of primers used in this PhD thesis study (°C: annealing temperature)**.**

PCR/qPCR PRIMERS			
GENE	**FORWARD PRIMER (5' – 3')**	**REVERSE PRIMER (5' – 3')**	**°C**
CUGBP1	GTGGAAGACAGGAAGCTGTTT	GCCGTCTGTGCCATGGCTCTTG	60
DEK	GCCATGTTAAAGAGCATCTGTG	CAGAAGGCTTTGGATGCATTA	60
HPRT	CCTGGCGTCGTGATTAGTGAT	AGACGTTCAGTCCTGTCCATAA	60
GAPDH	GAAGGTGAAGGTCGGAGTCAAC	TGATTTTGGAGGGATCTCGCTC	60
INSR	CCAAAGACAGACTCTCAGAT	AACATCGCCAAGGGACCTGC	54
SERCA1	GATGATCTTCAAGCTCCGGGC	CAGCTCTGCCTGAAGATGTG	54
FXR1	GATAATACAGAATCAGATCAG	CTGAAGGACCATGCTCTTCAA	54
FAM188A	GAGGAAACTGCTAGTATTTC	CCAAATTTATTTCCCCACAT	54
ANK2	TACCTCCAGACCCCAACATCC	TCTTTACCACGGTGTGTCCAT	54
ACTN1	CGGGCCTCCTTCAACCACTTT	TCCACAATGCTCATGATGCGG	54
MEF2A	GAATGAACAGTAGGAAACCAG	GCTGGTCAGTGAATAATCAGT	54
PPFIBP1	TAGTGAAATGGACAGTGAGA	CAATTTTTCTTGTAGCCTTT	54
DEK 3'UTR Fragment 1	see FLAG Forward Primer	GGTCAGCAGTAAGTTCTACTAAC	58
DEK 3'UTR Fragment 2	see FLAG Forward Primer	CATCTGTCACTTTTGTCATGCTG	58
DEK 3'UTR Fragment 3	see FLAG Forward Primer	GTGCTTGTACTTAATCCCACCC	58
DEK 3'UTR Fragment 4	see FLAG Forward Primer	CCTTTCCCTAGTGTCTGAGTAAC	58
FLAG	GATTACAAGGATGACGACGATAAG		58
CLONING PRIMERS			
FRAGMENT	**FORWARD PRIMER (5' – 3')**	**REVERSE PRIMER (5' – 3')**	**°C**
DEK 3'UTR Fragment 1	AGCCCTCGAGGATTACAAGGATGACGA CGATAAGGATAGAGGACAGAGAAGAT	TAGGGGATCCCACACTGACAGAGA TGTGTATTC	58
DEK 3'UTR Fragment 2	AGCCCTCGAGGATTACAAGGATGACGA CGATAAGAAAATTCAGCGGCAGTGTG	TAGGGGATCCGGGTAACTGTTCCT TCAGTGTTGCC	58
DEK 3'UTR Fragment 3	AGCCCTCGAGGATTACAAGGATGACGA CGATAAGTGCTTTGCCTCGAAAGTGT	TAGGGGATCCGGTGCAACAAATG TGTCATTGTGTC	58
DEK 3'UTR Fragment 4	AGCCCTCGAGGATTACAAGGATGACGACG ATAAGAATTAAGTGTTGAAAAATATCTTTGC	TAGGGGATCCTGGTGATACATCC ATTTAATAAGTGTGCG	58

4. CLONING OF DEK 3'UTR FRAGMENTS

DEK 3'UTR fragments were amplified with the indicated primers listed on Table 7 to obtain the following fragments (estimated UG repeats underlined).

Fragment 1

gauagaggacagagaagaugacucguucccauagauuugaagaucugauuuauaccauuauaccagcaaagagaauguauuucc uuuucuaaauccuuguuaagcaacguuaguagaacuuacugcugaccuuuuuuaucuugaguguuauugugaauuugaguuugc uguuuuaaaauugcauuucuaugccauuuuuaguuuaaaaucuugcauggcauuaauuguuccuugcuuuuuauaguuguauu uuguacauuuuggauuucuuuauauaaggucauagauucuugagcuguuguggguuuuuagugcacuuaauauuagcuugcu uaaggcauacuuuuaaucaaguagaacaaaaacuauuaucaccaggauuuauacauacagagauuguaguauuuaguauauga aauauuuugaauacacaucucugucagugug

Fragment 2

aaaauucagcggcaguguguccaucauauuaaaaauauacaagcuacaguuguccagaucacugaauuggaacuuuucuccugc auguguauauaugucaaauugucagcaugacaaaagugacagauguuauuuuuguauuuuuaaaaaacaauugguuguauau aaaguuuuuuuauuucuuuugugcagaucacuuuuuaaacucacauagguagguaucuuuauaguuguagacuauggaaugu caguguucagccaaacaguaugauggaacagugaaagucaauucagugauggcaacacugaaggaacaguuaccc

Fragment 3

ugcuuugccucgaaagugucaucaauuuguaauuuuaguauuaacucuguaaaagugucuguagguacguuuuauauuauau
aaggacagaccaaaaaucaaccuaucaaagcuucaaaaacuuugggaaaggguggggauuaaguacaagcacauuuggcuuacag
uaaaugaacugauuuuuauuaacugcuuuugcccauauaaaaugcugauauuuacuggaaaccuagccagcuucacgauuaug
acuaaaguaccagauuauaaaugccagaauauaaaugugcaggcaaucguggaugucucugacaaagugugucucaaaaauaaua
uacuuuuacauuaaagaaauuuaaauguuuucucuggaguuggggcucuuggcuuucagaguuugguuaaucaguguugauucu
agaugaucaacauaauggaccacuccugaaugagacuuaauuuuugucuuucaaauuuacugucuuaaaucaguuuauuaaauc
ugaauuuuaaaacaugcuguuuaugacacaaugacacauuuguugcacc

Fragment 4

aauuaaguguugaaaaauaucuuugcaucauagaacagaaauauauaaaaauauauguugaauguuaacagguauuuucaca
gguuuguuucuugauaguuacucagacacuagggaaaggguaaauacaagugaacaaaauaagcaacuaaaugagaccuaauaa
uuggccuucgauuuuaaaauauuuguucuuauaaaccuugucaauaaaaauaaaucuaaaucacugguguuuuaagucacuug
cauuugauaucuuauagguguauauagcauuuccuuaugggaauaauucugaaaagggauuuuuaaauugauucagcccua
uaaccuauacaauuuggaauacucuuuuguggguaauggaccauuuucuuggagugacuucacaaaacugaauaauuaagguua
auuuuaugaccauuugcuauaaagaagguaaguagucaugcauagaguauuuggaagugaggaaauggaguuguucuguaug
aaaguucuugaugaguacgcacacuuauuaaauggauguaucacca

PCR products were purified with PCR purification kit (Qiagen, cat. no. 28106) following manufacturer instructions. Amplified fragments and empty pLV-CMV-SV40-Puro vector were digested by XhoI (NEB Inc, cat. no. R0146) and BamHI (NEB Inc, cat. no. R0136) with NEBuffer 3 (NEB Inc, cat. no. B7003) and BSA (NEB Inc, cat. no. B9001). Ligation was performed (3:1, insert:vector molar ratio) with T4 DNA Ligase (NEB Inc, cat. no. M0202). Insertion was checked by sequencing.

5. GENE SILENCING VIA LENTIVIRAL TRANSDUCTION OF shRNAs

CUGBP1 expression was inhibited by lentiviral-driven gene silencing using two previously reported shRNAs[344], kindly donated by Roger Romis. Target sequences were; shCUGBP1-1: GCTGCATTAGAAGCTCAGAAT (Sigma-Aldrich-TRCN0000017284) and shCUGBP1-2: CGAGTCATGTTCTCTTCGTTT (Sigma-Aldrich-TRCN0000017285). As control, non-targeting shRNA from Sigma: CAACAAGATGAAGAGCACCAA was used. Viruses were produced in 293FT cells and infections were performed as previously described[91]. Downregulation efficiency was determined after puromycin selection (1µg/mL) by protein immunoblotting or RT-qPCR.

6. CELL PROLIFERATION ASSAYS

6.1. GROWTH CURVES

For growth curves, $1x10^3$ melanoma cells were plated in 96-well optical bottom plates at day 6 after lentiviral transduction. At the indicated time intervals (Day 0 is the following day after seeding), cells were fixed with 4% paraformaldehyde (Electron Microscopy Sciences) and stained

with DAPI (Invitrogen). For each time point, total cell number was quantified in triplicates by automated high throughput confocal detection of DAPI-stained nuclei using the OPERA HCS platform and the Acapella Analysis Software (Perkin Elmer).

6.2. COLONY FORMATION

Low confluency colony formation assays were performed seeding $1x10^3$ (SK-Mel-103, SK-Mel-147, 639V, A549, HeLa, HCT116, MiaPaca2 and U251) or $5x10^3$ (SK-Mel-5, SK-Mel-19, SK-Mel-28, SK-Mel-29, UACC-62, LU-1205 and BT-549) cells per well onto 6-well plates. Cells were allowed to grow for 10-14 days for low density assays, fixed with cold methanol for 10 minutes and the colonies were stained with 0.4g/L crystal violet (Sigma). Number of colonies was quantified by counting using ImageJ software.

7. CELL CYCLE PROFILE ANALYSIS BY FLOW CYTOMETRY

7.1. CELL SYNCHRONIZATION

For cell synchronization at G1/S border, control or shCUGBP1 depleted SK-Mel-103 cells were treated with 2.5 mM thymidine (Sigma) for 18 hours. Cells were fixed (see below) at 0, 4 and 8 hours after release of the thymidine block.

7.2. BRDU PULSE LABELING

For BrdU pulse, exponentially growing control or shCUGBP1 depleted SK-Mel-103 cells were incubated with 10µM BrdU (Sigma) for one hour. Cells were fixed with ice cold 70% ethanol and processed following the acidic protocol described before[345]. S-phase BrdU positive cells were stained with FITC-conjugated anti-BrdU antibody (BD Pharmigen), and DNA was counterstained with 50µg/mL propidium iodide (Sigma).

7.3. FLOW CYTOMETRY

Data was acquired using a FACS Calibur flow cytometer (Becton Dickinson). Cell aggregates were excluded using pulse processing and a minimum of 20000 single events were measured. Data was analyzed using FlowJo 9.6.4 software (Treestar). Cell percentages at G0/G1, S or G2/M phases in synchronized cells were calculated using Watson model[346].

8. TISSUE IMMUNOSTAINING, TISSUE IMMUNOFLUORESCENCE AND MICROSCOPY

8.1. IMMUNOHISTOCHEMISTRY (IHC)

Tissue microarrays containing a total of 185 (47 benign, 138 malignant) human specimens were stained with CUGBP1 antibody (Abcam, ab9549) using BondTM Automated System (Leica Microsystems) by the Monoclonal Antibodies Unit of CNIO. After automated dewaxing and rehydration of the samples, heat-induced antigen retrieval was performed using Bond Epitope

Retrieval Solution 2 (Leica Biosystems) and immunodetection was performed with BondTM Polymer Refine Detection (Leica Microsystems) following the manufacturer's instructions. CUGBP1 protein expression was scored blinded according to staining intensity by two independent dermatologists. The score system used for staining intensity was: 0 (no detectable), 1 (intermediate) and 2 (high). Digital images of IHC-stained sections were obtained at 40x magnification (0.12µm/ pixel) using a whole slide scanner (Mirax scan, Zeiss) fitted with a 40x/0.95 Plan Apochromat objective lens (Zeiss).

8.2. IMMUNOFLUORESCENCE (IF)

Paraffin embedded malignant melanoma tissues were processed as previously described[347] for CUGBP1 (Abcam, ab129115) and DEK (BD Transduction Laboratories, cat. no. 610948) co-staining. Antigen retrieval was performed using 10 mmol/L sodium citrate buffer at pH 6. Secondary antibodies used were anti-rabbit Alexa Fluor 555 and anti-mouse Alexa Fluor 488 (Life Technologies) and DNA was counterstained with DAPI. Negative controls were obtained by omitting the primary antibody. Image mosaics were acquired at 40xHCX PL APO 1.2 N.A. oil immersion objective using a confocal TCS-SP5 (AOBS-UV) confocal microscope and "intelligent matrix screening remote control" (iMSRC) tool[348]. Images were subsequently analyzed with Definiens XD software to determine CUGBP1 and DEK nuclear intensities per cell. The signal intensities were quantified in maximum range of RGB color scale (0-255). Data points were pseudo-colored based on red/green signal intensity ratio (red, ratio≥2; green, ratio≤0.5; yellow, 0.5<ratio<2).

9. RNA STABILITY (ACTINOMYCIN D TREATMENT) ASSAYS

Control or CUGBP1 depleted (shRNA) cells were seeded on day 4 after infection (250000 cells/6cm plate). Cells were treated with Actinomycin D (Sigma Aldrich, A9415) at 5 µg/ml concentration. After 30 minutes of pre-treatment, cells were washed with ice cold PBS and collected via scraping at indicated time points (0, 1, 2, 4 and 6 hour). RNA extraction, quantification, reverse transcription and qPCR were performed as described previously.

10. ANIMAL EXPERIMENTS

Mouse xenograft models were generated by subcutaneous implantation of $1.0x10^6$ (SK-Mel-103) or $2x10^6$ (UACC-62, LU-1205) cells in athymic nude (Crl:NU(NCr)-Foxn1nu) female mice (Charles Rivers). Cells were harvested at day 4 after transduction with control or CUGBP1 shRNAs, resuspended in Matrigel (BD Bioscience) at 1:3 ratio in PBS and injected in the back of the animals (n=5 per group). Tumor growth was measured blinded to the experimental conditions at the indicated time intervals. Tumor volume was estimated using a caliper and calculated as $V= axb^2x\pi/6$, where "a" stand for the bigger and "b" for the smaller diameter of the tumor. When

control tumors exceeded 1cm^3 size mice were sacrificed and xenografts were surgically excised and processed for histopathological and protein detection studies. All experiments with mice met the Animal Welfare guidelines and were performed in accordance with protocols approved by the Institutional Ethics Committee of CNIO.

11. RNA IMMUNOPRECIPITATION AND SEQUENCING (RIP-SEQ)

11.1. RNA IMMUNOPRECIPITATION

For RNA immunoprecipitation, non-infected cells at 80% confluence were fixed in 1% formaldehyde for 10 minutes at room temperature (RT), and fixation was stopped by adding 1M Glycine for 5 minutes at room temperature. After washing with ice cold PBS, cells were collected by scraping and lysed with in NT2 buffer (50 mM Tris–HCl pH 7.5, 150 mM NaCl, 1mM MgCl2, 0.5% Nonidet P-40 and 1 mM EDTA) supplemented with protease and RNase inhibitors (Applied Biosystems). For the solubilization of crosslinked complexes, lysates were sonicated in a Bioruptor Standard (Diagenode) for 10 minutes at medium intensity. After preclear by protein A Dynabeads for 30 minutes at 4°C, samples were immunoprecipitated using CUGBP1 antibody or mouse IgG coupled to protein A Dynabeads (Invitrogen) for 3h at 4°C. Immunoprecipitates were washed 6-8 times extensively and resuspended in NT2 buffer containing 50µg proteinase K (Roche Applied Science), 1% SDS, 200mM NaCl and 10mM EDTA. Sample was split into two (1:4 for protein, 3:4 for RNA extraction). Protein fraction was mixed with loading dye, boiled at 95°C for 5 minutes and supernatant was collected. RNA elution was done by consecutive incubations at 55°C for 30 minutes and at 65°C for 45 minutes. Supernatants were collected and digested with DNaseI for 10 minutes at RT. RNA was extracted with TRI Reagent (Sigma) following manufacturer´s protocol. For validation, independent RIP assays were performed. The total amount of RNA immunoprecipitated and 1µg of RNA extracted from inputs were retrotranscribed using cDNA reverse transcriptase kit and qPCR were performed as described before. Fold binding enrichment of target mRNAs in the immunoprecipitated fraction was calculated after normalization with the gene expression from the inputs. The primers used for RIP-qPCR are listed Table 7.

11.2. SEQUENCING AND BIOINFORMATICS ANALYSIS

RNA sequencing was performed by Genomics Unit from CNIO. Integrity of RNA was evaluated by Agilent 2100 Bioanalyzer using RNA 6000 Pico kit following manufacturer's recommendations. An estimated mass of 20 ng RNA per sample (1 µg for input samples) was processed with Ribo-Zero Gold Kit (Epicentre, cat. no. RZHM11106/RZG1224) for ribosomal RNAs removal. RNAs were randomly fragmented, converted to double stranded cDNA and processed through subsequent enzymatic treatments of end-repair, dA-tailing, ligation to adapters and amplification by PCR with Illumina PE primers. The purified cDNA library was applied to an Illumina flow cell for cluster

generation (TruSeq cluster generation kit v5) and sequenced on Illumina Genome Analyzer IIx with SBS TruSeq v5 reagents following manufacturer's protocols. Fastq[349] files with 40-nt single-end sequenced reads were quality-checked with FastQC[350] and aligned to the human genome (GRCh37/hg19) with TopHat-2.0.4[351], using Bowtie 0.12.7[352] and Samtools 0.1.16[353], allowing two mismatches. For each read, only the alignment with the best score was considered. RIP-seq peaks were called with Piranha 1.2.1[354] using the ZeroTruncatedPoissonRegression distribution, with a bin size of 20 and 0.05 FDR. From the total number of peaks obtained, only those with more than 30 reads were considered for further analysis. Peak annotation was performed with PeakAnalyzer 1.4[355], using the Homo sapiens GRCh37.72 annotation from Ensembl[356]. Common peaks among the three samples were obtained with BEDtools 2.16.2[357], and their corresponding nucleotide sequences were retrieved with the Ensembl API. CUGBP1 binding sequences in the binding region of the target was searched by Sequence Searcher[358] allowing two mismatches. Motifs enriched in the peaks were discovered with DREME[359].

12. CUSTOMIZED SPLICING SENSITIVE MICROARRAY

Melanoma cell lines SK-Mel-19 and SK-Mel-103; and primary human melanocytes were grown as indicated above. Melanoma cells were harvested by trypsination at a confluency of approximately 70% and the pellets were stored at -80°C. Melanocytes were harvested by trypsination at a confluency of approximately 70% confluency. Melanocytes derived from three different donors were pooled and the pellets stored at -80°C. Total RNA was purified using RNeasy Mini kit (Qiagen, 74104) and digested with DNase RNase free (Qiagen, 79254). Quality assessment of Total RNA samples were analyzed using the Agilent Bioanalyzer 2100 and the RNA 6000 LabChip Kit (Agilent) with the Eukaryote Total RNA Nano Assay (Agilent). Cy5-Cy3 labelled cRNA were generated from the total RNA using the Agilent Low RNA Input fluorescent linear amplification kit (Agilent, 5184-3526) and cyanine 5-CTP and cyanine 3-CTP (Perkin-Elmer NEL580, NEL581); the cRNA was purified using the RNeasy Mini kit (Qiagen, 74104). Quality control assessed by Agilent Bioanalyzer 2100. 6µg of each cRNA were used for the hybridization following Agilent In situ Hybridization Kit Plus, (Agilent, 5184-3568). Three biological replicates were hybridized, with both direct and dye-reversal hybridizations. Agilent hybridization oven was set to 60°C. Fluorescent images were obtained using the G2565BA Microarray Scanner System (Agilent) with 100% laser power and 100% PMT settings and 16-bit TIFF images, one for each channel, were quantified using GenePix Pro 6.0 microarray analysis software (Molecular Devices, www.moleculardevices.com). Mean foreground and background intensities were extracted from the red (Cy5) and green (Cy3) channels for every spot on the microarray. The background intensities are used to correct the foreground intensities for local variation on the array surface, resulting in corrected red and green intensities. Raw data were processed using SAPO (http://bioinfo.ciberehd.org/SAP.ang.htm) and CGEM (http://bioinfo.

ciberehd.org/CGEM.ang.html) alternative splicing analysis tools, obtaining lowess normalized log_2 ratios. General gene expression values represent the average of log_2 ratios for all the probes of a locus. Statistical analyses were carried out with Linear Models for Microarray Data[360,361]. The background correction method used in the analysis was Normexp[362]. Locally weighted linear regression (LOWESS) analysis was used as a normalization method[363].

13. HUMAN JUNCTION ARRAY (HJAY)

13.1. RNA LABELING AND HYBRIDIZATION

Affymetrix Human Junction Arrays (HJAY) were hybridized by GenoSplice Technology according to Affymetrix (Santa Clara, USA) labelling and hybridization recommendations. Microarrays were hybridized, washed and scanned using Affymetrix instruments. Total RNAs RIN values were between 9.8 and 10.0 (average: 9.98). Raw data are controlled with Expression console (Affymetrix).

13.2. MICROARRAY DATA ANALYSIS

Affymetrix HJAY dataset analysis was performed by GenoSplice technology. Data were normalized using quantile normalization. Background corrections were made with antigenomic probes and probes were selected according to their %GC, cross-hybridization status and potential overlap with repeat region as previously described[364,365]. Only probes targeting exons and exon-exon junctions annotated from FAST DB® transcripts (release fastdb_2013_1) were selected[366,367]. Only probes with a DABG P value ≤0.05 in at least half of the arrays were considered for statistical analysis[364,365]. Only genes expressed in at least one compared condition were analyzed. To be considered to be expressed, the DABG p-value was selected to be ≤0.05 for at least half of the gene probes. Student's t-test was performed to compare gene intensities between experimental conditions. Genes were considered significantly regulated when fold-change was ≥1.5 and p-value ≤0.05 (unadjusted p-value). Analysis at the splicing level was first performed taking into account only exon probes in order to potentially detect new alternative events that could be differentially regulated (i.e. without taking into account exon-exon junction probes). Analysis at the splicing level was also performed by taking into account exon-exon junction probes using the FAST DB® splicing patterns annotation (i.e. for each gene, all possible splicing patterns were defined and analyzed). Expression and alternative splicing analyses were performed using unpaired Student's t-test on the splicing-index as previously described[364,365]. Results were considered statistically significant for unadjusted p-values ≤ 0.05 and fold-changes ≥ 1.5 for alternative splicing analysis; and unadjusted p-values ≤ 0.05 and fold-changes ≥ 2.0 for expression analysis.

14. ISOBARIC TAG FOR RELATIVE AND ABSOLUTE QUANTITAION (iTRAQ)

Pellets obtained from control and CUGBP1 depleted SK-Mel-103 and UACC-62 cells were washed 3 times with cold PBS containing protease inhibitors (Halt™ Protease & Phosphatase inhibitor cocktail, EDTA-free) and resuspended in 500 µL of ice-cold RIPA lysis buffer (150 mM NaCl, 1.0% NP-40, 0.5% sodium deoxycholate, 0.1% SDS, 1 mM EDTA, 1 mM EGTA, 50 mM Tris, pH 8.0 plus protease inhibitors) and 0.1% Benzonase Nuclease (Novagen). Samples were vortexed, sonicated and clarified by centrifugation at 4°C for 15 minutes. The supernatants containing the protein fraction were collected and cleaned-up by methanol-chloroform precipitation. Pellets were dissolved in 7M urea 2M tiourea. Protein concentration was determined using the Pierce 660nm Protein Assay (Bio-Rad) using BSA as standard. Proteins were digested using the FASP protocol. Peptides were labeled with 4-plex iTRAQ reagents and samples were pooled. Then, the complex mixture was subjected to IEF fractionation. The resulting fractions were separated by on-line nano-LC and analyzed by electrospray MS/MS using a LTQ Orbitrap Velos mass spectrometer (Thermo Scientific). Raw files were searched against UniProtKB / Swiss-Prot human database (20,584 entries) using SequestHT as the search engine through the Proteome Discoverer (Thermo Scientific) software. Results were validated with Percolator and filtered to 1% FDR (peptide-level).

15. GSEA, NETWORKS, HEATMAPS and VENN DIAGRAMS

Significantly enriched ($p \leq 0.05$) GO Biological Processes (database 02.10.2015) between melanoma cells and primary melanocytes were identified by using Cytoscape v3.2.1[368] and the ClueGO v2.1.7 plug-in[369].

Gene Set Enrichment Analysis (GSEA) was performed using annotations from the Reactome pathways. Genes were ranked using the t statistic. After Kolmogorov-Smirnoff correction for multiple testing, only those pathways bearing a FDR <0.25 were considered significant[370]. Heatmap and correlation graphs for RNA and protein levels were created by Perseus v1.5.1.6. Protein networks were created by using Search Tool for the Retrieval of Interacting Genes/Proteins (STRING)[371] and Cytoscape v3.2.1. Venn diagrams were created by using online tools Venny v2.0[372] and jvenn[373].

16. STATISTICAL ANALYSES

CUGBP1 expression in human benign and malignant melanocytic lesions and cell proliferation curves were evaluated by two-tailed unpaired Student´s t-test. In all the cases $p<0.05$ was considered significant. CUGBP1 and DEK co-expression in human melanoma specimens was evaluated by Pearson test. R stands for Pearson correlation value.

VI.

RESULTS

RESULTADOS

1. GLOBAL ANALYSIS OF RNA BINDING PROTEINS IN MELANOMA CELLS

A recent census study has reported 692 mRNA binding proteins (mRBP) in human cells[218]. Given the potential of these factors to exert broad effects on gene expression, we decided to perform an unbiased analysis of their mutational status and allelic content in melanoma tumors. To this end, cBioPortal was used to mine the Cancer Genome Atlas (TCGA), which contains 478 annotated human melanoma specimens[374]. As summarized in Figure 7, none of the mRBPs appeared to be a frequent target of genomic alterations in this disease (see Table S1 for full detail on the individual genes and alteration rate).

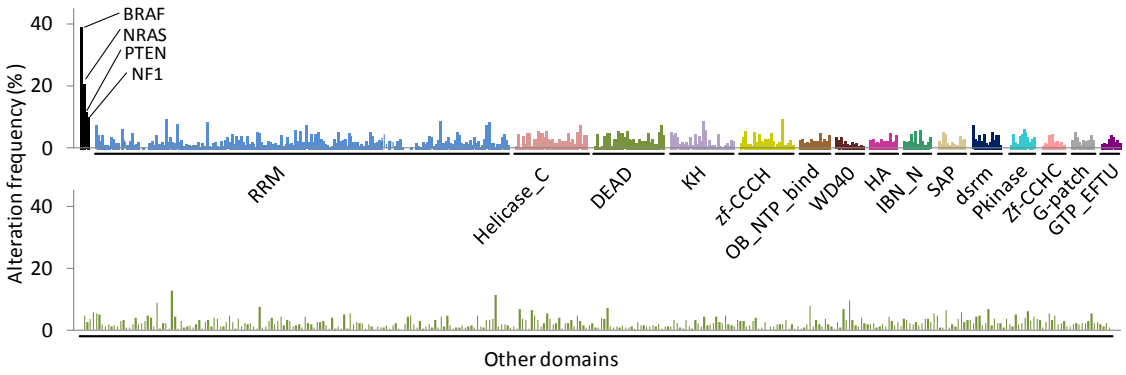

Figure 7: Genomic landscape of mRNA binding proteins in human melanoma. Shown is the frequency (%) of melanoma patients with mutations and/or copy number alterations (deletions or amplifications) in all known mRNA binding proteins (mRBPs, n=692), classified according to their RNA binding domains (Pfam nomenclature). Data was retrieved from the melanoma TCGA database (n=478 specimens) using cBioPortal and manual curation. *BRAF, NRAS* and *NF1* are included as references for classical melanoma-associated oncogenes, and *PTEN* as a classical melanoma-associated tumor suppression gene.

Therefore, we chose to perform comparative analyses of transcriptomic profiles of melanoma cell lines versus normal melanocytes as an initial strategy to screen for potential novel contributors to melanoma progression. While the large set of mRBPs listed in Figure 7 were extracted from computational analyses that mined for factors that contain bona fide RNA binding domains (RBDs)[218], only a fraction of these genes have been functionally addressed in cancer cells. Therefore, to increase the likelihood of identifying physiologically-relevant of melanoma genes, we chose to focus on RBPs with mechanistic evidence for key roles on mRNA polyadenylation, maturation, stability and/or translational control (n=180). These included mainly mRBPs, as well as factors known to recognize snRNAs, snoRNA, ncRNA and tRNA, for a more global analysis of the RNA binding family (see Table S2 for detailed information on the selected genes). A series of 302 cell signaling, proliferation, adhesion and apoptosis modulators with reported cancer-associated posttranscriptional gene regulation were also included in the array (Figure 8A) to guide in subsequent functional studies of identified RNA binding candidates (a strategy we have previously validated for gene discovery in Hodgkin lymphoma cells and in other systems)[375]. Total RNA was isolated from the well characterized SK-Mel-19 and SK-Mel-103 melanoma cell lines, used as

representative examples of cases bearing the *BRAF*^{V600E} and *NRAS*^{Q61R} characteristic mutations in this disease (see Table 6)[376]. Hybridizations were performed using pools of primary melanocytes as a reference (see Methods section for additional detail). Gene Ontology (GO) functional term enrichment analyses were performed by Cytoscape and the ClueGO plug-in for maximum p value of 0.05. Interestingly, we identified a selective deregulation of 29% (50/180) of RBPs in melanoma cells (Figure 8B and Table S3) with enriched functions in RNA splicing and spliceosome formation, ribonucleoprotein (RNP) complex assembly, mRNA 3'end processing and termination of RNA transcription (see gene clusters 1-22 in Figure 8C). Among the cancer-associated genes we identified changes in 19.5% of the analyzed cases (59/302) which intriguingly clustered preferentially around cell cycle, chromosome organization and mitotic cell cycle checkpoints (clusters 23-75 in Figure 8C; see Table S4 for details of the specific GO terms and the genes on each cluster). We then set to investigate these 75 GO clusters for candidate selection.

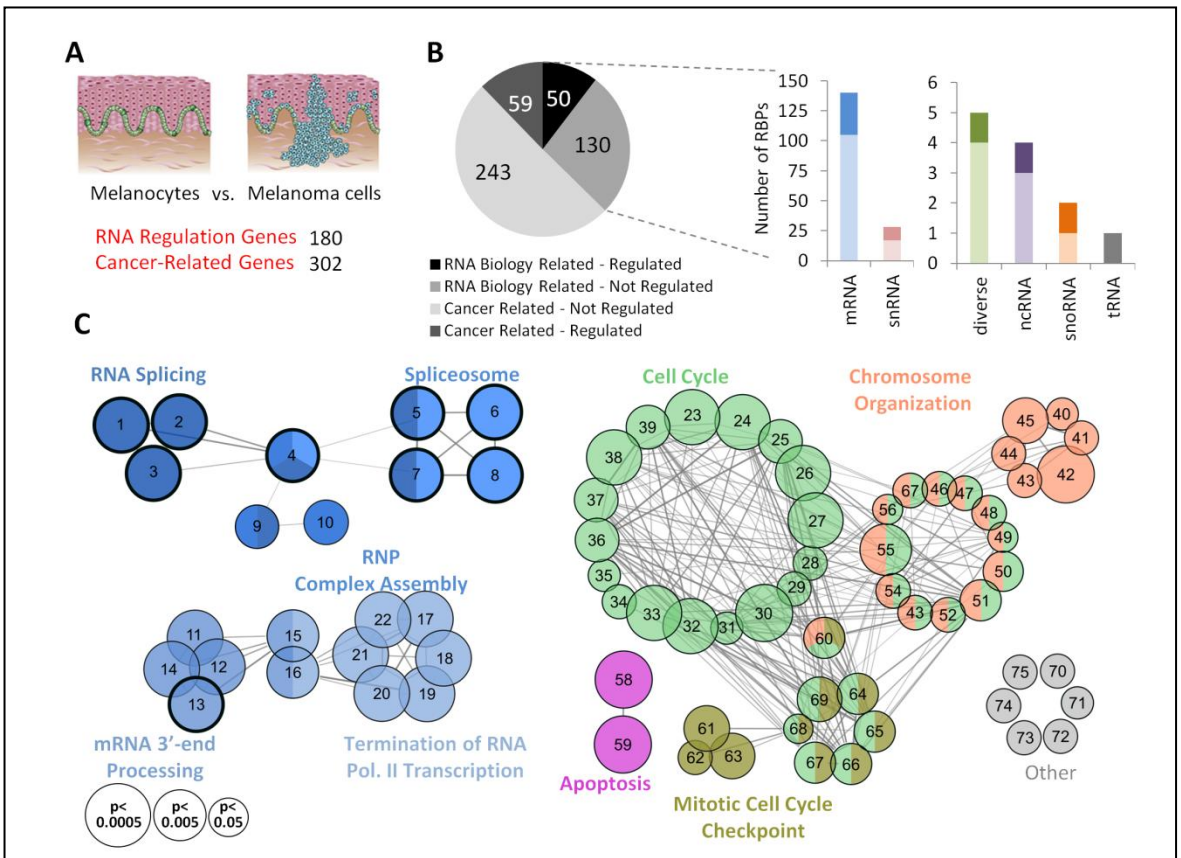

Figure 8: Global analysis of RBPs and post-transcriptionally regulated cancer-associated genes in melanoma vs. normal melanocytes. A, Schematic representation of experimental design. **B,** Differentially expressed cancer- and RNA biology related genes in melanoma cells compared to the primary melanocytes with specific detail on changes in the indicated RBP families. Dark colors represent differential regulation. **C,** Network of enriched GO terms in SK-Mel-19 and SK-Mel-103 cell lines. Size of the nodes reversely reflects the statistical significance of the terms ($p<0.0005$, $p<0.005$ or $p<0.05$). Bold bordered terms refer to GO terms containing CUGBP1. mRNA: messenger RNA, snRNA: small nuclear RNA, ncRNA: non-coding RNA, snoRNA: small nucleolar RNA, tRNA: transfer RNA.

2. CUGBP1 IS AN EARLY-INDUCED RBP IN MELANOMA CELL LINES AND MALIGNANT TISSUES

Given the inherent pleiotropic nature of RBPs, we considered essential a detailed validation that integrated histological assessment of expression in clinical biopsies, functional studies in cultured cells and in animal models, and genome-wide transcriptomic/proteomic analyses for the identification of direct targets. Given the challenge of performing such a comprehensive characterization for each of the 50 RBPs described above in Figure 8B (Table S2), an additional filtering step was performed with the following criteria: (i) no reported link to melanoma, (ii) participation in the melanoma-enriched GO-terms associated with RNA metabolism (i.e. networks labeled in blue in Figure 8C), and (iii) relationship to the cancer-related categories with a particular deregulation in the melanoma cell lines tested (Clusters 23-75 in Figure 8C). Among the top genes in this list (Table S4) we chose to focus on CELF1 (CUG repeat binding protein, Elav-like family member 1), also referred to as CUGBP1 for its ability to bind GU-rich elements (GREs) in target mRNAs. As mentioned in the introduction, CUGBP1 has the attractive feature of being able to act on pre-mRNAs (modulating alternative splicing) and on mature mRNAs, controlling translation and transcript stability. CUGBP1 is best known for its contribution to post-transcriptional events in muscle differentiation and myotonic dystrophy. Nevertheless, a few studies in gastric carcinoma[339], hepatocellular carcinoma[338] and oesophageal[340] carcinoma have reported a requirement of CUGBP1 for proper tumor cell proliferation. No common CUGBP1 cellular targets have been identified from these studies (see additional detail below), offering the possibility of gene discovery.

Our customized microarray revealed an increased *CUGBP1* mRNA expression melanoma cell lines compared to primary melanocytes. To start defining the impact of this deregulation at the protein level, total cell extracts were prepared from a panel of melanoma cell lines that recapitulate main genetic alterations in this disease (see *BRAF, NRAS, PTEN* and *p53* status in Table 6 in Materials and Methods section). Immunoblots were then performed using as a reference normal skin cells (including various independent isolates of primary melanocytes and as well as fibroblasts and keratinocytes). As shown in Figure 9A, all melanoma cells displayed a marked upregulation of CUGBP1 compared to normal controls. Of note, this differential expression was not detected for CUGBP2, another member of the CUG binding protein family (Figure 9A). Additional comparative analyses were performed with respect to the well known Mel-STV immortalized melanocytes[377]. Interestingly, Mel-STV, which has been used in the field as surrogates for early transformation events[377,378] showed also higher CUGBP1 than normal melanocytes, to levels similar to melanoma cell lines (Figure 9B). These results therefore, suggest an early activation of CUGBP1 during melanoma progression. To confirm this hypothesis, a retrospective series of benign nevi (n=47) and clinically annotated melanoma (n=138) paraffin-embedded biopsies (see Methods for additional

details on the number of primary and metastatic specimens analyzed) were processed by immunohistochemistry, using a 0-2 scoring for CUGBP1 on the basis of negative, intermediate or high expression (Figure 9C; see the Methods section). As summarized in Figures 9D and 9E, a significant enrichment for high expression of CUGBP1 was found in malignant lesions ($p<0.005$), particularly on vertical growth phase (VGP) cutaneous melanomas (see examples in Figure 9E). Together, these results identify CUGBP1 as a new RBP with an early induction during melanoma progression.

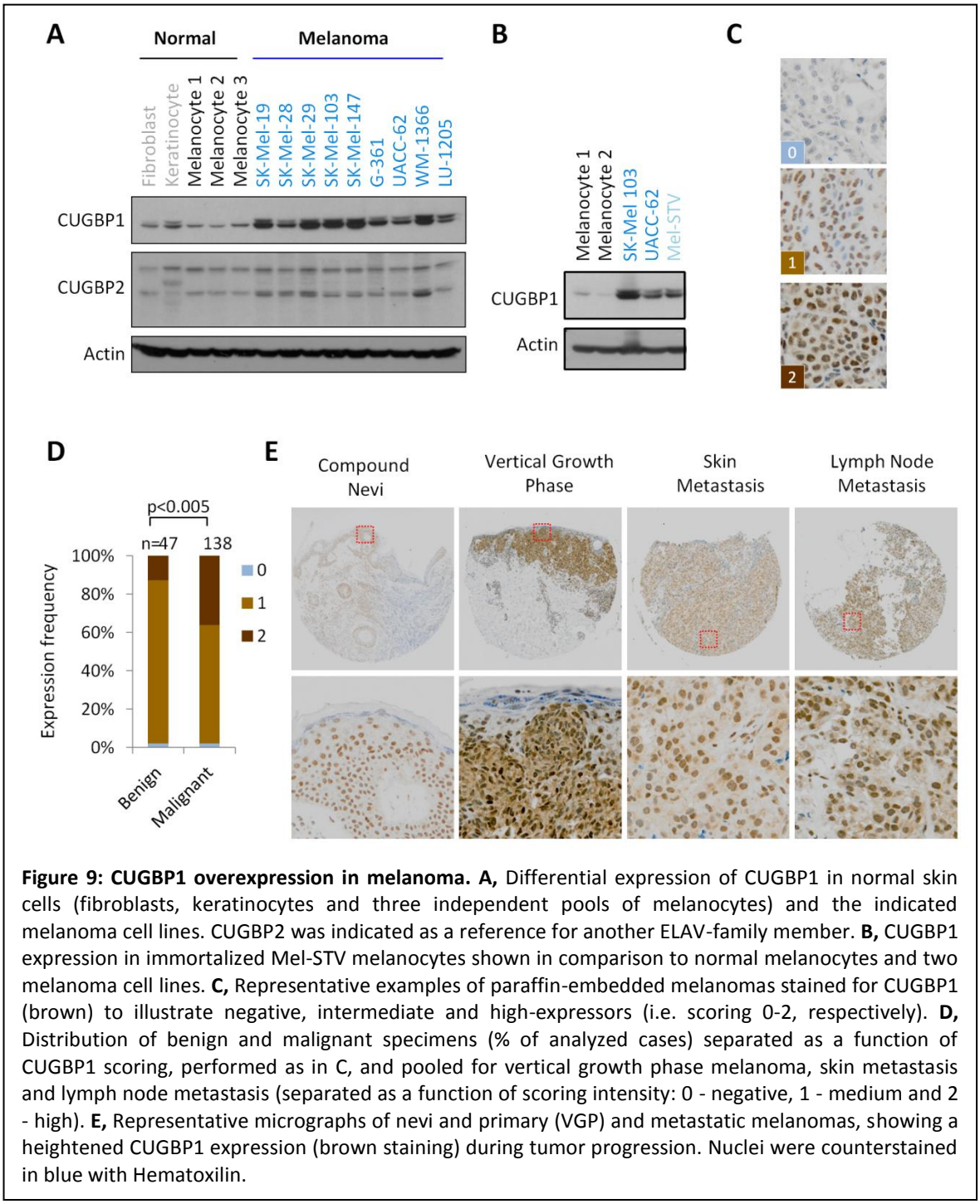

Figure 9: CUGBP1 overexpression in melanoma. A, Differential expression of CUGBP1 in normal skin cells (fibroblasts, keratinocytes and three independent pools of melanocytes) and the indicated melanoma cell lines. CUGBP2 was indicated as a reference for another ELAV-family member. **B,** CUGBP1 expression in immortalized Mel-STV melanocytes shown in comparison to normal melanocytes and two melanoma cell lines. **C,** Representative examples of paraffin-embedded melanomas stained for CUGBP1 (brown) to illustrate negative, intermediate and high-expressors (i.e. scoring 0-2, respectively). **D,** Distribution of benign and malignant specimens (% of analyzed cases) separated as a function of CUGBP1 scoring, performed as in C, and pooled for vertical growth phase melanoma, skin metastasis and lymph node metastasis (separated as a function of scoring intensity: 0 - negative, 1 - medium and 2 - high). **E,** Representative micrographs of nevi and primary (VGP) and metastatic melanomas, showing a heightened CUGBP1 expression (brown staining) during tumor progression. Nuclei were counterstained in blue with Hematoxilin.

3. DEFECTIVE PROLIFERATIVE CAPACITY OF MELANOMA CELLS DEPLETED FOR CUGBP1

To deplete CUGBP1 and define functional impact in melanoma cells, we used a lentiviral-based gene transfer of two previously reported short hairpin interfering RNAs (shRNA)[344]. These constructs, allowing for puromycin-based selection of infected cells, were used to transduce SK-Mel-103 (NRAS^{Q61R} mutated) and UACC-62 (BRAF^{V600E}) (see downregulation efficacy in Figure 10A). Cell proliferation was monitored at different time points after infection by DAPI-based nuclei count (see Methods). Both cell lines responded to CUGBP1 depletion with a marked inhibition of cell proliferation (Figure 10B). To further characterize the effect of CUGBP1 on proliferation, SK-Mel-103 cells were infected with control or CUGBP1-shRNA expressing lentiviruses. Two days after puromycin selection, cells were synchronized at G1/S phase of the cell cycle by a standard thymidine block. Propidium iodide staining was then performed for assessment of DNA content by flow cytometry. While control shRNA-cells recovered a normal proliferation within 8h after releasing from the block, CUGBP1-shRNA cells showed a significant G1 phase accumulation, with a concomitant reduction in S-phase proliferating cells (see flow cytometry profiles in Figure 10C and quantification in Figure 10D).

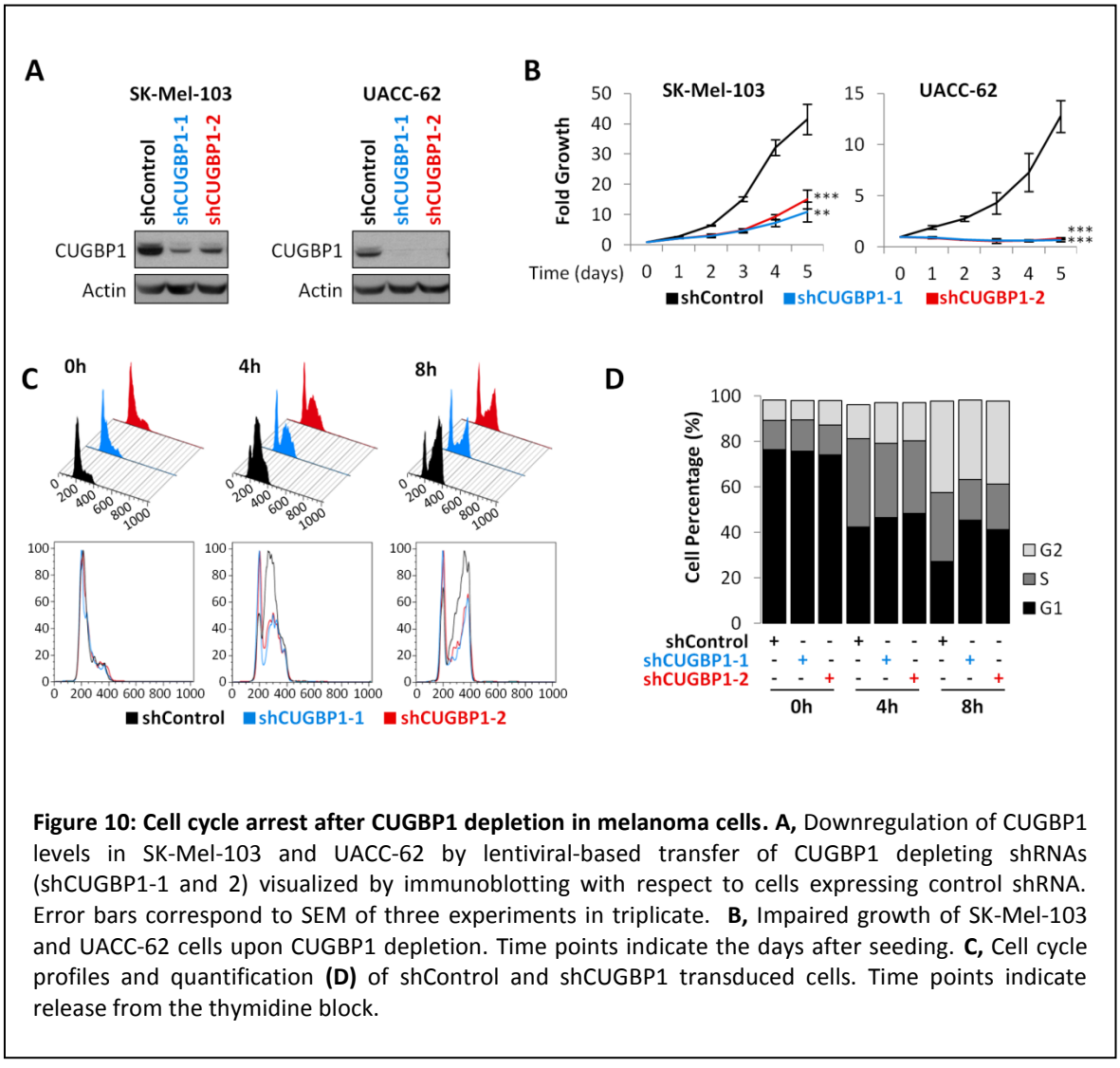

Figure 10: Cell cycle arrest after CUGBP1 depletion in melanoma cells. A, Downregulation of CUGBP1 levels in SK-Mel-103 and UACC-62 by lentiviral-based transfer of CUGBP1 depleting shRNAs (shCUGBP1-1 and 2) visualized by immunoblotting with respect to cells expressing control shRNA. Error bars correspond to SEM of three experiments in triplicate. **B,** Impaired growth of SK-Mel-103 and UACC-62 cells upon CUGBP1 depletion. Time points indicate the days after seeding. **C,** Cell cycle profiles and quantification **(D)** of shControl and shCUGBP1 transduced cells. Time points indicate release from the thymidine block.

To determine whether impaired cell proliferation is a general feature of CUGBP1-depleted melanoma cells, long-term colony formation assays were performed in panel of 8 independent cell lines (n=8, see CUGBP1 downregulation in Figure 11A). Interestingly, albeit with different efficacies, all melanoma cell lines tested responded to CUGBP1 shRNA with an inhibited proliferative capacity (see Figure 11B for crystal violet-stained colonies 10-14 days after seeding and Figure 11C for

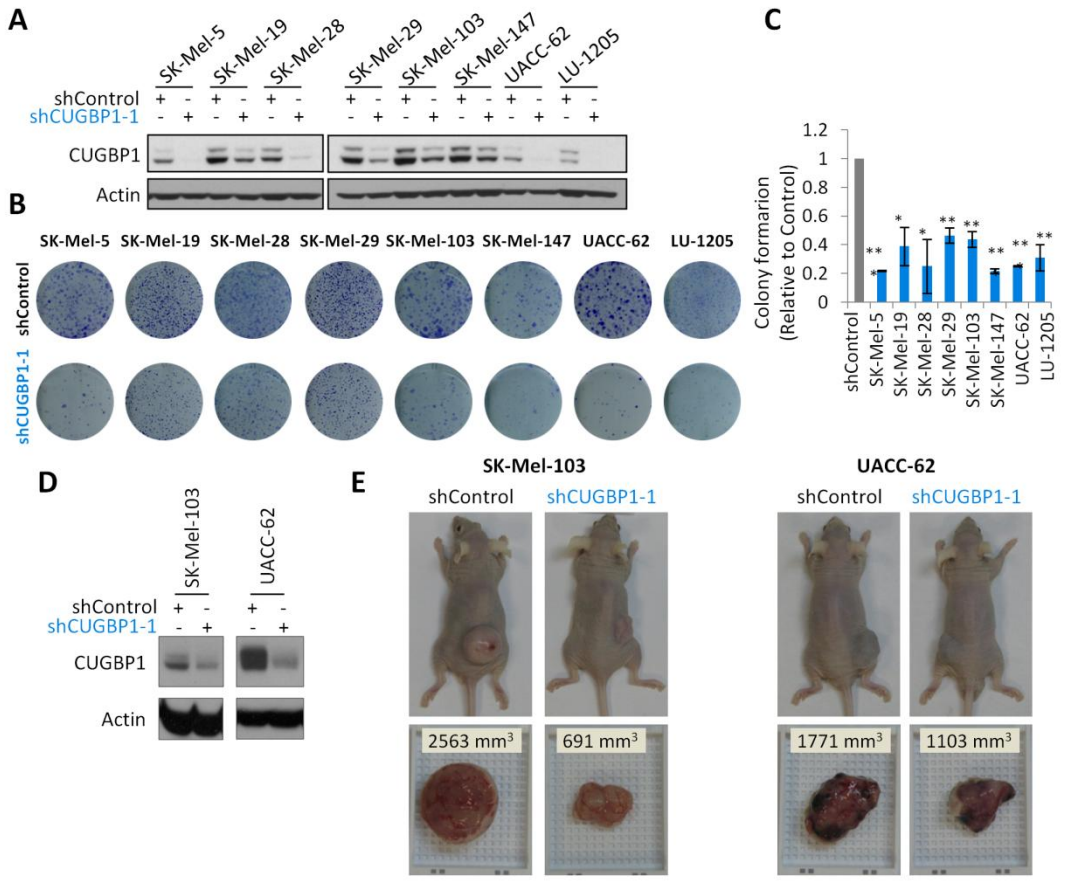

Figure 11: Impaired proliferative potential of CUGBP1-depleted melanoma cells. A, Downregulation of CUGBP1 by lentiviral-mediated transduction of CUGBP1 shRNA (1) in the indicated cell lines, defined by immunoblotting 2 days after puromycin selection of positively-transduced cells. **B,** Colony formation of the cell populations in (A) determined by crystal violet 12 days after cell seeding. **C,** Quantification of inhibited colony formation activity. Data are represented as the ratio of inhibition with respect to control shRNA-transduced cells (for simplicity here shown as a gray bar only for SK-Mel-5). Error bars correspond to SEM of two experiments in duplicates. **D, E,** Depletion of CUGBP1 in the indicated cell lines (D) for subcutaneous implantation in nude mice (E). Shown are photographs and images of excised lesions generated by the indicated cell populations showing the impact of sustained CUGBP1 depletion.

quantification). To further define the physiological relevance of these results, control- and CUGBP1-depleted melanoma cells (SK-Mel-103 or UACC-62) were injected subcutaneously into the flanks of 7 week-old athymic nude (*Crl:NU(NCr)-Foxn1^{nu}*) female mice. While some CUGBP1-depleted lesions were observed with a marked reduction in growth (Figures 11D and 11E), most tumors recovered CUGBP1 expression which may indicate that tumors could not be formed without CUGBP1. Thus, post-mortem analyses (protein immunoblotting and immunohistochemical

stainings) revealed that intriguingly, actively growing melanoma xenografts selected for cells that retained CUGBP1 expression (data not shown). Together, these *in vitro* and *in vivo* results support a relevant impact of CUGBP1 on the tumorigenic potential of melanoma cells.

4. KNOWN CUGBP1 TARGETS ARE NOT SHARED BY MELANOMA

Next, we interrogated CUGBP1 targets that may underline the inhibited proliferative capacity of melanoma cells when this factor is depleted. As indicated in the introduction, one the main functions of CUGBP1 is the regulation of alternative splicing[303,305]. Characteristically-regulated CUGBP1 splicing targets are *INSR*[302-304], *SERCA1*[305], *FXR1*[305], *FAM188A*[305], *ANK2*[305], *ACTN1*[306,307], *MEF2A*[306,307] and *PPFIBP1*[306,307], among others (see Figures 12A and 12B for the corresponding exon

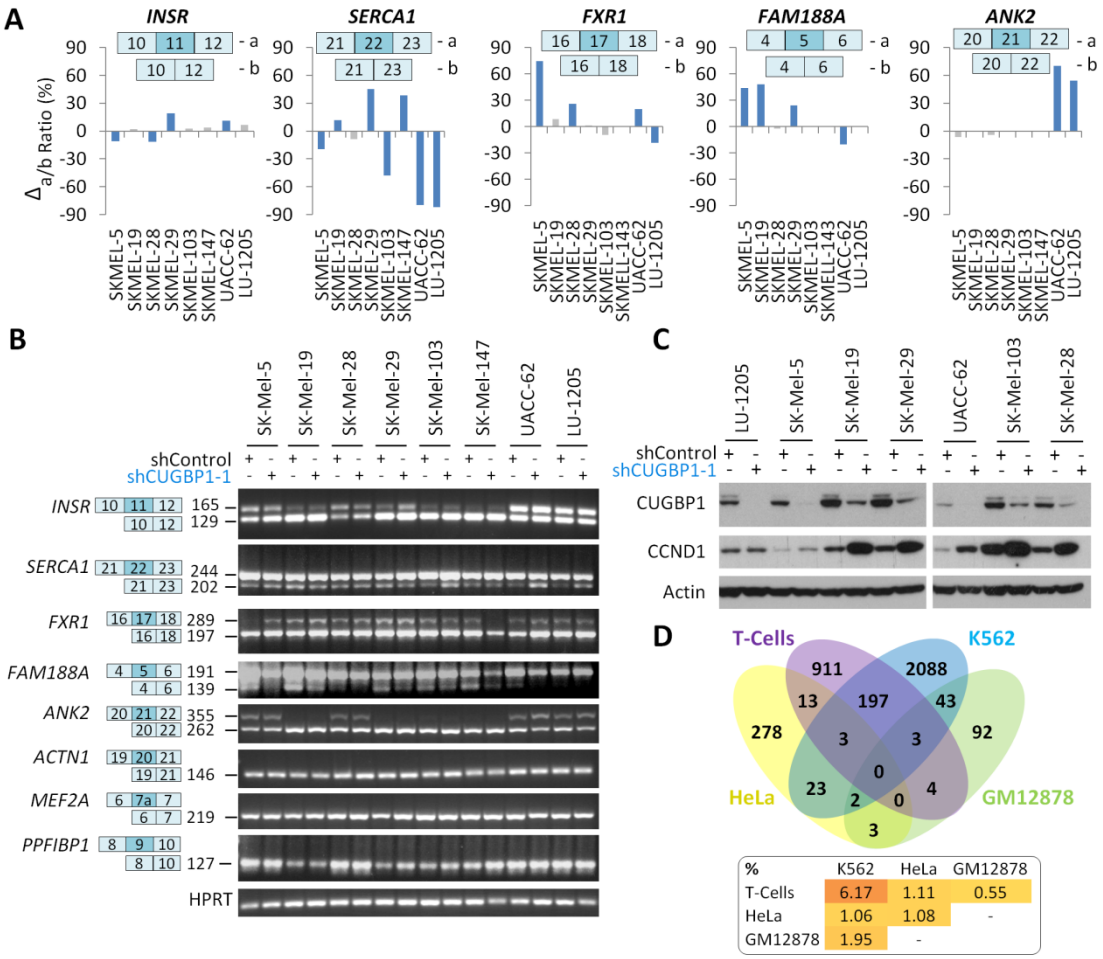

Figure 12: Known CUGBP1 targets are not shared by melanoma cells. A, Ratio of splicing variants of the indicated genes in melanoma cell lines transduced with control or CUGBP1-1 shRNAs. Data correspond to quantification of semi-quantitative PCRs (with concrete examples in panel **B,** visualized after electrophoretic separation in agarose gels). **C,** CCND1 protein levels in the indicated populations of melanoma cells, detected by immunoblotting. **D,** Venn diagrams to assess the overlap of CUGBP1 binding targets in the indicated cell lines. The table below lists this overlap as percentages.

inclusion/exclusion events). Therefore, a panel of 8 melanoma cell lines was transduced with control or shCUGBP1-1 for isoform analysis by semi quantitative PCR. Spliced variants of *INSR,*

SERCA1, FXR1, FAM188A, and *ANK2* were found in the melanoma cell lines tested, but however, no consistent changes in isoform ratio were observed after CUGBP1 depletion (see quantifications in Figure 12A and representative examples of electrophoretic analyses in Figure 12B). For *ACTN1, MEF2A and PPFIBP1*, only one isoform was detected by RT-PCR, with no obvious changes in expression in CUGPB1-depleted cells (Figure 12B). Similar lack of selective changes in splicing variants was detected for other tumor cell types, indicating that these factors may not be frequent downstream targets of CUGBP1 (Figures 19A and 19B). We then tested cyclin D1 (CCND1) for its known roles in cell cycle control, but also an example of a gene which can be either upregulated or downregulated by CUGBP1 depending on the system (i.e. in HepG2 hepatocellular carcinoma[338] and MGC-803 gastric cancer[339] cell lines, respectively). As shown in Figure 12C, most melanoma cells tested responded to CUGBP1 depletion by increasing CCND1 protein levels, a feature consistent with delayed S-phase progression[379]. However, these changes in CCND1 were variable and indeed not consistent among cell lines (see for example negligible changes in LU-1205, Figure 12C). We therefore chose to pursue a genome-wide characterization of CUGBP1 targets in melanoma.

Gene sets corresponding to the two RNA immunoprecipitation (RIP)-based assessment of CUGBP1 targets reported to our knowledge in human cells (i.e, in HeLa[284] and in T-cells[327]) were then mined to identify commonly modulated factors that could be used as a guideline in melanoma. A search in the ENCODE project[331] was also performed, identifying two additional cell lines, K562 (myelogenous leukemia) and GM12878 (an EBV-transformed B-cells), were there unpublished, but available data for CUGBP1 binding. Intriguingly, maximum overlap among these data sets was less than 6% (in T cells vs. K562 cells, Figure 12D). Notably, no gene was found to be shared by these 4 studies (Figure 12D). Together, these results further emphasize the need for a comprehensive unbiased search for novel CUGBP1 targets in melanoma.

5. TRANSCRIPTOMIC AND PROTEOMIC ANALYSES IDENTIFY CUGBP1 REGULATED GENES

As mentioned before CUGBP1 is an RNA binding protein with wide range of functions, ranging from the modulation of splicing[302-307], to transcriptional activation/repression[285,309,313,314,322-325] or mRNA stability modulation[284,327-329]. In order to explore all these functions we used two high throughput systems: (i) Human Junction Array (HJAY), which allows to monitor both changes in mRNA levels and alternative splicing events by using a high coverage of probes for the detection of constitutive exons and retained/excluded exons (5.4 million probes), and (ii) isobaric tags for relative and absolute quantification (iTRAQ) for global assessment of proteomic profiles. As model systems, we used SK-Mel-103 and UACC-62 melanoma cell lines, which were processed for RNA and total protein isolation 4 days after infection with lentiviral-driven control or CUGBP1 shRNA

(i.e. time points before cell cycle arrest). HJAY identified 1361 and 698 altered genes by CUGBP1 depletion in SK-Mel-103 and UACC-62, respectively (Figure 13A). Of those changes, the vast majority (96.4 and 95%) corresponded to differential gene expression, with just a minority of factors with additional alteration of splicing sites (Figure 13B). Therefore, we focused on iTRAQ proteomic analyses, which to our knowledge have not been previously performed for CUGBP1 targets.

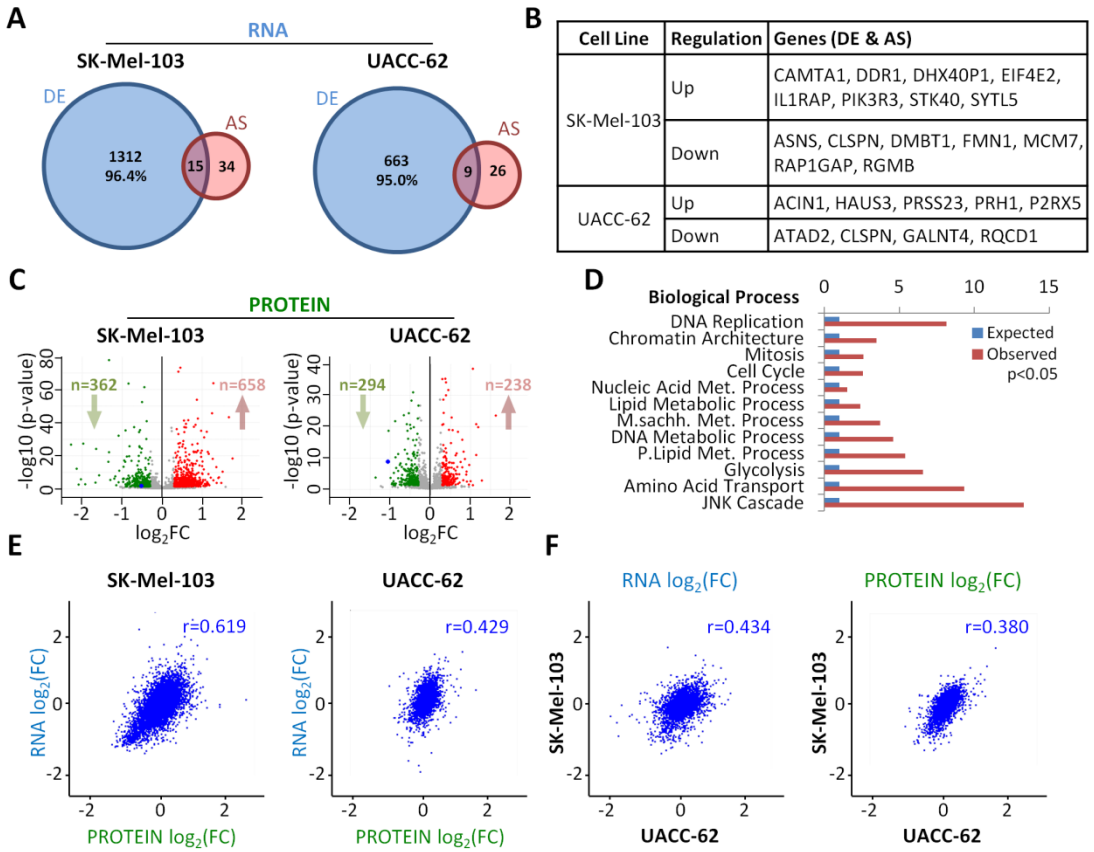

Cell Line	Regulation	Genes (DE & AS)
SK-Mel-103	Up	CAMTA1, DDR1, DHX40P1, EIF4E2, IL1RAP, PIK3R3, STK40, SYTL5
	Down	ASNS, CLSPN, DMBT1, FMN1, MCM7, RAP1GAP, RGMB
UACC-62	Up	ACIN1, HAUS3, PRSS23, PRH1, P2RX5
	Down	ATAD2, CLSPN, GALNT4, RQCD1

Figure 13: Genome-wide transcriptomic and proteomic analysis (HJAY and iTRAQ LC-MS/MS, respectively) for the identification of CUGBP1-regulated cellular targets. A, Venn diagrams showing differentially expressed (DE) and alternatively spliced (AS) genes identified by HJAY in SK-Mel-103 and UACC-62 cells upon shCUGBP1-1 transduction. **B,** Genes undergoing differential mRNA expression and splicing regulation in CUGBP1 shRNA melanoma cells. **C,** Volcano plots showing up- and downregulated proteins identified by iTRAQ LC-MS/MS analyses in SK-Mel-103 and UACC-62 cells upon shCUGBP1-1 transduction. Factors indicated in green and red are those with significant changes in protein expression. **D,** Enriched biological processes identified from significant changes in the proteome ($p<0.05$) of the indicated cell lines defined by monitoring Panther database. **E,** Correlation scatter plots of global changes in RNA and protein levels upon CUGBP1 depletion in SK-Mel-103 and UACC-62 melanoma cell lines. **F,** Overlap in RNA and protein level changes between these two cell lines.

Setting proteomic changes to be significant for $p<0.05$ and 1.5-fold deviation with respect to shRNA controls we identified 1020 and 532 CUGBP1-regulated proteins in SK-Mel-103 and UACC-62 cell lines, respectively (see Volcano plots in Figure 13C). Enrichment analyses using Panther databases revealed a preferential enrichment for biological processes related to DNA replication, chromatin architecture, mitosis, cell cycle and various stress-related programmes (Figure 13D). Of note, these differentially expressed proteins were found to reflect changes in mRNA expression (Figure 13E), with a significant overlap in the two cell lines tested (RNA, r=0.43; and protein, r=0.38; Figure 13F). Together, these results support a broad spectrum of proteins whose expression is modulated by CUGBP1 in melanoma as a result of defining mRNA levels, rather than acting as a regulator of alternative splicing.

6. IDENTIFICATION OF CUGBP1-REGULATED NETWORKS

To further address CUGBP1 targets in melanoma, transcriptomic and proteomic datasets reported above were subjected to gene set enrichment analyses through Reactome databases for pathway (network) identification (Figures 14A and 14B). DNA synthesis/replication and cell cycle related pathways were downregulated in both cell lines at both RNA and protein levels (Figure 14A). Interestingly, the impact of CUGBP1 in these cellular processes appeared to be broad, but selective (i.e. only a fraction of genes in each functional category was significantly deregulated by CUGBP1 shRNA (Figure 14B). To identify key hubs in these processes, functional networks were then built using the STRING database with the Cytoscape v3.2.1 for visualization. As shown in Figure 14C a series of highly interconnected proteins were revealed by this analysis to be deregulated both at the protein and RNA levels (mostly by inhibition in expression, green columns) in the two cell lines (the direction and magnitude of these changes are indicated in the insets of Figure 14C as columns labeled A-D). Validating this approach, CCNB1 and POLA1, two genes required for cell cycle progression and reported as CUGBP1 targets in hepatocellular[338] carcinomas, gastric carcinomas[339] and myeloid leukemia[331] (unpublished data), respectively, were also found modulated by CUGBP1 in both melanoma cell lines. Nevertheless, the rest of the factors and network interactions uncovered by our comprehensive transcriptomic and proteomic analyses had not been previously linked to CUGBP1, further emphasizing the significance of our results. Focusing on newly-identified cell cycle and DNA synthesis/replication networks that could underlie the phenotype of CUGBP1-depleted melanoma cells (Figure 10), our analyses revealed various MCM proteins (MCM-2, -3, -4, -5, -6, -7) as well as other well known DNA synthesis and replication factors such as RPA-2 and RPA-3 (Figure 14C). Other downregulated genes included FANCA, FAND2 and FANC1 (Figure 14C), likely reflecting DNA damage associated to replicative stress. An additional gene unknown to be modulated by CUGBP1 and identified in our analysis was the chromatin remodeler DEK (Figure 14C), an oncogene upregulated in multiple tumor types[165-170], including

melanoma[185], where we had previously demonstrated critical for cell cycle progression and cell survival[185]. In summary, these studies further expand our knowledge on CUGBP1 roles in the regulation of key cancer-associated signaling networks.

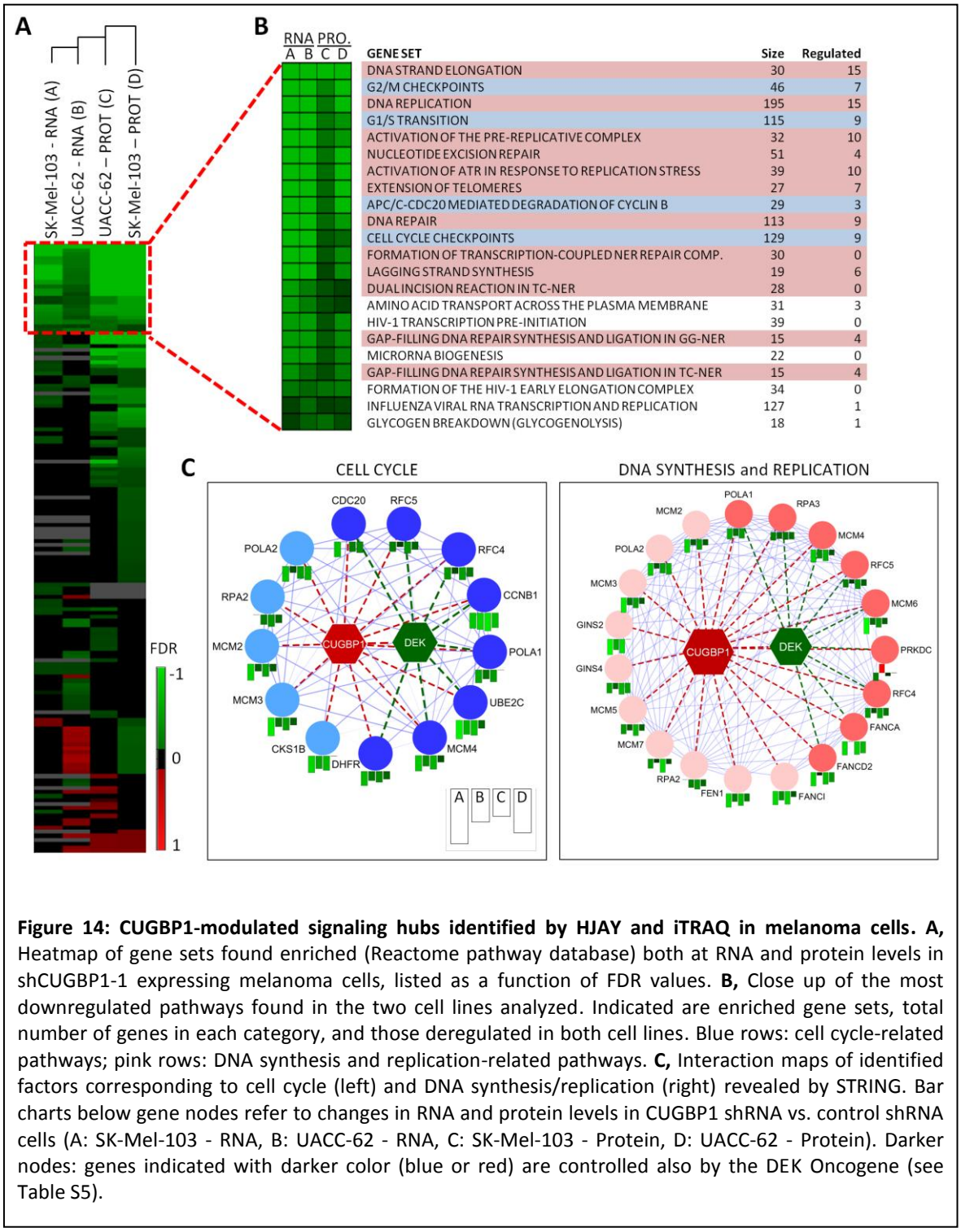

Figure 14: CUGBP1-modulated signaling hubs identified by HJAY and iTRAQ in melanoma cells. A, Heatmap of gene sets found enriched (Reactome pathway database) both at RNA and protein levels in shCUGBP1-1 expressing melanoma cells, listed as a function of FDR values. **B,** Close up of the most downregulated pathways found in the two cell lines analyzed. Indicated are enriched gene sets, total number of genes in each category, and those deregulated in both cell lines. Blue rows: cell cycle-related pathways; pink rows: DNA synthesis and replication-related pathways. **C,** Interaction maps of identified factors corresponding to cell cycle (left) and DNA synthesis/replication (right) revealed by STRING. Bar charts below gene nodes refer to changes in RNA and protein levels in CUGBP1 shRNA vs. control shRNA cells (A: SK-Mel-103 - RNA, B: UACC-62 - RNA, C: SK-Mel-103 - Protein, D: UACC-62 - Protein). Darker nodes: genes indicated with darker color (blue or red) are controlled also by the DEK Oncogene (see Table S5).

7. RIP-SEQ ASSAYS IDENTIFY NOVEL DIRECT CUGBP1 TARGETS IN MELANOMA

Next, RNA immunoprecipitation followed by sequencing of retrieved transcripts (RIP-seq) was performed to determine which of the genes whose expression is modulated by CUGBP1 are indeed direct targets of this protein. To this end, RNAs binding to the endogenous CUGBP1 were precipitated after crosslinking with a CUGBP1 antibody in SK-Mel-103 and UACC-62 (three biological replicates). This was followed by RNA-Seq with 20 million reads per sample, using inputs as a reference. Validating this approach, we identified higher number of reads in CUGBP1 IP samples compared to input at the 3'UTR of CCND1 (see an example for SK-Mel-103 in Figure 15A visualized on the UCSC genome browser), which was validated by RIP and qPCR in additional melanoma cell lines (Figure 15B). Factors with FDR value smaller than 0.05 (n=2024) were then compared to the reported RIP studies for HeLa[284] and T-cells[327] mentioned above as well as the candidates we had identified as CUGBP1 targets in K562 and GM12878 in unpublished data from ENCODE. The overlap with these datasets was rather low: with only 8.5% and 13.7% of targets shared with K562 and T-cells and a global minimal binding conservation (Figure 15C, Table S6). Thus, we uncovered transcripts of 1197 (out of 2024) unreported CUGBP1-bound genes in melanoma (Figure 15C). Peak calling was then performed with the Piranha software[354] to identify regions of statistically significant read enrichment. In order to minimize false positive results by using a large bin size, instead a bin size of 20 was used considering that canonical CUGBP1 binding sequences are typically 11-mers[284]. The distribution of binding regions on target mRNA indicated that CUGBP1 bound the majority its targets (59%) on their 3'UTRs (Figure 15D, left pie charts). Sequence Searcher[358] was used to mine for the common CUGBP1 recognition sites UGUGUGUGUGU and UGUUUGUUUGU[284,323] allowing up to two mismatches. As shown in Figure 15D, right chart, 78% of targets in our RIP-Seq indeed contained CUGBP1 sites in their regions of CUGBP1 binding. The motif discovery DREME algorithm[359] was then applied to further define the CUGBP1-binding sites enriched in both SK-Mel-103 and UACC-62 CUGBP1 RIP-Seq. Importantly, 5 significant motifs were found, all of which were UG rich sequences, with p values ranging from 10^{-7} to 10^{-40} (Figure 15E).

In conclusion, the results above identify a broad spectrum of novel cellular targets that CUGBP1 binds preferentially at 3'UTR-containing UG-rich repeats. This 3'UTR binding is consistent with global effects on mRNA stability, therefore, providing a mechanistic explanation for the changes in mRNA expression (Figure 13) discovered in CUGBP1-depleted melanoma cells (i.e. rather than involving intron/exon binding and modulation of RNA splicing).

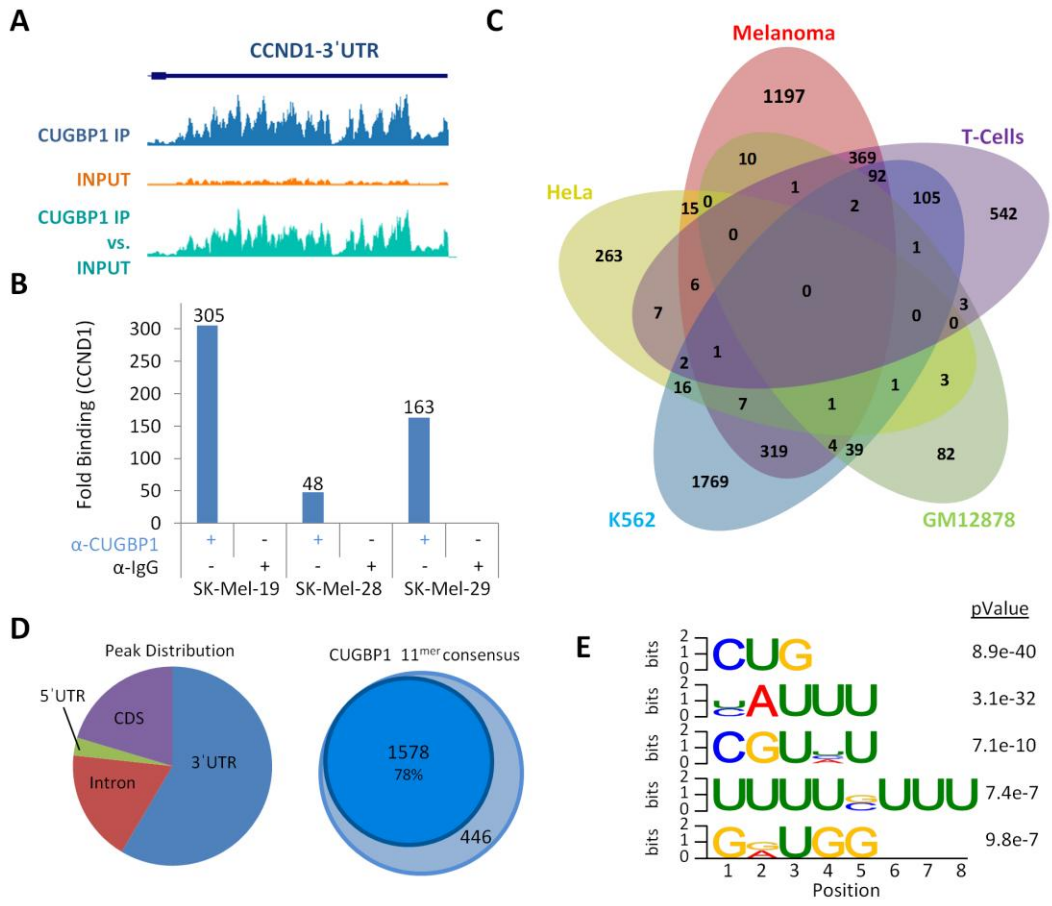

Figure 15: Identification of direct targets of CUGBP1 by RIP-Seq analyses. A, Validation of the crosslinking/immunoprecipitation of CUGBP1-bound transcripts in SK-Mel-103 showing the enrichment identified for the 3'UTR of CCND1 in CUGBP1-IP samples (blue), with respect to input (orange); the CUGBP1-IP/Input ratio (green). **B,** Confirmation of CCND1 3'UTR pulldown by RIP for the indicated melanoma cell lines. **C,** Venn diagrams to assess the overlap of RIP-based analyses in melanoma cells (SK-Mel-103 and UACC-62) versus the indicated cell populations. **D,** *Left chart*, peak calling distribution defined by the Piranha algorithm indicating preferential binding of CUGBP1 to 3'UTR sites in both SK-Mel-103 and UACC-62. *Right chart,* results obtained by Sequence Searcher for classical CUGBP1 11-mers as defined in the text, represented for the total of 2024 RIP-Seq identified transcripts. **E,** Enriched sequences from the melanoma CUGBP1 RIP-Seq data defined by the DREME algorithm ($p<0.005$).

8. VALIDATION OF DEK AS A FUNCTIONAL DOWNSTREAM TARGET OF CUGBP1 IN MELANOMA

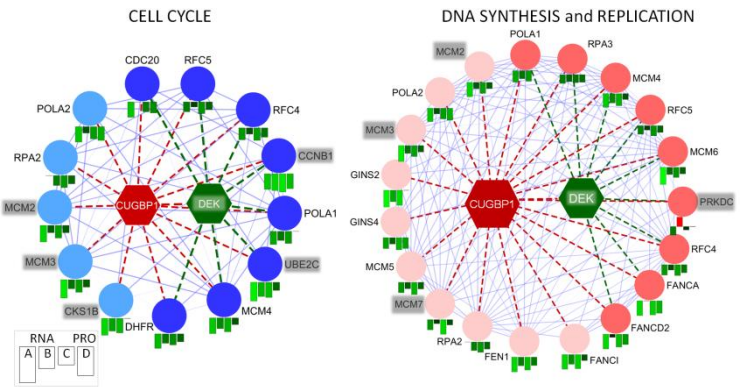

Figure 16: CUGBP1 targets (grey boxes) undergoing changes in mRNA and protein levels as indicated in Figure 14C. Genes under the control of DEK as defined by cDNA arrays are marked with green dashed lines. See text for detail.

Next, the RIP-Seq data was integrated with our transcriptomic and proteomic analyses. Of note, a fraction, but not all key cell cycle/DNA synthesis interacting networks controlled at mRNA levels by CUGBP1 are indeed direct targets of this RBP (see genes marked with gray boxes in Figure 16). Therefore, we questioned whether any of these direct interactors (i.e. CCNB1, CKS1B, DEK, MCM2, MCM3, MCM7, PRKDC or UBE2C) could in turn act downstream of CUGBP1, broadening its spectrum of action. We hypothesized of DEK as a likely candidate, since as indicated above, it is an oncogenic RNA-[190,191] and chromatin-interacting[171,172] factor with key roles in cycle progression and modulation of apoptosis in melanoma cells[186]. Therefore, a further detailed mechanistic and computational analysis was performed (i) to validate DEK as a CUGBP1-modulated factor; (ii) define how CUGBP1 regulates DEK expression, (iii) demonstrate physiological relevance by modulating DEK and rescuing CUGBP1 shRNA-related effects, and if the case (iv) assess co-expression of CUGBP1 and DEK *in vivo* (human melanoma specimens). To start answering the objectives indicated above, a panel of melanoma cell lines was infected with lentiviruses coding for CUGBP1 shRNA, and the subsequent effect on DEK protein expression was determined by immunoblotting. As summarized in Figs. 17A and B, DEK levels were clearly reduced in 5 of the 6 CUGBP1-downregulated melanoma cell lines. Therefore, CUGBP1 is required to sustain a high expression of DEK. A further characterization of the RIP-Seq data described in Figure 15 revealed CUGBP1 bound to the 3'UTR of DEK (Figure 17C), a feature confirmed by independent immunoprecipitation and amplification of this whole genomic region by semi-quantitative RT-PCR (see data for SK-Mel-103 and UACC-62 in Figs. 17D, E, and similar supportive results for additional melanoma cell lines in Figs. 17F, G).

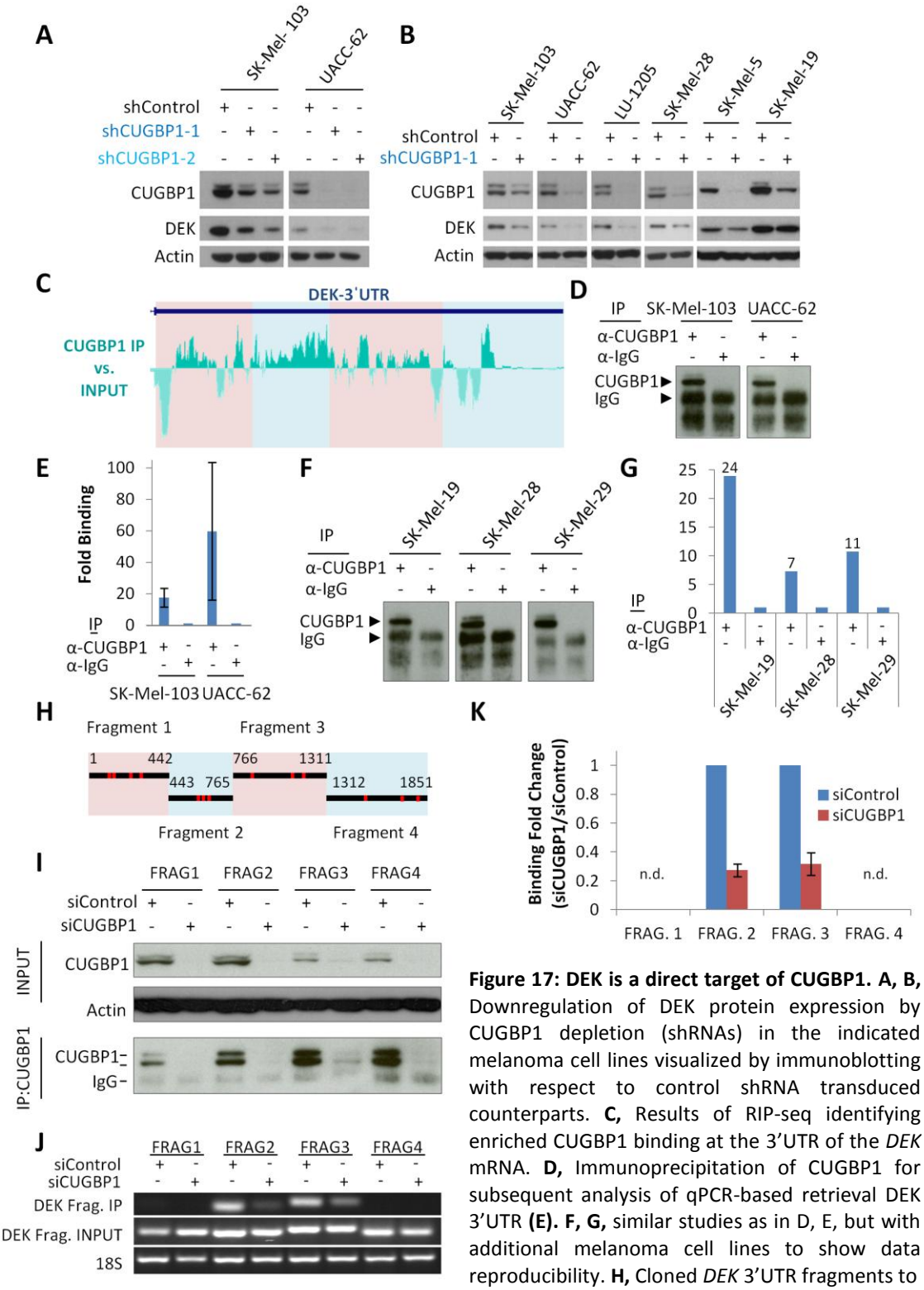

Figure 17: DEK is a direct target of CUGBP1. A, B, Downregulation of DEK protein expression by CUGBP1 depletion (shRNAs) in the indicated melanoma cell lines visualized by immunoblotting with respect to control shRNA transduced counterparts. **C,** Results of RIP-seq identifying enriched CUGBP1 binding at the 3'UTR of the *DEK* mRNA. **D,** Immunoprecipitation of CUGBP1 for subsequent analysis of qPCR-based retrieval DEK 3'UTR **(E). F, G,** similar studies as in D, E, but with additional melanoma cell lines to show data reproducibility. **H,** Cloned *DEK* 3'UTR fragments to further assess CUGBP1 recognition. **I,** Input and immunoprecipitated CUGBP1 in UACC-62 expressing the indicated DEK 3' UTR fragments. As a control for specificity of the CUGBP1 antibodies, similar pulldowns were performed in cells expressing CUGBP1 siRNA. **J,** Amplification of the corresponding *DEK* 3'UTR fragments determined by semi-quantitative RT-PCR fragments to further assess CUGBP1 recognition. **K,** Quantification of data as in J.

We have identified 13 UG-rich areas at the DEK 3'UTR (red boxes in Figure 17H). A PCR-based amplification was then set to clone these sites (distributed into 4 fragments; Figure 17H) for expression via lentiviral vectors. Four isogenic UACC-62 populations were therefore generated to individually express these DEK 3'UTR fragments. In turn, each of these populations was divided in two sets, for transduction of control or CUGBP1 siRNAs (the latter for a negative control for the selectivity of the CUGBP1 antibodies; Figure 17I). As shown in Figure 17J, K, this strategy revealed a significant and preferential binding of CUGBP1 to the central area of the 3'UTR of DEK. Together, these data confirm DEK as a new class of bona-fide CUGBP1 targets.

9. CUGBP1 ALSO CONTROLS PROLIFERATION AND DEK EXPRESSION IN OTHER TUMOR TYPES

As mentioned above, published genome-wide analyses for CUGBP1 targets are only available for HeLa and T-cells. Interestingly, mining the corresponding datasets, we identified DEK bound by CUGBP1 in T-cells, supporting our data in melanoma. However, there was no information for CUGBP1-DEK RIP in HeLa, nor additional information in other cancer types. Therefore, a panel of cell lines from different tumor types was analyzed to define to which our results in melanoma were applicable to other malignancies. Interestingly, and as summarized in Figure 18A, a variety of cell lines from multiple tumor types expressed CUGBP1 levels comparable to those in melanoma cell lines (i.e. higher than in normal skin cells). Moreover, CUGBP1 depletion also compromised cell proliferation as demonstrated by impaired colony formation ability (Figures 18B and 18C).

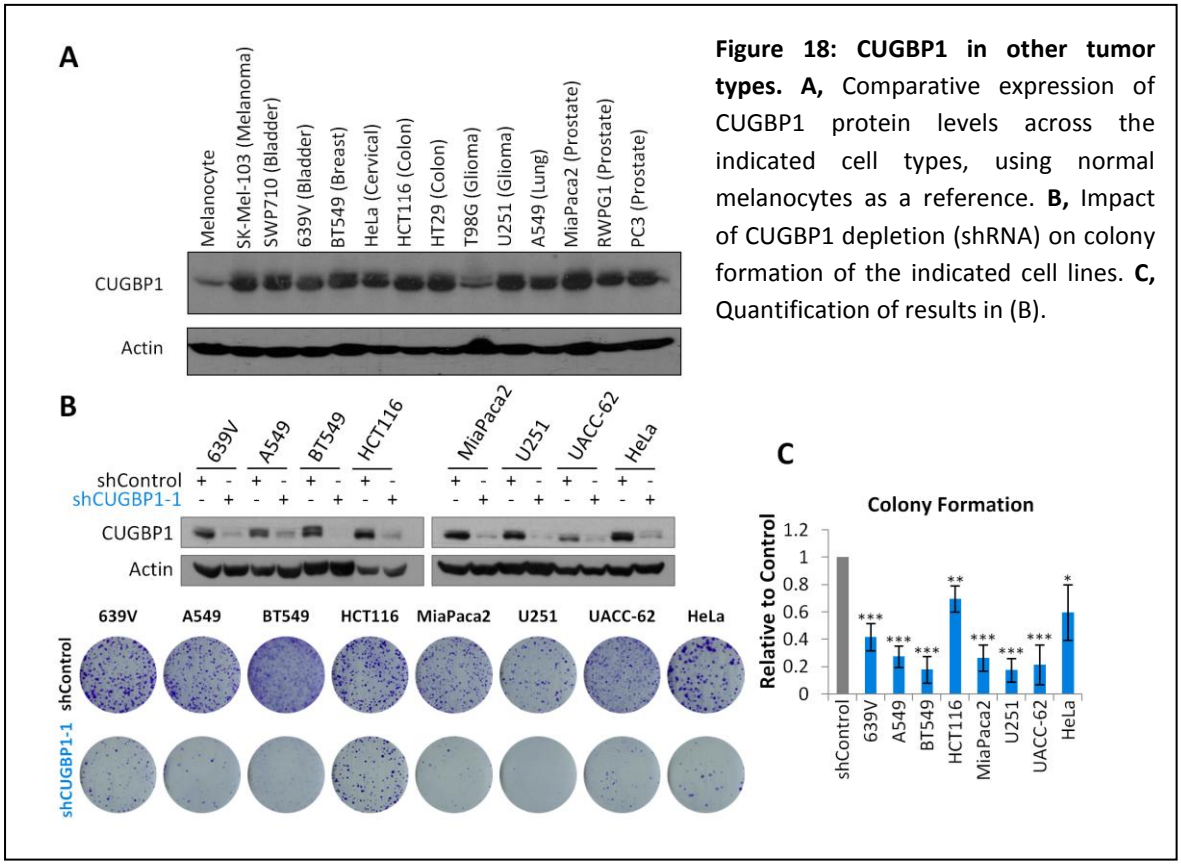

Figure 18: CUGBP1 in other tumor types. A, Comparative expression of CUGBP1 protein levels across the indicated cell types, using normal melanocytes as a reference. **B,** Impact of CUGBP1 depletion (shRNA) on colony formation of the indicated cell lines. **C,** Quantification of results in (B).

Of note, no significant changes in isoform levels of known CUGBP1 targets as a splicing regulator, neither on CCND1 protein expression were detected after CUGBP1 depletion in these cell lines (Figures 19A and 19B). Instead, CUGBP1 downregulation resulted in a clearly identifiable reduction in DEK in 4 out of the 7 lines analyzed (Figure 19C). Therefore, these data expand the spectrum of tumor types with DEK as a downstream target of CUGBP1.

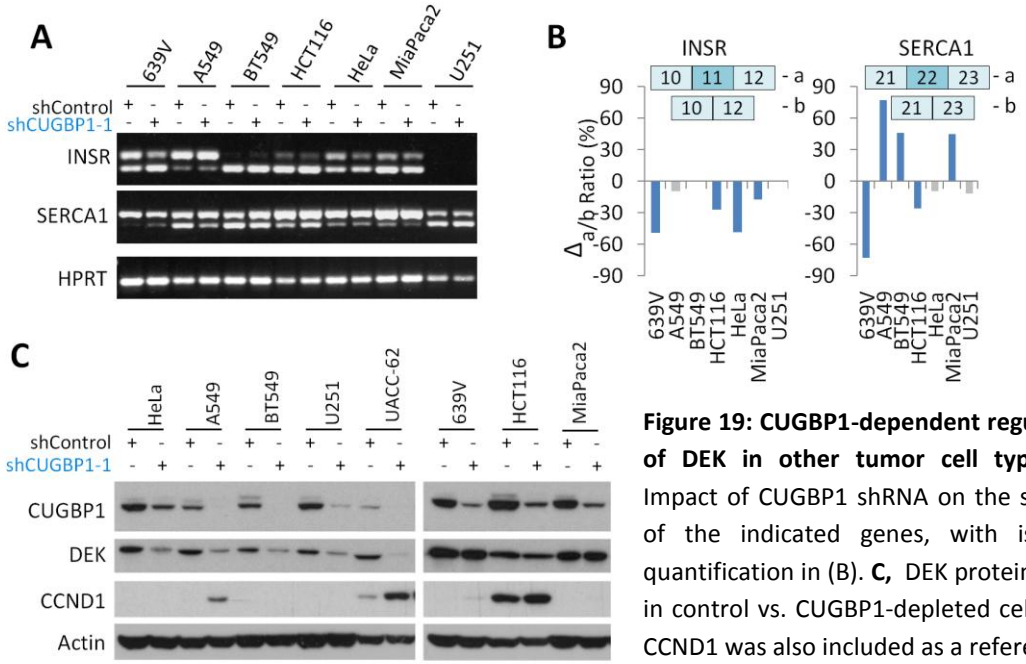

Figure 19: CUGBP1-dependent regulation of DEK in other tumor cell types. A, Impact of CUGBP1 shRNA on the splicing of the indicated genes, with isoform quantification in (B). **C,** DEK protein levels in control vs. CUGBP1-depleted cell lines. CCND1 was also included as a reference.

10. CUGBP1 STABILIZES DEK mRNA

Next, we interrogated how CUGBP1 binding to the DEK mRNA affected gene expression. As this binding was found to occur at the 3' UTR region, we hypothesized effects on mRNA stability. Therefore, we compared the half life of the DEK mRNA in melanoma and non-melanoma cell lines. To this end, transcription was blocked with Actinomycin D in control and CUGBP1 shRNA-expressing cells, and DEK mRNA half life was measured thereafter. Importantly, in those lines where CUGBP1 depletion reduced DEK protein expression, DEK mRNA half life was significantly

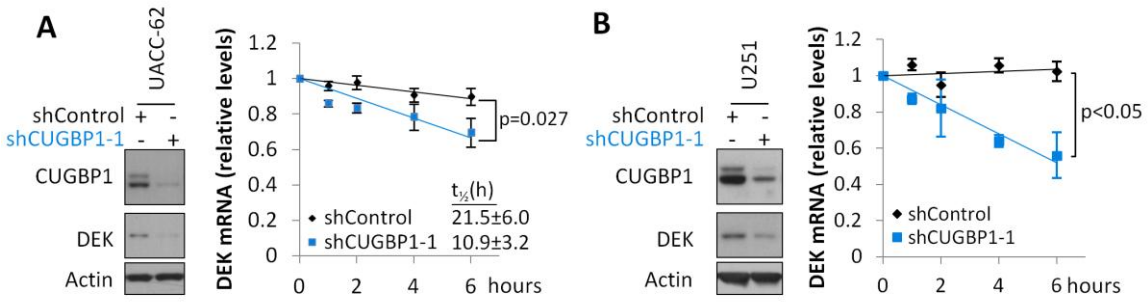

Figure 20: CUGBP1 stabilizes DEK mRNA. A, CUGBP1 depletion efficiency (left) and remaining DEK mRNA levels after Actinomycin D treatment in UACC-62 melanoma cell line. **B,** CUGBP1 depletion efficiency (left) and remaining DEK mRNA levels after Actinomycin D treatment in U251 glioblastoma cell line.

shortened (see data for the melanoma UACC-62 in Figure 20A, and for the glioblastoma U251 in Figure 20B). Therefore, while other regulatory mechanisms may modulate DEK expression[192-194,198], our data supports an unanticipated control of its mRNA stability (and consequently protein levels) by CUGBP1 in a large fraction of tumor cell lines.

11. DEK OVEREXPRESSION RESCUES CUGBP1 DEPLETION-DEPENDENT PHENOTYPE

As indicated above, one of the main findings of this PhD thesis is the identification of a broad spectrum of proteomic and transcriptomic changes induced by CUGBP1 depletion. Therefore, we questioned to which extent DEK depletion was ultimately responsible for main effect of CUGBP1 depletion, namely, impairment in the defective proliferative capacity of melanoma cells. Therefore, the DEK coding sequence was cloned in lentiviral vectors for stable transduction in representative cell lines. This ectopically expressed DEK (which not having the 3'UTR was not downregulated by CUGBP1 depletion; Figure 21A) largely counteracted the inhibitory effect of CUGBP1 shRNA on colony formation ability (Figures 21B and 21C). Therefore, this data solidifies the concept of DEK as a functionally-relevant target of CUGBP1.

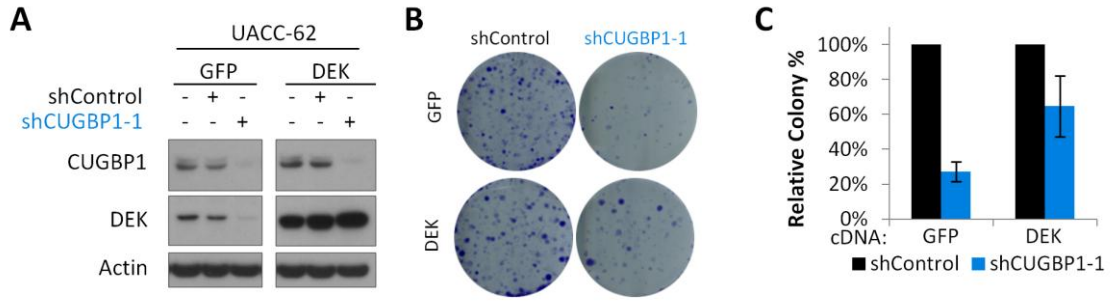

Figure 21: Functional impact of DEK downstream of CUGBP1. A, Expression of the indicated protein in SK-Mel-103 transduced with GFP-expressing lentiviruses either empty or coding for the coding region of DEK (lacking 5' or 3' UTRs). **B,** Crystal violet staining of colonies formed in the indicated cell populations infected with control or shCUGBP1-1. **C,** Quantification of data in (B).

12. POSITIVE CORRELATION BETWEEN CUGBP1 AND DEK EXPRESSION *IN VIVO*

A corollary of our findings is that DEK and CUGBP1 expression should be positively correlated in human melanoma biopsies. Supporting this hypothesis, mRNA levels of both genes showed a relevant Pearson correlation (R=0.35) in the n=278 melanomas of the TCGA database (Figure 22A). This correlation was even stronger when analyzing the expression of both proteins by automated single-cell analysis of co-immunostained sections of malignant human melanoma biopsies. An example of this dual DEK/CUGBP1 visualization (green and red fluorescence, respectively) can be found in Figure 22B in a representative melanoma skin metastasis. Similarly significant coexpression was identified in vertical growth phase, and LN metastasis (Figure 23C, see also additional examples for skin metastases). Together, these provide further physiological support for a tight interplay between DEK and CUGBP1 expression.

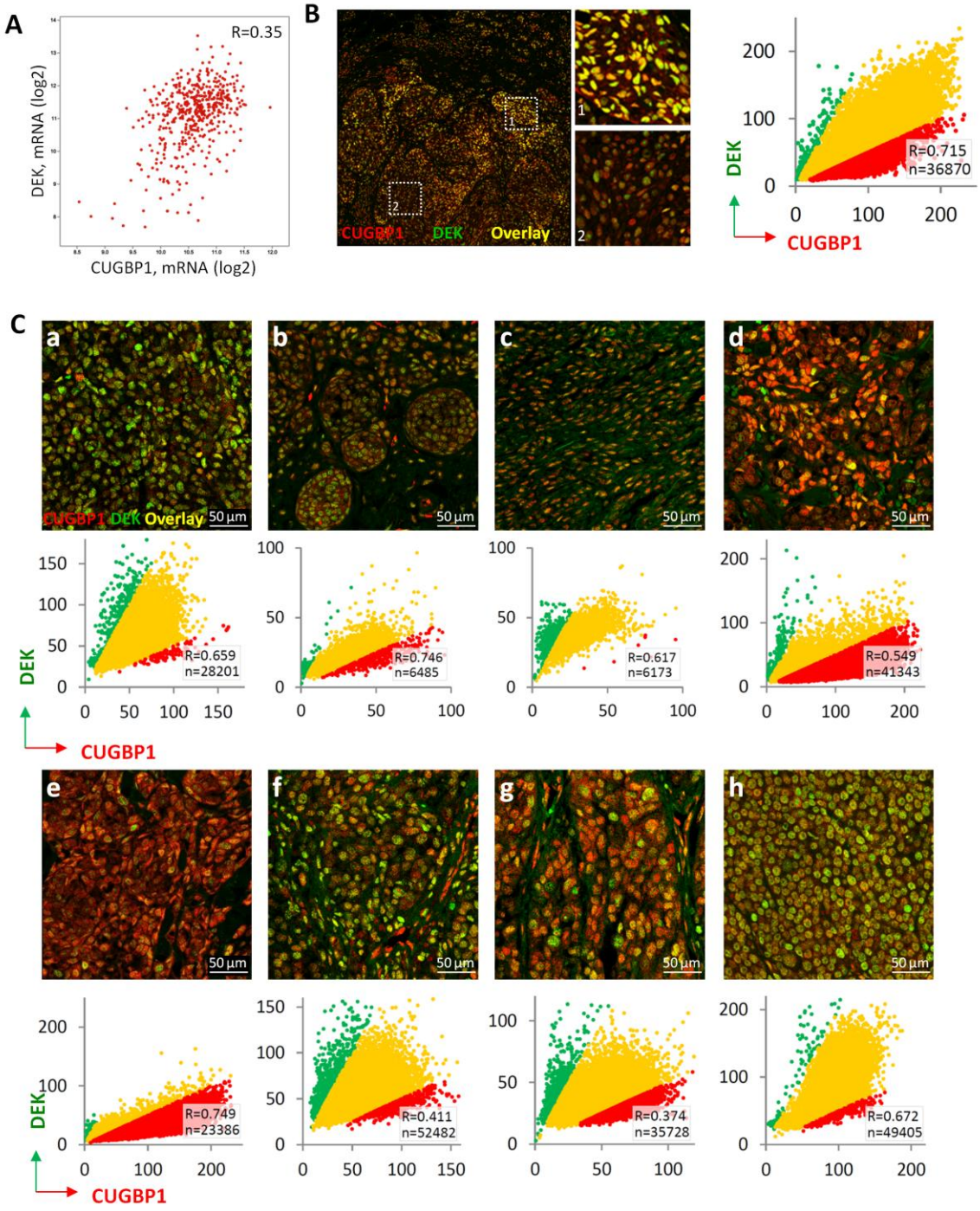

Figure 22: Positive correlation between CUGBP1 and DEK expression *in vivo*. A, Correlation plots of DEK vs. CUGBP1 mRNA in melanoma patients (data obtained from TCGA, n=278). **B,** CUGBP1 (red) and DEK (green) protein levels in a skin metastasis human biopsy sample. Chart below: the quantification of nuclear staining of CUGBP1 and DEK in the human biopsy. Images on the right show higher magnification of selected areas of the lesion. **C,** Immunofluorescence staining of CUGBP1 and DEK in malignant melanoma lesions of human biopsies (a-c, VGP; d-e, skin metastasis; f-h, lymph node metastasis). Charts show the quantification of nuclear staining of CUGBP1 and DEK in each biopsy (R, Pearson correlation coefficient; n, total number of quantified cells in whole tissue).

VII.

DISCUSSION

DISCUSIÓN

Melanomas are prime examples of aggressive tumors that proceed with massive changes in the transcriptome and proteome[126-129]. RNA regulatory mechanisms are attractive as key contributors to this complexity for their potential to modulate multiple pro-tumorigenic signaling cascades[243,246,247]. Yet, knowledge on the expression and function of RNA binding proteins (RBPs) are puzzlingly incomplete. Here we identify CUGBP1/CELF1 as an early-induced melanoma factor required for proper cell cycle progression. Target identification was then performed by genome-wide RIP-Seq, transcriptomic and proteomic analyses. This integrated approach, to our knowledge, the first in class for human RBPs, revealed a relatively minor set of genes controlled by CUGBP1 in the context of alternative splicing. These results therefore separate melanomas from developmental processes (i.e. in muscle cells) where this gene has been better characterized[285,286]. Instead, CUGBP1 was found to regulate mRNA levels (and their protein expression) of a broad spectrum of cellular factors, enriched for an interconnected network of key cell cycle/DNA replication modulators. Canonical UG rich domains were identified at 3'UTR of CUGBP1 bound transcripts, supporting a key role of this RBP in the control of mRNA stability. A novel CUGBP1-target discovered with these 3'UTR-associated features was the oncogene DEK. The physiological relevance of DEK as a downstream effector of CUGBP1 was supported by rescue experiments, and further emphasized by histological analyses in human clinical specimens. Interestingly, DEK was found under the control of CUGBP1 in cell lines from various additional cancer types. Together, these data provide new insights on mechanisms of RNA regulation in melanoma, identifying new roles and functions of CUGBP1, with unanticipated links to the oncogenic DEK that may have a broader impact on tumor development.

1. RBPs IN MELANOMA AND BEYOND: CUGBP1 IN CELL CYCLE CONTROL

The starting point of this PhD thesis was the finding that despite the almost 80000 somatic mutations and the plethora of chromosomal reorganizations reported for human melanoma specimens[217], mRBPs (with more than 650 family members) are not a frequent subject of mutations or copy number variations. Hypothesizing a post-transcriptional control, we exploited an array specifically designed for a high coverage survey of functionally annotated representatives of main RBP families (i.e. recognition to mRNA, snRNA, snoRNA and ncRNA)[218]. This microarray also contained probes for 302 cancer-related factors, which ultimately guided our validation efforts towards the analysis of RBPs able to both modulate cell cycle control checkpoints and chromatin organizers. This strategy revealed 50 RBPs with an enhanced mRNA expression with respect to normal melanocytes. Of those, only 9 (C1QBP, DEK, DYRK1A, EIF6, MAGOH, PTBP1, SNRPD1, SNRPE and SRSF3 – see Table 8 for details) had been previously found with key roles in melanoma. Therefore our new discoveries have important basic and translational implications.

Table 8: RBPs enriched in melanoma melanocyte microarray with defined functions in melanoma.

GENE	FINDING	REF
C1QBP	C1QBP driven enhanced migration and tumor growth of B16F10 melanoma cells in C57/BL6 mice through MT1-MMP and MMP-2 activation.	380
DEK	DEK dependent melanoma growth and chemoresistance.	185
DYRK1A	Higher DYRK1A levels in primary melanoma compared to nevi.	381
EIF6	Cell migration and invasion enhancement in eIF6 overexpressing melanoma cell lines through activation of cdc42.	382
MAGOH	MAGOH-regulated proliferation of melanoblasts in the dermis.	383
PTBP1	PTBP1 dependent CD44v6 (brain metastasis driver) overexpression in advanced melanomas.	384
SNRPD1	SNRPD1 depletion dependent reduction of cell viability in melanoma cell lines.	385
SNRPE	SNRPE depletion dependent reduction of cell viability in melanoma cell lines through increased autophagy.	385
SRSF3	SRSF3-dependent MDM4-driven melanoma growth.	386

With the objective of providing insight into novel mechanisms of gene regulation in melanoma, we focused on genes not previously reported to this disease. CUGBP1 was of interest for its recent links to hepatocellular carcinoma, non-small cell lung cancer, esophageal carcinoma and gastric cancer[336-342], although genome-wide analyses for regulated transcripts have yet to be defined (Table 5). Finding CUGBP1 induced in semi-transformed melanocytes (Mel-STV) and at early stages of melanoma progression thus further emphasizes tumor-associated roles of RBPs. Moreover, our data showing a high protein expression of CUGBP1 (and functional impact) in cell lines from bladder, breast, colon, glioma, lung and prostate cancer cell lines (Figure 18) further expands the breadth of malignancies where high throughput analyses of CUGBP1 targets may prove highly informative. In addition, we anticipate the identification of upstream modulators of CUGBP1 as a useful strategy to further link pro-oncogenic events to global regulators of gene expression. In this context, it is interesting to note that an E-box motif has been identified at the *CUGBP1* promoter: analyses in normal and differentiated myoblasts reported binding of the TCF3, CBP and p300 transcription factors[294], also with reported links to malignancy. The development of inducible CRISPR-Cas9 now offers the possibility of assessing not only upstream modulators of CUGBP1, but also to define cooperating (or antagonistic) effects *in vivo* of the additional RBPs we found deregulated in melanoma cells.

2. SYSTEM-DEPENDENT ROLES OF CUGBP1

One of the most unanticipated result was the relatively modest overlap of the CUGBP1-bound transcripts we discovered in melanoma, with respect to the two genome-wide analyses available in the literature for HeLa and T-cells[284,327]. This minor overlap was also obvious for information available through ENCODE on the K562 and GM12878 cell lines[331]. The mechanisms underlying this

variability will have to be defined in future studies. However, it is tempting to speculate the involvement of alternative 3'UTRs that are differentially used depending on the cellular context[387,388]. Additionally, the differential outcome of CUGBP1 in different cellular settings may reflect the expression of other RBPs which may act in a compensatory manner. Competition and collaboration between different RBPs and microRNAs has been reported in several studies[389-391]. In particular for CUGBP1, this agonistic and antagonistic functions have been demonstrated for MBNL1[283,333] and HuR[392]. The extent to which these compensatory proteins act in melanoma cells is unclear, but preliminary studies from our lab suggest an important contribution of MBNL1 (unpublished data).

3. NOVEL CUGBP1 TARGETS IN MELANOMA CELLS

Regarding the mechanism of action of CUGBP1 in melanoma, our initial studies aimed to assess alternative splicing. The rationale stemmed from the large body of literature for CUGBP1 in the modulation of isoform selection in the context of physiological and pathogenic developmental processes in muscle cells[294,303,332,334,393]. However, we found that CUGBP1 shRNA had a minor impact on known CUGBP1 targets such as exon 11 or INSR[302-304], exon 22 of SERCA1[305], exon 17 of FXR1[305], exon 5 of FAM188A[305] and exon 20 of ANK2[305]. In addition, we failed to detect the splicing event of exon 7a MEF2A and exon 9 of PPFIBP1 in cancer cell lines tested. Moreover, genome-wide analyses using Human Junction Arrays (HJAY), which cover a total of 5.4 million probes, revealed a surprisingly small number of genes found to show changes in splicing in both cell lines upon CUGBP1 depletion (see Table 9).

Table 9: Common alternative splicing events observed in both SK-Mel 103 and UACC-62 cells upon CUGBP1 depletion.

SK-MEL 103		UACC-62			
GENE	**Fold Index**	**GENE**	**Fold Index**	**EXON**	**EVENT**
ATP5G3	3.14	ATP5G3	2.11	ae4	intron retention
CLDND1	3.04	CLDND1	3.07	e2	alternative first exon, exon skipping
CLSPN	2.22	CLSPN	2.21	ae1	alternative first exon
CSNK1G1	3.00	CSNK1G1	2.01	e5	alternative last exon, exon skipping
DHX40P1	3.04	DHX40P1	2.41	e10	unknown
DHX40P1	2.77	DHX40P1	2.27	e8	unknown
DHX40P1	2.52	DHX40P1	2.48	e12	unknown
DHX40P1	2.27	DHX40P1	2.22	ae5	unknown
DHX40P1	2.07	DHX40P1	2.21	e7	unknown
EIF4E2	3.07	EIF4E2	2.40	ae6	alternative last exon
MACF1	3.09	MACF1	2.87	e41	alternative first exon, exon skipping
MBNL1	2.02	MBNL1	2.14	e3	exon skipping
RREB1	2.44	RREB1	3.60	ae6	intron retention

In the light of the small number of genes with altered splicing, we decided to proceed to an unbiased transcriptomic and proteomic analysis. Interestingly, a significant correlation between mRNA and protein levels, supporting the concept that CUGBP1 controls gene expression by modulating translation[285,309,322] and mRNA stability[284,327]. Another objective of this work was to unravel and build network of genes regulated by CUGBP1 in melanoma cells. Enrichment analyses revealed cell cycle and DNA replication/cellular stress as key signaling cascades modulated by CUGBP1. Interestingly, and while both cellular processes are modulated by a large set of cellular factors, CUGBP1 appear to modulate mRNA and protein expression of a selective set of highly interacting signaling hubs. In particular, we identified an unexpected coordinated regulation of minichromosome maintenance proteins (MCM2, MCM3, MCM4, MCM5, MCM6 and MCM7), replication factor C protein complex (RFC4 and RCF5) and DNA polymerase alpha complex (POLA1 and POLA2). This indicates an aberration in the DNA synthesis initiation and elongation. Downregulation of these genes upon CUGBP1 depletion might explain the delayed progression through the G1 phase of the cycle phase. In addition, GINS family members (GINS2 and GINS4) essential for initiation of DNA replication, and progression of DNA replication forks were also found as CUGBP1 modulating factors. DNA replication stress has been proposed to be one of the hallmarks of cancer, which is a source of DNA strand breaks and genomic instability[394]. The deregulation of FANCA, FANCD2 or FANCC1 (Figure 16) may further contribute to replicative stress and a subsequent impairment of tumor progression. The inability of CUGBP1-depleted melanoma cells to grow efficiently as xenografts further supports the requirement of this RBP to avoid detrimental effects related to aberrant proliferation.

Intriguingly, RIP-Seq identified various MCMs (i.e. MCM2, MDCM3 and MCM7) as well as other cell cycle and DNA synthesis modulators such as CCNB1, UBE2C or PRKDC (Figure 16) as direct binding targets of CUGBP1 in melanoma cells. However, this was not the case for multiple additional controllers of cell proliferation that CUGBP1 modulates at the protein and mRNA levels. In this context, finding that chromatin organization and chromatin architecture were enriched terms identified in microarrays and whole genome transcriptomic and proteomic analysis was found critical to identify CUGBP1 “intermediaries” that broaden the control of pro-tumorigenic factors with no consensus UG-rich sites in their mRNA. Thus, integrating all these unbiased analyses ultimately revealed the chromatin binding factor DEK as a direct CUGBP1 target. Moreover, we identified 13 UG-rich repeats at the 3’UTR of *DEK*. Of those, repeats contained in between nucleotides 442-1311 in this region appear to define recognition by CUGBP1. This binding of CUGBP1 extended the half life of the DEK transcript. While additional studies are required to determine how CUGBP1 stabilizes and protects DEK and other targets from degradation, a possible mechanism involve competing for other mRNA binding proteins such as HuR, ARE-BP and/or PABP

thus inhibiting the formation of destabilizing complex which would enable the PARN to degrade the target mRNA.

The power of genome-wide analyses was also illustrated in the identification of downstream effectors of DEK (Table S5). We had previously linked the oncogenic functions of DEK to the control of cell cycle progression and modulation of cell survival. Here we now identified specific proteins that may mediate these functions of DEK. Certainly, given the inherent pleiotropic nature of RPBs, it would not be expected that DEK would completely restore the deficient proliferation of CUGBP1-depleted melanoma cells. Therefore, finding that a significant recovery of colony formation was possible after rescuing DEK expression in CUGBP1 shRNA-expressing melanoma cells is highly significant (Figure 21). In this context, it is important to note that DEK has been shown to counteract replication stress and ensure cell proliferation by resolving DNA and/or chromatin structures at the replication fork due to its function on changing the DNA topology[395]. The physiological relevance of DEK is emphasized by its overexpression in human melanoma specimens[185], and the finding demonstrated here of a positive correlation with CUGBP1. Histopathological validation in human melanoma tissues is supported by the identification of DEK as a downstream modulator of CUGBP1 in other cell types.

In summary, these findings presented in this PhD thesis helped us to expand the information on the functional impact of CUGBP1 in cancer, and in more detail in melanoma. Importantly, we have identified a large set of novel CUGBP1-bound transcripts which expand spectrum of targets (and functions) of this gene. Together, this information furthers our knowledge on the crosstalk between cell cycle, DNA synthesis and chromatin organization, via the RNA binding features of CUGBP1, incorporating DEK as a fundamental mediator of these processes.

VIII.

CONCLUSIONS

CONCLUSIONES

CONCLUSIONS

In the light of the results represented in this PhD thesis we withdraw the following conclusions:

1. RNA binding proteins (RBPs) are not a frequent mutational target in melanoma. However, a subset of 50 members of this family was found to undergo selective deregulation at the mRNA level in melanoma cell lines.
2. From these newly-identified melanoma-overexpressed RBPs, the CUG repeat binding protein 1, CUGBP1, was found upregulated at early stages of tumor progression, being required to maintain cell proliferation (*in vitro* and *in vivo*). Depletion of CUGBP1 in melanoma cells results in delayed cell cycle, resulting from defective G1-S cell cycle progression.
3. Genome-wide analyses (transcriptomic and proteomic analyses) identified a highly interconnected network of novel CUGBP1 regulated genes. In particular, enrichment studies uncovered cell cycle and DNA synthesis/replication modulators previously unknown to be modulated by CUGBP1 at protein and mRNA levels.
4. RIP-seq revealed a large set of direct binding targets of CUGBP1, which contained GU-rich repeats preferentially at 3'UTR sites. A key characteristic target of CUGBP1 with these features is the *DEK* chromatin organizer. The binding occurs between bases 433-1311 of 3'UTR of DEK mRNA, representing an unanticipated mechanism of regulation for this oncogene.
5. DEK is a functionally-relevant CUGBP1 target, alleviating inhibitory effects of CUGBP1 shRNA in clonogenic capacity.
6. CUGBP1 and DEK levels (RNA and protein) positively correlate in human melanoma biopsies.
7. The interplay between CUGBP1-DEK and cell cycle proliferation/DNA synthesis identified in melanoma, was also demonstrated to apply to other tumor types, expanding the roles and mechanistic impact of RBPs in cancer.

CONCLUSIONES

A raíz de los resultados presentados en la presente Tesis Doctoral, concluimos lo siguiente:

1. Las proteínas de unión a ARN (RBPs) no representan una diana mutacional frecuente en el melanoma. Sin embargo, aquí identificamos una serie de 50 miembros de esta familia que sufren una regulación particular a nivel de ARNm en el melanoma humano.
2. Entre estas nuevas RBPs enriquecidas en el melanoma, la "CUG repeat binding protein 1", CUGBP1, se identificó como un factor sobre-expresado en fases iniciales de esta enfermedad, requerido para mantener la proliferación celular (*in vitro* and *in vivo*). La depleción de CUGBP1 en células de melanoma conduce a una reducción en la capacidad proliferativa derivada de una progresión deficiente a través de las fases G1-S del ciclo celular.
3. Análisis de perfiles transcriptómicos y proteómicos correspondientes al genoma completo revelaron una red altamente interconectada de nuevos genes regulados por CUGBP1. En particular, estudios de enriquecimiento resultaron en el descubrimiento de reguladores de ciclo celular y de síntesis/replicación del ADN, previamente desconocidos como dianas reguladas por CUGBP1 a nivel de ARNm y proteína.
4. RIP-seq reveló un gran grupo de dianas directas de CUGBP1, conteniendo repeticiones ricas en UG preferentemente en sitios 3'UTR. Uno de los genes con esta característica es el organizador de cromatina DEK. CUGBP1 reconoce los residuos 433-1311 de 3'UTR en el ARNm de *DEK*, representando un mecanismo de regulación desconocido para este oncogén.
5. DEK ejerce un efecto funcionalmente relevante como efector de CUGBP1, disminuyendo los efectos inhibidores de CUGBP1 shRNA en la capacidad clonogénica de las células del melanoma.
6. Los niveles de CUGBP1 y DEK (ARN and proteína) correlacionan de forma positiva en biopsias de melanoma humano.
7. La interconexión entre CUGBP1, DEK y proliferación celular/síntesis de ADN identificada en el melanoma se demostró aplicable a otros tipos tumorales, reforzando y expandiendo el impacto fisiológico de las RBPs en el cáncer.

IX.

REFERENCES

BIBLIOGRAFÍA

1. Zabierowski, S.E. & Herlyn, M. Embryonic stem cells as a model for studying melanocyte development. *Methods Mol Biol* **584**, 301-316 (2010).
2. Dupin, E. & Le Douarin, N.M. Development of melanocyte precursors from the vertebrate neural crest. *Oncogene* **22**, 3016-3023 (2003).
3. Slominski, A.*, et al.* Hair follicle pigmentation. *J Invest Dermatol* **124**, 13-21 (2005).
4. Cable, J. & Steel, K.P. Identification of two types of melanocyte within the stria vascularis of the mouse inner ear. *Pigment Cell Res* **4**, 87-101 (1991).
5. Barden, H. & Levine, S. Histochemical observations on rodent brain melanin. *Brain Res Bull* **10**, 847-851 (1983).
6. Hu, D.N., Savage, H.E. & Roberts, J.E. Uveal melanocytes, ocular pigment epithelium, and Muller cells in culture: in vitro toxicology. *Int J Toxicol* **21**, 465-472 (2002).
7. Nichols, S.E., Jr. & Reams, W.M., Jr. The occurrence and morphogenesis of melanocytes in the connective tissues of the PET/MCV mouse strain. *J Embryol Exp Morphol* **8**, 24-32 (1960).
8. Mjaatvedt, C.H., Kern, C.B., Norris, R.A., Fairey, S. & Cave, C.L. Normal distribution of melanocytes in the mouse heart. *Anat Rec A Discov Mol Cell Evol Biol* **285**, 748-757 (2005).
9. Coit, D.G.*, et al.* Melanoma, version 2.2013: featured updates to the NCCN guidelines. *J Natl Compr Canc Netw* **11**, 395-407 (2013).
10. Miller, A.J. & Mihm, M.C., Jr. Melanoma. *N Engl J Med* **355**, 51-65 (2006).
11. Schadendorf, D.*, et al.* Melanoma. *Nature Reviews Disease Primers*, 15055 (2015).
12. Scott, K.L.*, et al.* Proinvasion metastasis drivers in early-stage melanoma are oncogenes. *Cancer Cell* **20**, 92-103 (2011).
13. National Cancer Institute. SEER Stat Fact Sheets: Melanoma of the Skin. Vol. 2016 (2015).
14. Siegel, R.L., Miller, K.D. & Jemal, A. Cancer statistics, 2015. *CA Cancer J Clin* **65**, 5-29 (2015).
15. American Cancer Society. Cancer Facts & Figures 2016. *Atlanta: American Cancer Society* (2016).
16. Bernal, M., Souza, D., Gomez, G. & Gomez, F. Projections of Incidence, Prevalence and Mortality from Melanoma in Spain. *Journal of Cosmetics, Dermatological Sciences and Applications* **Vol.3**(2013).
17. Gilchrest, B.A., Eller, M.S., Geller, A.C. & Yaar, M. The pathogenesis of melanoma induced by ultraviolet radiation. *N Engl J Med* **340**, 1341-1348 (1999).
18. Gandini, S.*, et al.* Meta-analysis of risk factors for cutaneous melanoma: II. Sun exposure. *Eur J Cancer* **41**, 45-60 (2005).
19. Gandini, S.*, et al.* Meta-analysis of risk factors for cutaneous melanoma: III. Family history, actinic damage and phenotypic factors. *Eur J Cancer* **41**, 2040-2059 (2005).
20. Tsao, H. & Niendorf, K. Genetic testing in hereditary melanoma. *J Am Acad Dermatol* **51**, 803-808 (2004).
21. Goldstein, A.M.*, et al.* Features associated with germline CDKN2A mutations: a GenoMEL study of melanoma-prone families from three continents. *J Med Genet* **44**, 99-106 (2007).
22. Holly, E.A., Kelly, J.W., Shpall, S.N. & Chiu, S.H. Number of melanocytic nevi as a major risk factor for malignant melanoma. *J Am Acad Dermatol* **17**, 459-468 (1987).
23. Titus-Ernstoff, L.*, et al.* Pigmentary characteristics and moles in relation to melanoma risk. *Int J Cancer* **116**, 144-149 (2005).
24. Moloney, F.J.*, et al.* A population-based study of skin cancer incidence and prevalence in renal transplant recipients. *Br J Dermatol* **154**, 498-504 (2006).
25. Jensen, P.*, et al.* Skin cancer in kidney and heart transplant recipients and different long-term immunosuppressive therapy regimens. *J Am Acad Dermatol* **40**, 177-186 (1999).
26. Pantanowitz, L., Schlecht, H.P. & Dezube, B.J. The growing problem of non-AIDS-defining malignancies in HIV. *Curr Opin Oncol* **18**, 469-478 (2006).
27. Stein, L.*, et al.* The spectrum of human immunodeficiency virus-associated cancers in a South African black population: results from a case-control study, 1995-2004. *Int J Cancer* **122**, 2260-2265 (2008).

28. Whiteman, D.C., Pavan, W.J. & Bastian, B.C. The melanomas: a synthesis of epidemiological, clinical, histopathological, genetic, and biological aspects, supporting distinct subtypes, causal pathways, and cells of origin. *Pigment Cell Melanoma Res* **24**, 879-897 (2011).
29. Quintana, E.*, et al.* Phenotypic heterogeneity among tumorigenic melanoma cells from patients that is reversible and not hierarchically organized. *Cancer Cell* **18**, 510-523 (2010).
30. Chin, L., Garraway, L.A. & Fisher, D.E. Malignant melanoma: genetics and therapeutics in the genomic era. *Genes Dev* **20**, 2149-2182 (2006).
31. Tsao, H., Chin, L., Garraway, L.A. & Fisher, D.E. Melanoma: from mutations to medicine. *Genes Dev* **26**, 1131-1155 (2012).
32. Desmond, R.A. & Soong, S.J. Epidemiology of malignant melanoma. *Surg Clin North Am* **83**, 1-29 (2003).
33. Sneyd, M.J. & Cox, B. A comparison of trends in melanoma mortality in New Zealand and Australia: the two countries with the highest melanoma incidence and mortality in the world. *BMC Cancer* **13**, 372 (2013).
34. de Vries, E., Bray, F.I., Coebergh, J.W. & Parkin, D.M. Changing epidemiology of malignant cutaneous melanoma in Europe 1953-1997: rising trends in incidence and mortality but recent stabilizations in western Europe and decreases in Scandinavia. *Int J Cancer* **107**, 119-126 (2003).
35. Breslow, A. Thickness, cross-sectional areas and depth of invasion in the prognosis of cutaneous melanoma. *Ann Surg* **172**, 902-908 (1970).
36. Balch, C.M.*, et al.* Final version of 2009 AJCC melanoma staging and classification. *J Clin Oncol* **27**, 6199-6206 (2009).
37. Brenn, T. Pitfalls in the evaluation of melanocytic lesions. *Histopathology* **60**, 690-705 (2012).
38. Troxel, D.B. Pitfalls in the diagnosis of malignant melanoma: findings of a risk management panel study. *Am J Surg Pathol* **27**, 1278-1283 (2003).
39. Weinstein, D., Leininger, J., Hamby, C. & Safai, B. Diagnostic and prognostic biomarkers in melanoma. *J Clin Aesthet Dermatol* **7**, 13-24 (2014).
40. Abbas, O., Miller, D.D. & Bhawan, J. Cutaneous malignant melanoma: update on diagnostic and prognostic biomarkers. *Am J Dermatopathol* **36**, 363-379 (2014).
41. Lin, J.Y. & Fisher, D.E. Melanocyte biology and skin pigmentation. *Nature* **445**, 843-850 (2007).
42. Swope, V.*, et al.* Significance of the melanocortin 1 receptor in the DNA damage response of human melanocytes to ultraviolet radiation. *Pigment Cell Melanoma Res* **27**, 601-610 (2014).
43. Rodriguez, C.I. & Setaluri, V. Cyclic AMP (cAMP) signaling in melanocytes and melanoma. *Arch Biochem Biophys* **563**, 22-27 (2014).
44. Bastian, B.C. The molecular pathology of melanoma: an integrated taxonomy of melanocytic neoplasia. *Annu Rev Pathol* **9**, 239-271 (2014).
45. LeBoit, P., Burg, G., Weedon, D. & Sarasain, A. *Pathology and genetics of skin tumours. World Health Organization classification of tumours.*, (*IARC Press*, Lyon, 2006).
46. Clark, W.H., Jr., From, L., Bernardino, E.A. & Mihm, M.C. The histogenesis and biologic behavior of primary human malignant melanomas of the skin. *Cancer Res* **29**, 705-727 (1969).
47. Kincannon, J. & Boutzale, C. The physiology of pigmented nevi. *Pediatrics* **104**, 1042-1045 (1999).
48. Argenziano, G., Zalaudek, I., Ferrara, G., Hofmann-Wellenhof, R. & Soyer, H.P. Proposal of a new classification system for melanocytic naevi. *Br J Dermatol* **157**, 217-227 (2007).
49. Zayour, M. & Lazova, R. Congenital melanocytic nevi. *Clin Lab Med* **31**, 267-280 (2011).
50. Swerdlow, A.J.*, et al.* Benign melanocytic naevi as a risk factor for malignant melanoma. *Br Med J (Clin Res Ed)* **292**, 1555-1559 (1986).

51. Farber, M.J., Heilman, E.R. & Friedman, R.J. Dysplastic nevi. *Dermatol Clin* **30**, 389-404 (2012).
52. Duffy, K. & Grossman, D. The dysplastic nevus: from historical perspective to management in the modern era: part I. Historical, histologic, and clinical aspects. *J Am Acad Dermatol* **67**, 1 e1-16; quiz 17-18 (2012).
53. Shain, A.H.*, et al.* The Genetic Evolution of Melanoma from Precursor Lesions. *N Engl J Med* **373**, 1926-1936 (2015).
54. Silva, J.H., Sa, B.C., Avila, A.L., Landman, G. & Duprat Neto, J.P. Atypical mole syndrome and dysplastic nevi: identification of populations at risk for developing melanoma - review article. *Clinics (Sao Paulo)* **66**, 493-499 (2011).
55. Zhang, G. & Herlyn, M. Human nevi: no longer precursors of melanomas? *J Invest Dermatol* **132**, 2133-2134 (2012).
56. Bastian, B.C., LeBoit, P.E. & Pinkel, D. Mutations and copy number increase of HRAS in Spitz nevi with distinctive histopathological features. *Am J Pathol* **157**, 967-972 (2000).
57. Bauer, J., Curtin, J.A., Pinkel, D. & Bastian, B.C. Congenital melanocytic nevi frequently harbor NRAS mutations but no BRAF mutations. *J Invest Dermatol* **127**, 179-182 (2007).
58. Pollock, P.M.*, et al.* High frequency of BRAF mutations in nevi. *Nat Genet* **33**, 19-20 (2003).
59. Van Raamsdonk, C.D.*, et al.* Frequent somatic mutations of GNAQ in uveal melanoma and blue naevi. *Nature* **457**, 599-602 (2009).
60. Troxel, D.B. Error in surgical pathology. *Am J Surg Pathol* **28**, 1092-1095 (2004).
61. Pacheco, I., Buzea, C. & Tron, V. Towards new therapeutic approaches for malignant melanoma. *Expert Rev Mol Med* **13**, e33 (2011).
62. Greenwald, H.S., Friedman, E.B. & Osman, I. Superficial spreading and nodular melanoma are distinct biological entities: a challenge to the linear progression model. *Melanoma Res* **22**, 1-8 (2012).
63. Durbec, F., Martin, L., Derancourt, C. & Grange, F. Melanoma of the hand and foot: epidemiological, prognostic and genetic features. A systematic review. *Br J Dermatol* **166**, 727-739 (2012).
64. McGovern, V.J., Cochran, A.J., Van der Esch, E.P., Little, J.H. & MacLennan, R. The classification of malignant melanoma, its histological reporting and registration: a revision of the 1972 Sydney classification. *Pathology* **18**, 12-21 (1986).
65. Laver, N.V., McLaughlin, M.E. & Duker, J.S. Ocular melanoma. *Arch Pathol Lab Med* **134**, 1778-1784 (2010).
66. Davies, H.*, et al.* Mutations of the BRAF gene in human cancer. *Nature* **417**, 949-954 (2002).
67. Mihajlovic, M., Vlajkovic, S., Jovanovic, P. & Stefanovic, V. Primary mucosal melanomas: a comprehensive review. *Int J Clin Exp Pathol* **5**, 739-753 (2012).
68. Jain, S. & Allen, P.W. Desmoplastic malignant melanoma and its variants. A study of 45 cases. *Am J Surg Pathol* **13**, 358-373 (1989).
69. Martin, R.C.*, et al.* So-called "malignant blue nevus": a clinicopathologic study of 23 patients. *Cancer* **115**, 2949-2955 (2009).
70. Blessing, K.*, et al.* Small cell malignant melanoma: a variant of naevoid melanoma. Clinicopathological features and histological differential diagnosis. *J Clin Pathol* **53**, 591-595 (2000).
71. Kemp, S., Gallagher, G., Kabani, S. & Moskal, R. Persistent melanoma in situ: case report and review. *J Oral Maxillofac Surg* **66**, 1945-1948 (2008).
72. Hendrickson, M.R. & Ross, J.C. Neoplasms arising in congenital giant nevi: morphologic study of seven cases and a review of the literature. *Am J Surg Pathol* **5**, 109-135 (1981).
73. Jen, M., Murphy, M. & Grant-Kels, J.M. Childhood melanoma. *Clin Dermatol* **27**, 529-536 (2009).
74. Clark, W.H., Jr.*, et al.* A study of tumor progression: the precursor lesions of superficial spreading and nodular melanoma. *Hum Pathol* **15**, 1147-1165 (1984).

75. Chudnovsky, Y., Khavari, P.A. & Adams, A.E. Melanoma genetics and the development of rational therapeutics. *J Clin Invest* **115**, 813-824 (2005).
76. Seuradge, J. & Wong, E. Melanoma: Mcmaster Pathophysiology Review. Vol. 2016 (ed. Chaudhry, S.) (2015).
77. Bevona, C., Goggins, W., Quinn, T., Fullerton, J. & Tsao, H. Cutaneous melanomas associated with nevi. *Arch Dermatol* **139**, 1620-1624; discussion 1624 (2003).
78. Crucioli, V. & Stilwell, J. The histogenesis of malignant melanoma in relation to pre-existing pigmented lesions. *J Cutan Pathol* **9**, 396-404 (1982).
79. Marks, R., Dorevitch, A.P. & Mason, G. Do all melanomas come from "moles"? A study of the histological association between melanocytic naevi and melanoma. *Australas J Dermatol* **31**, 77-80 (1990).
80. Naeyaert, J.M. & Brochez, L. Clinical practice. Dysplastic nevi. *N Engl J Med* **349**, 2233-2240 (2003).
81. Sagebiel, R.W. Melanocytic nevi in histologic association with primary cutaneous melanoma of superficial spreading and nodular types: effect of tumor thickness. *J Invest Dermatol* **100**, 322S-325S (1993).
82. Takata, M., Murata, H. & Saida, T. Molecular pathogenesis of malignant melanoma: a different perspective from the studies of melanocytic nevus and acral melanoma. *Pigment Cell Melanoma Res* **23**, 64-71 (2010).
83. Damsky, W.E., Rosenbaum, L.E. & Bosenberg, M. Decoding melanoma metastasis. *Cancers (Basel)* **3**, 126-163 (2010).
84. Chin, L. The genetics of malignant melanoma: lessons from mouse and man. *Nat Rev Cancer* **3**, 559-570 (2003).
85. Ross, A.L., Sanchez, M.I. & Grichnik, J.M. Molecular nevogenesis. *Dermatol Res Pract* **2011**, 463184 (2011).
86. Bennett, D.C. Human melanocyte senescence and melanoma susceptibility genes. *Oncogene* **22**, 3063-3069 (2003).
87. Collado, M. & Serrano, M. Senescence in tumours: evidence from mice and humans. *Nat Rev Cancer* **10**, 51-57 (2010).
88. Mooi, W.J. & Peeper, D.S. Oncogene-induced cell senescence--halting on the road to cancer. *N Engl J Med* **355**, 1037-1046 (2006).
89. Bansal, R. & Nikiforov, M.A. Pathways of oncogene-induced senescence in human melanocytic cells. *Cell Cycle* **9**, 2782-2788 (2010).
90. Collado, M. & Serrano, M. The power and the promise of oncogene-induced senescence markers. *Nat Rev Cancer* **6**, 472-476 (2006).
91. Denoyelle, C*., et al.* Anti-oncogenic role of the endoplasmic reticulum differentially activated by mutations in the MAPK pathway. *Nat Cell Biol* **8**, 1053-1063 (2006).
92. Gray-Schopfer, V.C*., et al.* Cellular senescence in naevi and immortalisation in melanoma: a role for p16? *Br J Cancer* **95**, 496-505 (2006).
93. Healy, E*., et al.* Prognostic significance of allelic losses in primary melanoma. *Oncogene* **16**, 2213-2218 (1998).
94. Keller-Melchior, R., Schmidt, R. & Piepkorn, M. Expression of the tumor suppressor gene product p16INK4 in benign and malignant melanocytic lesions. *J Invest Dermatol* **110**, 932-938 (1998).
95. Kuilman, T., Michaloglou, C., Mooi, W.J. & Peeper, D.S. The essence of senescence. *Genes Dev* **24**, 2463-2479 (2010).
96. Maldonado, J.L., Timmerman, L., Fridlyand, J. & Bastian, B.C. Mechanisms of cell-cycle arrest in Spitz nevi with constitutive activation of the MAP-kinase pathway. *Am J Pathol* **164**, 1783-1787 (2004).
97. Michaloglou, C*., et al.* BRAFE600-associated senescence-like cell cycle arrest of human naevi. *Nature* **436**, 720-724 (2005).
98. Prieur, A. & Peeper, D.S. Cellular senescence in vivo: a barrier to tumorigenesis. *Curr Opin Cell Biol* **20**, 150-155 (2008).

99. Bianchi-Smiraglia, A. & Nikiforov, M.A. Controversial aspects of oncogene-induced senescence. *Cell Cycle* **11**, 4147-4151 (2012).
100. Cotter, M.A., Florell, S.R., Leachman, S.A. & Grossman, D. Absence of senescence-associated beta-galactosidase activity in human melanocytic nevi in vivo. *J Invest Dermatol* **127**, 2469-2471 (2007).
101. Gray-Schopfer, V.C., Soo, J.K. & Bennett, D.C. Comment on "Absence of senescence-associated beta-galactosidase activity in human melanocytic nevi in vivo". *J Invest Dermatol* **128**, 1581; author reply 1583-1584 (2008).
102. Michaloglou, C., Soengas, M.S., Mooi, W.J. & Peeper, D.S. Comment on "Absence of senescence-associated beta-galactosidase activity in human melanocytic nevi in vivo". *J Invest Dermatol* **128**, 1582-1583; author reply 1583-1584 (2008).
103. Tran, S.L*., et al.* Absence of distinguishing senescence traits in human melanocytic nevi. *J Invest Dermatol* **132**, 2226-2234 (2012).
104. Chin, L*., et al.* Cooperative effects of INK4a and ras in melanoma susceptibility in vivo. *Genes Dev* **11**, 2822-2834 (1997).
105. Dankort, D*., et al.* Braf(V600E) cooperates with Pten loss to induce metastatic melanoma. *Nat Genet* **41**, 544-552 (2009).
106. Kim, M. Cooperative interactions of PTEN deficiency and RAS activation in melanoma metastasis. *Small GTPases* **1**, 161-164 (2010).
107. Dovey, M., White, R.M. & Zon, L.I. Oncogenic NRAS cooperates with p53 loss to generate melanoma in zebrafish. *Zebrafish* **6**, 397-404 (2009).
108. Bardeesy, N*., et al.* Dual inactivation of RB and p53 pathways in RAS-induced melanomas. *Mol Cell Biol* **21**, 2144-2153 (2001).
109. Maertens, O*., et al.* Elucidating distinct roles for NF1 in melanomagenesis. *Cancer Discov* **3**, 338-349 (2013).
110. Cheung, M., Sharma, A., Madhunapantula, S.V. & Robertson, G.P. Akt3 and mutant V600E B-Raf cooperate to promote early melanoma development. *Cancer Res* **68**, 3429-3439 (2008).
111. Garraway, L.A*., et al.* Integrative genomic analyses identify MITF as a lineage survival oncogene amplified in malignant melanoma. *Nature* **436**, 117-122 (2005).
112. Gimotty, P.A*., et al.* Biologic and prognostic significance of dermal Ki67 expression, mitoses, and tumorigenicity in thin invasive cutaneous melanoma. *J Clin Oncol* **23**, 8048-8056 (2005).
113. Bennett, D.C. How to make a melanoma: what do we know of the primary clonal events? *Pigment Cell Melanoma Res* **21**, 27-38 (2008).
114. Mahabeleshwar, G.H. & Byzova, T.V. Angiogenesis in melanoma. *Semin Oncol* **34**, 555-565 (2007).
115. Kuzel, P. & Chien, A.J. *The Role of Cellular Differentiation and Cell Fate in Malignant Melanoma*, (INTECH Open Access Publisher, 2011).
116. Jensen, E.H*., et al.* Down-regulation of pro-apoptotic genes is an early event in the progression of malignant melanoma. *Ann Surg Oncol* **14**, 1416-1423 (2007).
117. Mueller, D.W. & Bosserhoff, A.K. Role of miRNAs in the progression of malignant melanoma. *Br J Cancer* **101**, 551-556 (2009).
118. Bonazzi, V.F., Stark, M.S. & Hayward, N.K. MicroRNA regulation of melanoma progression. *Melanoma Res* **22**, 101-113 (2012).
119. Redondo, P., Lloret, P., Idoate, M. & Inoges, S. Expression and serum levels of MMP-2 and MMP-9 during human melanoma progression. *Clin Exp Dermatol* **30**, 541-545 (2005).
120. Matarrese, P*., et al.* Cathepsin B inhibition interferes with metastatic potential of human melanoma: an in vitro and in vivo study. *Mol Cancer* **9**, 207 (2010).
121. Lade-Keller, J*., et al.* E- to N-cadherin switch in melanoma is associated with decreased expression of phosphatase and tensin homolog and cancer progression. *Br J Dermatol* **169**, 618-628 (2013).

122. van Kempen, L.C., van Muijen, G.N. & Ruiter, D.J. Melanoma progression in a changing environment. *Eur J Cell Biol* **86**, 65-67 (2007).
123. Brychtova, S.*, et al. Stromal Microenvironment Alterations in Malignant Melanoma*, (INTECH Open Access Publisher, 2011).
124. Postow, M.A., Harding, J. & Wolchok, J.D. Targeting immune checkpoints: releasing the restraints on anti-tumor immunity for patients with melanoma. *Cancer J* **18**, 153-159 (2012).
125. Karagiannis, P.*, et al.* IgG4 subclass antibodies impair antitumor immunity in melanoma. *J Clin Invest* **123**, 1457-1474 (2013).
126. Hoek, K.S. DNA microarray analyses of melanoma gene expression: a decade in the mines. *Pigment Cell Res* **20**, 466-484 (2007).
127. Haqq, C.*, et al.* The gene expression signatures of melanoma progression. *Proc Natl Acad Sci U S A* **102**, 6092-6097 (2005).
128. Smith, A.P., Hoek, K. & Becker, D. Whole-genome expression profiling of the melanoma progression pathway reveals marked molecular differences between nevi/melanoma in situ and advanced-stage melanomas. *Cancer Biol Ther* **4**, 1018-1029 (2005).
129. Riker, A.I.*, et al.* The gene expression profiles of primary and metastatic melanoma yields a transition point of tumor progression and metastasis. *BMC Med Genomics* **1**, 13 (2008).
130. Alonso, S.R.*, et al.* A high-throughput study in melanoma identifies epithelial-mesenchymal transition as a major determinant of metastasis. *Cancer Res* **67**, 3450-3460 (2007).
131. Bourgault-Villada, I.*, et al. Current Insight Into the Metastatic Process and Melanoma Cell Dissemination*, (INTECH Open Access Publisher, 2011).
132. Peinado, H., Lavotshkin, S. & Lyden, D. The secreted factors responsible for pre-metastatic niche formation: old sayings and new thoughts. *Semin Cancer Biol* **21**, 139-146 (2011).
133. Paget, S. The distribution of secondary growths in cancer of the breast. 1889. *Cancer Metastasis Rev* **8**, 98-101 (1889).
134. Liersch, R., Hirakawa, S., Berdel, W.E., Mesters, R.M. & Detmar, M. Induced lymphatic sinus hyperplasia in sentinel lymph nodes by VEGF-C as the earliest premetastatic indicator. *Int J Oncol* **41**, 2073-2078 (2012).
135. Rinderknecht, M. & Detmar, M. Tumor lymphangiogenesis and melanoma metastasis. *J Cell Physiol* **216**, 347-354 (2008).
136. Peinado, H.*, et al.* Melanoma exosomes educate bone marrow progenitor cells toward a pro-metastatic phenotype through MET. *Nat Med* **18**, 883-891 (2012).
137. Hood, J.L., San, R.S. & Wickline, S.A. Exosomes released by melanoma cells prepare sentinel lymph nodes for tumor metastasis. *Cancer Res* **71**, 3792-3801 (2011).
138. Goel, V.K., Lazar, A.J., Warneke, C.L., Redston, M.S. & Haluska, F.G. Examination of mutations in BRAF, NRAS, and PTEN in primary cutaneous melanoma. *J Invest Dermatol* **126**, 154-160 (2006).
139. Ribas, A. & Flaherty, K.T. BRAF targeted therapy changes the treatment paradigm in melanoma. *Nat Rev Clin Oncol* **8**, 426-433 (2011).
140. Holderfield, M., Deuker, M.M., McCormick, F. & McMahon, M. Targeting RAF kinases for cancer therapy: BRAF-mutated melanoma and beyond. *Nat Rev Cancer* **14**, 455-467 (2014).
141. Cantwell-Dorris, E.R., O'Leary, J.J. & Sheils, O.M. BRAFV600E: implications for carcinogenesis and molecular therapy. *Mol Cancer Ther* **10**, 385-394 (2011).
142. Mercer, K.E. & Pritchard, C.A. Raf proteins and cancer: B-Raf is identified as a mutational target. *Biochim Biophys Acta* **1653**, 25-40 (2003).
143. Carracedo, A. & Pandolfi, P.P. The PTEN-PI3K pathway: of feedbacks and cross-talks. *Oncogene* **27**, 5527-5541 (2008).
144. Robertson, G.P. Functional and therapeutic significance of Akt deregulation in malignant melanoma. *Cancer Metastasis Rev* **24**, 273-285 (2005).
145. Pomerantz, J.*, et al.* The Ink4a tumor suppressor gene product, p19Arf, interacts with MDM2 and neutralizes MDM2's inhibition of p53. *Cell* **92**, 713-723 (1998).

146. Flaherty, K.T., Hodi, F.S. & Fisher, D.E. From genes to drugs: targeted strategies for melanoma. *Nat Rev Cancer* **12**, 349-361 (2012).
147. Hodis, E.*, et al.* A landscape of driver mutations in melanoma. *Cell* **150**, 251-263 (2012).
148. Curtin, J.A., Busam, K., Pinkel, D. & Bastian, B.C. Somatic activation of KIT in distinct subtypes of melanoma. *J Clin Oncol* **24**, 4340-4346 (2006).
149. Kwei, K.A.*, et al.* Genomic profiling identifies TITF1 as a lineage-specific oncogene amplified in lung cancer. *Oncogene* **27**, 3635-3640 (2008).
150. Johnstone, C.N.*, et al.* Analysis of the regulation of the A33 antigen gene reveals intestine-specific mechanisms of gene expression. *J Biol Chem* **277**, 34531-34539 (2002).
151. Visakorpi, T.*, et al.* In vivo amplification of the androgen receptor gene and progression of human prostate cancer. *Nat Genet* **9**, 401-406 (1995).
152. Holst, F.*, et al.* Estrogen receptor alpha (ESR1) gene amplification is frequent in breast cancer. *Nat Genet* **39**, 655-660 (2007).
153. Garraway, L.A. & Sellers, W.R. Lineage dependency and lineage-survival oncogenes in human cancer. *Nat Rev Cancer* **6**, 593-602 (2006).
154. Garraway, L.A.*, et al.* "Lineage addiction" in human cancer: lessons from integrated genomics. *Cold Spring Harb Symp Quant Biol* **70**, 25-34 (2005).
155. Carreira, S.*, et al.* Mitf regulation of Dia1 controls melanoma proliferation and invasiveness. *Genes Dev* **20**, 3426-3439 (2006).
156. Du, J.*, et al.* Critical role of CDK2 for melanoma growth linked to its melanocyte-specific transcriptional regulation by MITF. *Cancer Cell* **6**, 565-576 (2004).
157. Haq, R.*, et al.* BCL2A1 is a lineage-specific antiapoptotic melanoma oncogene that confers resistance to BRAF inhibition. *Proc Natl Acad Sci U S A* **110**, 4321-4326 (2013).
158. McGill, G.G.*, et al.* Bcl2 regulation by the melanocyte master regulator Mitf modulates lineage survival and melanoma cell viability. *Cell* **109**, 707-718 (2002).
159. Chiaverini, C.*, et al.* Microphthalmia-associated transcription factor regulates RAB27A gene expression and controls melanosome transport. *J Biol Chem* **283**, 12635-12642 (2008).
160. Widlund, H.R. & Fisher, D.E. Microphthalamia-associated transcription factor: a critical regulator of pigment cell development and survival. *Oncogene* **22**, 3035-3041 (2003).
161. The Cancer Genome Atlas. Cancers Selected for Study. Vol. 2016 (2015).
162. Santos, G.C., Zielenska, M., Prasad, M. & Squire, J.A. Chromosome 6p amplification and cancer progression. *J Clin Pathol* **60**, 1-7 (2007).
163. Curtin, J.A.*, et al.* Distinct sets of genetic alterations in melanoma. *N Engl J Med* **353**, 2135-2147 (2005).
164. Namiki, T.*, et al.* Genomic alterations in primary cutaneous melanomas detected by metaphase comparative genomic hybridization with laser capture or manual microdissection: 6p gains may predict poor outcome. *Cancer Genet Cytogenet* **157**, 1-11 (2005).
165. Lin, L.*, et al.* Mechanisms underlying cancer growth and apoptosis by DEK overexpression in colorectal cancer. *PLoS One* **9**, e111260 (2014).
166. Ying, G. & Wu, Y. DEK: A novel early screening and prognostic marker for breast cancer. *Mol Med Rep* **12**, 7491-7495 (2015).
167. Wu, Q.*, et al.* DEK overexpression in uterine cervical cancers. *Pathol Int* **58**, 378-382 (2008).
168. Lin, L.J. & Chen, L.T. The role of DEK protein in hepatocellular carcinoma for progression and prognosis. *Pak J Med Sci* **29**, 778-782 (2013).
169. Yi, H.C.*, et al.* Overexpression of DEK gene is correlated with poor prognosis in hepatocellular carcinoma. *Mol Med Rep* **11**, 1318-1323 (2015).
170. Han, S.*, et al.* Clinicopathological significance of DEK overexpression in serous ovarian tumors. *Pathol Int* **59**, 443-447 (2009).
171. Hu, H.G., Illges, H., Gruss, C. & Knippers, R. Distribution of the chromatin protein DEK distinguishes active and inactive CD21/CR2 gene in pre- and mature B lymphocytes. *Int Immunol* **17**, 789-796 (2005).

172. Hu, H.G., Scholten, I., Gruss, C. & Knippers, R. The distribution of the DEK protein in mammalian chromatin. *Biochem Biophys Res Commun* **358**, 1008-1014 (2007).
173. Campillos, M., Garcia, M.A., Valdivieso, F. & Vazquez, J. Transcriptional activation by AP-2alpha is modulated by the oncogene DEK. *Nucleic Acids Res* **31**, 1571-1575 (2003).
174. Koleva, R.I.*, et al.* C/EBPalpha and DEK coordinately regulate myeloid differentiation. *Blood* **119**, 4878-4888 (2012).
175. Shibata, T.*, et al.* DEK oncoprotein regulates transcriptional modifiers and sustains tumor initiation activity in high-grade neuroendocrine carcinoma of the lung. *Oncogene* **29**, 4671-4681 (2010).
176. Kappes, F.*, et al.* The DEK oncoprotein is a Su(var) that is essential to heterochromatin integrity. *Genes Dev* **25**, 673-678 (2011).
177. Hollenbach, A.D., McPherson, C.J., Mientjes, E.J., Iyengar, R. & Grosveld, G. Daxx and histone deacetylase II associate with chromatin through an interaction with core histones and the chromatin-associated protein Dek. *J Cell Sci* **115**, 3319-3330 (2002).
178. Sammons, M.*, et al.* Negative regulation of the RelA/p65 transactivation function by the product of the DEK proto-oncogene. *J Biol Chem* **281**, 26802-26812 (2006).
179. Kim, D.W.*, et al.* Proteomic analysis of apoptosis related proteins regulated by proto-oncogene protein DEK. *J Cell Biochem* **106**, 1048-1059 (2009).
180. Ko, S.I.*, et al.* Regulation of histone acetyltransferase activity of p300 and PCAF by proto-oncogene protein DEK. *FEBS Lett* **580**, 3217-3222 (2006).
181. Mor-Vaknin, N.*, et al.* The DEK nuclear autoantigen is a secreted chemotactic factor. *Mol Cell Biol* **26**, 9484-9496 (2006).
182. Saha, A.K.*, et al.* Intercellular trafficking of the nuclear oncoprotein DEK. *Proc Natl Acad Sci U S A* **110**, 6847-6852 (2013).
183. Privette Vinnedge, L.M.*, et al.* The human DEK oncogene stimulates beta-catenin signaling, invasion and mammosphere formation in breast cancer. *Oncogene* **30**, 2741-2752 (2011).
184. Wise-Draper, T.M.*, et al.* DEK proto-oncogene expression interferes with the normal epithelial differentiation program. *Am J Pathol* **174**, 71-81 (2009).
185. Khodadoust, M.S.*, et al.* Melanoma proliferation and chemoresistance controlled by the DEK oncogene. *Cancer Res* **69**, 6405-6413 (2009).
186. Wise-Draper, T.M.*, et al.* Apoptosis inhibition by the human DEK oncoprotein involves interference with p53 functions. *Mol Cell Biol* **26**, 7506-7519 (2006).
187. Kappes, F.*, et al.* DEK is a poly(ADP-ribose) acceptor in apoptosis and mediates resistance to genotoxic stress. *Mol Cell Biol* **28**, 3245-3257 (2008).
188. Kavanaugh, G.M.*, et al.* The human DEK oncogene regulates DNA damage response signaling and repair. *Nucleic Acids Res* **39**, 7465-7476 (2011).
189. Wise-Draper, T.M.*, et al.* Overexpression of the cellular DEK protein promotes epithelial transformation in vitro and in vivo. *Cancer Res* **69**, 1792-1799 (2009).
190. Soares, L.M., Zanier, K., Mackereth, C., Sattler, M. & Valcarcel, J. Intron removal requires proofreading of U2AF/3' splice site recognition by DEK. *Science* **312**, 1961-1965 (2006).
191. McGarvey, T.*, et al.* The acute myeloid leukemia-associated protein, DEK, forms a splicing-dependent interaction with exon-product complexes. *J Cell Biol* **150**, 309-320 (2000).
192. Carro, M.S.*, et al.* DEK Expression is controlled by E2F and deregulated in diverse tumor types. *Cell Cycle* **5**, 1202-1207 (2006).
193. Sitwala, K.V., Adams, K. & Markovitz, D.M. YY1 and NF-Y binding sites regulate the transcriptional activity of the dek and dek-can promoter. *Oncogene* **21**, 8862-8870 (2002).
194. Privette Vinnedge, L.M., Ho, S.M., Wikenheiser-Brokamp, K.A. & Wells, S.I. The DEK oncogene is a target of steroid hormone receptor signaling in breast cancer. *PLoS One* **7**, e46985 (2012).
195. Kappes, F.*, et al.* Phosphorylation by protein kinase CK2 changes the DNA binding properties of the human chromatin protein DEK. *Mol Cell Biol* **24**, 6011-6020 (2004).
196. Sawatsubashi, S.*, et al.* A histone chaperone, DEK, transcriptionally coactivates a nuclear receptor. *Genes Dev* **24**, 159-170 (2010).

197. Cleary, J.*, et al.* p300/CBP-associated factor drives DEK into interchromatin granule clusters. *J Biol Chem* **280**, 31760-31767 (2005).
198. Cheung, T.H.*, et al.* Maintenance of muscle stem-cell quiescence by microRNA-489. *Nature* **482**, 524-528 (2012).
199. Riveiro-Falkenbach, E. & Soengas, M.S. Control of tumorigenesis and chemoresistance by the DEK oncogene. *Clin Cancer Res* **16**, 2932-2938 (2010).
200. Yi, J.H.*, et al.* Dacarbazine-based chemotherapy as first-line treatment in noncutaneous metastatic melanoma: multicenter, retrospective analysis in Asia. *Melanoma Res* **21**, 223-227 (2011).
201. Serrone, L., Zeuli, M., Sega, F.M. & Cognetti, F. Dacarbazine-based chemotherapy for metastatic melanoma: thirty-year experience overview. *J Exp Clin Cancer Res* **19**, 21-34 (2000).
202. Atkins, M.B., Kunkel, L., Sznol, M. & Rosenberg, S.A. High-dose recombinant interleukin-2 therapy in patients with metastatic melanoma: long-term survival update. *Cancer J Sci Am* **6 Suppl 1**, S11-14 (2000).
203. Atkins, M.B.*, et al.* High-dose recombinant interleukin 2 therapy for patients with metastatic melanoma: analysis of 270 patients treated between 1985 and 1993. *J Clin Oncol* **17**, 2105-2116 (1999).
204. Young, K., Minchom, A. & Larkin, J. BRIM-1, -2 and -3 trials: improved survival with vemurafenib in metastatic melanoma patients with a BRAF(V600E) mutation. *Future Oncol* **8**, 499-507 (2012).
205. Chapman, P.B.*, et al.* Improved survival with vemurafenib in melanoma with BRAF V600E mutation. *N Engl J Med* **364**, 2507-2516 (2011).
206. Flaherty, K.T.*, et al.* Improved survival with MEK inhibition in BRAF-mutated melanoma. *N Engl J Med* **367**, 107-114 (2012).
207. Kudchadkar, R., Paraiso, K.H. & Smalley, K.S. Targeting mutant BRAF in melanoma: current status and future development of combination therapy strategies. *Cancer J* **18**, 124-131 (2012).
208. Robert, L.*, et al.* Distinct immunological mechanisms of CTLA-4 and PD-1 blockade revealed by analyzing TCR usage in blood lymphocytes. *Oncoimmunology* **3**, e29244 (2014).
209. Hodi, F.S. Overcoming immunological tolerance to melanoma: Targeting CTLA-4. *Asia Pac J Clin Oncol* **6 Suppl 1**, S16-23 (2010).
210. Robert, C. & Ghiringhelli, F. What is the role of cytotoxic T lymphocyte-associated antigen 4 blockade in patients with metastatic melanoma? *Oncologist* **14**, 848-861 (2009).
211. Lipson, E.J.*, et al.* Durable cancer regression off-treatment and effective reinduction therapy with an anti-PD-1 antibody. *Clin Cancer Res* **19**, 462-468 (2013).
212. Brahmer, J.R.*, et al.* Safety and activity of anti-PD-L1 antibody in patients with advanced cancer. *N Engl J Med* **366**, 2455-2465 (2012).
213. Francisco, L.M., Sage, P.T. & Sharpe, A.H. The PD-1 pathway in tolerance and autoimmunity. *Immunol Rev* **236**, 219-242 (2010).
214. Tumeh, P.C.*, et al.* PD-1 blockade induces responses by inhibiting adaptive immune resistance. *Nature* **515**, 568-571 (2014).
215. Spranger, S., Bao, R. & Gajewski, T.F. Melanoma-intrinsic beta-catenin signalling prevents anti-tumour immunity. *Nature* **523**, 231-235 (2015).
216. Lawrence, M.S.*, et al.* Mutational heterogeneity in cancer and the search for new cancer-associated genes. *Nature* **499**, 214-218 (2013).
217. Berger, M.F.*, et al.* Melanoma genome sequencing reveals frequent PREX2 mutations. *Nature* **485**, 502-506 (2012).
218. Gerstberger, S., Hafner, M. & Tuschl, T. A census of human RNA-binding proteins. *Nat Rev Genet* **15**, 829-845 (2014).
219. Cooper, T.A., Wan, L. & Dreyfuss, G. RNA and disease. *Cell* **136**, 777-793 (2009).

220. Vindry, C., Vo Ngoc, L., Kruys, V. & Gueydan, C. RNA-binding protein-mediated post-transcriptional controls of gene expression: integration of molecular mechanisms at the 3' end of mRNAs? *Biochem Pharmacol* **89**, 431-440 (2014).
221. Glisovic, T., Bachorik, J.L., Yong, J. & Dreyfuss, G. RNA-binding proteins and post-transcriptional gene regulation. *FEBS Lett* **582**, 1977-1986 (2008).
222. Bywater, M.J., Pearson, R.B., McArthur, G.A. & Hannan, R.D. Dysregulation of the basal RNA polymerase transcription apparatus in cancer. *Nat Rev Cancer* **13**, 299-314 (2013).
223. Jurica, M.S. & Moore, M.J. Pre-mRNA splicing: awash in a sea of proteins. *Mol Cell* **12**, 5-14 (2003).
224. Wahl, M.C., Will, C.L. & Luhrmann, R. The spliceosome: design principles of a dynamic RNP machine. *Cell* **136**, 701-718 (2009).
225. Pan, Q., Shai, O., Lee, L.J., Frey, B.J. & Blencowe, B.J. Deep surveying of alternative splicing complexity in the human transcriptome by high-throughput sequencing. *Nat Genet* **40**, 1413-1415 (2008).
226. Mendes Soares, L.M. & Valcarcel, J. The expanding transcriptome: the genome as the 'Book of Sand'. *EMBO J* **25**, 923-931 (2006).
227. Nilsen, T.W. & Graveley, B.R. Expansion of the eukaryotic proteome by alternative splicing. *Nature* **463**, 457-463 (2010).
228. Nigita, G., Veneziano, D. & Ferro, A. A-to-I RNA Editing: Current Knowledge Sources and Computational Approaches with Special Emphasis on Non-Coding RNA Molecules. *Front Bioeng Biotechnol* **3**, 37 (2015).
229. Valente, L. & Nishikura, K. ADAR gene family and A-to-I RNA editing: diverse roles in posttranscriptional gene regulation. *Prog Nucleic Acid Res Mol Biol* **79**, 299-338 (2005).
230. Shoshan, E.*, et al.* Reduced adenosine-to-inosine miR-455-5p editing promotes melanoma growth and metastasis. *Nat Cell Biol* **17**, 311-321 (2015).
231. Pestova, T.V.*, et al.* Molecular mechanisms of translation initiation in eukaryotes. *Proc Natl Acad Sci U S A* **98**, 7029-7036 (2001).
232. Eckmann, C.R., Rammelt, C. & Wahle, E. Control of poly(A) tail length. *Wiley Interdiscip Rev RNA* **2**, 348-361 (2011).
233. Zhang, X., Virtanen, A. & Kleiman, F.E. To polyadenylate or to deadenylate: that is the question. *Cell Cycle* **9**, 4437-4449 (2010).
234. Pique, M., Lopez, J.M., Foissac, S., Guigo, R. & Mendez, R. A combinatorial code for CPE-mediated translational control. *Cell* **132**, 434-448 (2008).
235. Fernandez-Miranda, G. & Mendez, R. The CPEB-family of proteins, translational control in senescence and cancer. *Ageing Res Rev* **11**, 460-472 (2012).
236. Peng, S.S., Chen, C.Y., Xu, N. & Shyu, A.B. RNA stabilization by the AU-rich element binding protein, HuR, an ELAV protein. *EMBO J* **17**, 3461-3470 (1998).
237. Serini, S.*, et al.* DHA induces apoptosis and differentiation in human melanoma cells in vitro: involvement of HuR-mediated COX-2 mRNA stabilization and beta-catenin nuclear translocation. *Carcinogenesis* **33**, 164-173 (2012).
238. Chen, C.Y.*, et al.* AU binding proteins recruit the exosome to degrade ARE-containing mRNAs. *Cell* **107**, 451-464 (2001).
239. Kiesler, E., Miralles, F. & Visa, N. HEL/UAP56 binds cotranscriptionally to the Balbiani ring pre-mRNA in an intron-independent manner and accompanies the BR mRNP to the nuclear pore. *Curr Biol* **12**, 859-862 (2002).
240. Swinburne, I.A., Meyer, C.A., Liu, X.S., Silver, P.A. & Brodsky, A.S. Genomic localization of RNA binding proteins reveals links between pre-mRNA processing and transcription. *Genome Res* **16**, 912-921 (2006).
241. Viphakone, N.*, et al.* Luzp4 defines a new mRNA export pathway in cancer cells. *Nucleic Acids Res* **43**, 2353-2366 (2015).
242. Guil, S. & Caceres, J.F. The multifunctional RNA-binding protein hnRNP A1 is required for processing of miR-18a. *Nat Struct Mol Biol* **14**, 591-596 (2007).

243. Vanharanta, S*., et al.* Loss of the multifunctional RNA-binding protein RBM47 as a source of selectable metastatic traits in breast cancer. *Elife* **3**(2014).
244. Sawicka, K., Bushell, M., Spriggs, K.A. & Willis, A.E. Polypyrimidine-tract-binding protein: a multifunctional RNA-binding protein. *Biochem Soc Trans* **36**, 641-647 (2008).
245. Blech-Hermoni, Y., Stillwagon, S.J. & Ladd, A.N. Diversity and conservation of CELF1 and CELF2 RNA and protein expression patterns during embryonic development. *Dev Dyn* **242**, 767-777 (2013).
246. Yu, C*., et al.* Oral squamous cancer cell exploits hnRNP A1 to regulate cell cycle and proliferation. *J Cell Physiol* **230**, 2252-2261 (2015).
247. Gao, C., Yu, Z., Liu, S., Xin, H. & Li, X. Overexpression of CUGBP1 is associated with the progression of non-small cell lung cancer. *Tumour Biol* **36**, 4583-4589 (2015).
248. Darnell, R.B. RNA regulation in neurologic disease and cancer. *Cancer Res Treat* **42**, 125-129 (2010).
249. Castello, A., Fischer, B., Hentze, M.W. & Preiss, T. RNA-binding proteins in Mendelian disease. *Trends Genet* **29**, 318-327 (2013).
250. Kechavarzi, B. & Janga, S.C. Dissecting the expression landscape of RNA-binding proteins in human cancers. *Genome Biol* **15**, R14 (2014).
251. Dasgupta, T. & Ladd, A.N. The importance of CELF control: molecular and biological roles of the CUG-BP, Elav-like family of RNA-binding proteins. *Wiley Interdiscip Rev RNA* **3**, 104-121 (2012).
252. Barreau, C., Paillard, L., Mereau, A. & Osborne, H.B. Mammalian CELF/Bruno-like RNA-binding proteins: molecular characteristics and biological functions. *Biochimie* **88**, 515-525 (2006).
253. Amato, M.A*., et al.* Comparison of the expression patterns of five neural RNA binding proteins in the Xenopus retina. *J Comp Neurol* **481**, 331-339 (2005).
254. Wu, J., Li, C., Zhao, S. & Mao, B. Differential expression of the Brunol/CELF family genes during Xenopus laevis early development. *Int J Dev Biol* **54**, 209-214 (2010).
255. Tahara, N., Bessho, Y. & Matsui, T. Celf1 is required for formation of endoderm-derived organs in zebrafish. *Int J Mol Sci* **14**, 18009-18023 (2013).
256. Brimacombe, K.R. & Ladd, A.N. Cloning and embryonic expression patterns of the chicken CELF family. *Dev Dyn* **236**, 2216-2224 (2007).
257. Karunakaran, D.K*., et al.* The expression analysis of Sfrs10 and Celf4 during mouse retinal development. *Gene Expr Patterns* **13**, 425-436 (2013).
258. Ladd, A.N., Charlet, N. & Cooper, T.A. The CELF family of RNA binding proteins is implicated in cell-specific and developmentally regulated alternative splicing. *Mol Cell Biol* **21**, 1285-1296 (2001).
259. Ladd, A.N. & Cooper, T.A. Multiple domains control the subcellular localization and activity of ETR-3, a regulator of nuclear and cytoplasmic RNA processing events. *J Cell Sci* **117**, 3519-3529 (2004).
260. Lichtner, P*., et al.* Expression and mutation analysis of BRUNOL3, a candidate gene for heart and thymus developmental defects associated with partial monosomy 10p. *J Mol Med (Berl)* **80**, 431-442 (2002).
261. Meins, M*., et al.* Identification and characterization of murine Brunol4, a new member of the elav/bruno family. *Cytogenet Genome Res* **97**, 254-260 (2002).
262. Ladd, A.N., Nguyen, N.H., Malhotra, K. & Cooper, T.A. CELF6, a member of the CELF family of RNA-binding proteins, regulates muscle-specific splicing enhancer-dependent alternative splicing. *J Biol Chem* **279**, 17756-17764 (2004).
263. Dev, A*., et al.* Mice deficient for RNA-binding protein brunol1 show reduction of spermatogenesis but are fertile. *Mol Reprod Dev* **74**, 1456-1464 (2007).
264. Horb, L.D. & Horb, M.E. BrunoL1 regulates endoderm proliferation through translational enhancement of cyclin A2 mRNA. *Dev Biol* **345**, 156-169 (2010).

265. Halgren, C.*, et al.* Haploinsufficiency of CELF4 at 18q12.2 is associated with developmental and behavioral disorders, seizures, eye manifestations, and obesity. *Eur J Hum Genet* **20**, 1315-1319 (2012).
266. Sun, W.*, et al.* Aberrant sodium channel activity in the complex seizure disorder of Celf4 mutant mice. *J Physiol* **591**, 241-255 (2013).
267. Yang, Y.*, et al.* Complex seizure disorder caused by Brunol4 deficiency in mice. *PLoS Genet* **3**, e124 (2007).
268. Dougherty, J.D.*, et al.* The disruption of Celf6, a gene identified by translational profiling of serotonergic neurons, results in autism-related behaviors. *J Neurosci* **33**, 2732-2753 (2013).
269. Levers, T.E., Tait, S., Birling, M.C., Brophy, P.J. & Price, D.J. Etr-r3/mNapor, encoding an ELAV-type RNA binding protein, is expressed in differentiating cells in the developing rodent forebrain. *Mech Dev* **112**, 191-193 (2002).
270. Naha, N.*, et al.* Ethanol inhibited apoptosis-related RNA binding protein, Napor-3 gene expression in the prenatal rat brain. *Med Sci Monit* **15**, BR6-12 (2009).
271. Otsuka, N.*, et al.* Transcriptional induction and translational inhibition of Arc and Cugbp2 in mice hippocampus after transient global ischemia under normothermic condition. *Brain Res* **1287**, 136-145 (2009).
272. Pacini, A.*, et al.* NAPOR-3 RNA binding protein is required for apoptosis in hippocampus. *Brain Res Mol Brain Res* **140**, 34-44 (2005).
273. Zhang, W., Liu, H., Han, K. & Grabowski, P.J. Region-specific alternative splicing in the nervous system: implications for regulation by the RNA-binding protein NAPOR. *RNA* **8**, 671-685 (2002).
274. Ladd, A.N. CUG-BP, Elav-like family (CELF)-mediated alternative splicing regulation in the brain during health and disease. *Mol Cell Neurosci* **56**, 456-464 (2013).
275. Lu, X., Timchenko, N.A. & Timchenko, L.T. Cardiac elav-type RNA-binding protein (ETR-3) binds to RNA CUG repeats expanded in myotonic dystrophy. *Hum Mol Genet* **8**, 53-60 (1999).
276. Subramaniam, D.*, et al.* RNA binding protein CUGBP2/CELF2 mediates curcumin-induced mitotic catastrophe of pancreatic cancer cells. *PLoS One* **6**, e16958 (2011).
277. Mukhopadhyay, D., Houchen, C.W., Kennedy, S., Dieckgraefe, B.K. & Anant, S. Coupled mRNA stabilization and translational silencing of cyclooxygenase-2 by a novel RNA binding protein, CUGBP2. *Mol Cell* **11**, 113-126 (2003).
278. Natarajan, G.*, et al.* CUGBP2 downregulation by prostaglandin E2 protects colon cancer cells from radiation-induced mitotic catastrophe. *Am J Physiol Gastrointest Liver Physiol* **294**, G1235-1244 (2008).
279. Ramalingam, S., Ramamoorthy, P., Subramaniam, D. & Anant, S. Reduced Expression of RNA Binding Protein CELF2, a Putative Tumor Suppressor Gene in Colon Cancer. *Immunogastroenterology* **1**, 27-33 (2012).
280. Mukhopadhyay, D.*, et al.* CUGBP2 plays a critical role in apoptosis of breast cancer cells in response to genotoxic injury. *Ann N Y Acad Sci* **1010**, 504-509 (2003).
281. Murmu, N.*, et al.* Dynamic antagonism between RNA-binding protein CUGBP2 and cyclooxygenase-2-mediated prostaglandin E2 in radiation damage. *Proc Natl Acad Sci U S A* **101**, 13873-13878 (2004).
282. Subramaniam, D.*, et al.* Translation inhibition during cell cycle arrest and apoptosis: Mcl-1 is a novel target for RNA binding protein CUGBP2. *Am J Physiol Gastrointest Liver Physiol* **294**, G1025-1032 (2008).
283. Masuda, A.*, et al.* CUGBP1 and MBNL1 preferentially bind to 3' UTRs and facilitate mRNA decay. *Sci Rep* **2**, 209 (2012).
284. Rattenbacher, B.*, et al.* Analysis of CUGBP1 targets identifies GU-repeat sequences that mediate rapid mRNA decay. *Mol Cell Biol* **30**, 3970-3980 (2010).
285. Timchenko, N.A., Iakova, P., Cai, Z.J., Smith, J.R. & Timchenko, L.T. Molecular basis for impaired muscle differentiation in myotonic dystrophy. *Mol Cell Biol* **21**, 6927-6938 (2001).

286. Timchenko, L.T.*, et al.* Identification of a (CUG)n triplet repeat RNA-binding protein and its expression in myotonic dystrophy. *Nucleic Acids Res* **24**, 4407-4414 (1996).
287. Michalowski, S.*, et al.* Visualization of double-stranded RNAs from the myotonic dystrophy protein kinase gene and interactions with CUG-binding protein. *Nucleic Acids Res* **27**, 3534-3542 (1999).
288. Takahashi, N., Sasagawa, N., Suzuki, K. & Ishiura, S. The CUG-binding protein binds specifically to UG dinucleotide repeats in a yeast three-hybrid system. *Biochem Biophys Res Commun* **277**, 518-523 (2000).
289. Vlasova, I.A.*, et al.* Conserved GU-rich elements mediate mRNA decay by binding to CUG-binding protein 1. *Mol Cell* **29**, 263-270 (2008).
290. Edwards, J.*, et al.* Sequence determinants for the tandem recognition of UGU and CUG rich RNA elements by the two N--terminal RRMs of CELF1. *Nucleic Acids Res* **39**, 8638-8650 (2011).
291. Teplova, M., Song, J., Gaw, H.Y., Teplov, A. & Patel, D.J. Structural insights into RNA recognition by the alternate-splicing regulator CUG-binding protein 1. *Structure* **18**, 1364-1377 (2010).
292. Tsuda, K.*, et al.* Structural basis for the sequence-specific RNA-recognition mechanism of human CUG-BP1 RRM3. *Nucleic Acids Res* **37**, 5151-5166 (2009).
293. Mori, D., Sasagawa, N., Kino, Y. & Ishiura, S. Quantitative analysis of CUG-BP1 binding to RNA repeats. *J Biochem* **143**, 377-383 (2008).
294. Huichalaf, C.H., Sakai, K., Wang, G.L., Timchenko, N.A. & Timchenko, L. Regulation of the promoter of CUG triplet repeat binding protein, Cugbp1, during myogenesis. *Gene* **396**, 391-402 (2007).
295. Kalsotra, A., Wang, K., Li, P.F. & Cooper, T.A. MicroRNAs coordinate an alternative splicing network during mouse postnatal heart development. *Genes Dev* **24**, 653-658 (2010).
296. Xiao, L.*, et al.* Regulation of cyclin-dependent kinase 4 translation through CUG-binding protein 1 and microRNA-222 by polyamines. *Mol Biol Cell* **22**, 3055-3069 (2011).
297. Cui, Y.H.*, et al.* miR-503 represses CUG-binding protein 1 translation by recruiting CUGBP1 mRNA to processing bodies. *Mol Biol Cell* **23**, 151-162 (2012).
298. Kuyumcu-Martinez, N.M., Wang, G.S. & Cooper, T.A. Increased steady-state levels of CUGBP1 in myotonic dystrophy 1 are due to PKC-mediated hyperphosphorylation. *Mol Cell* **28**, 68-78 (2007).
299. Wang, G.S.*, et al.* PKC inhibition ameliorates the cardiac phenotype in a mouse model of myotonic dystrophy type 1. *J Clin Invest* **119**, 3797-3806 (2009).
300. Salisbury, E.*, et al.* Ectopic expression of cyclin D3 corrects differentiation of DM1 myoblasts through activation of RNA CUG-binding protein, CUGBP1. *Exp Cell Res* **314**, 2266-2278 (2008).
301. Timchenko, L.T.*, et al.* Age-specific CUGBP1-eIF2 complex increases translation of CCAAT/enhancer-binding protein beta in old liver. *J Biol Chem* **281**, 32806-32819 (2006).
302. Savkur, R.S., Philips, A.V. & Cooper, T.A. Aberrant regulation of insulin receptor alternative splicing is associated with insulin resistance in myotonic dystrophy. *Nat Genet* **29**, 40-47 (2001).
303. Ho, T.H., Bundman, D., Armstrong, D.L. & Cooper, T.A. Transgenic mice expressing CUG-BP1 reproduce splicing mis-regulation observed in myotonic dystrophy. *Hum Mol Genet* **14**, 1539-1547 (2005).
304. Paul, S.*, et al.* Interaction of muscleblind, CUG-BP1 and hnRNP H proteins in DM1-associated aberrant IR splicing. *EMBO J* **25**, 4271-4283 (2006).
305. Orengo, J.P.*, et al.* Expanded CTG repeats within the DMPK 3' UTR causes severe skeletal muscle wasting in an inducible mouse model for myotonic dystrophy. *Proc Natl Acad Sci U S A* **105**, 2646-2651 (2008).
306. Ladd, A.N., Taffet, G., Hartley, C., Kearney, D.L. & Cooper, T.A. Cardiac tissue-specific repression of CELF activity disrupts alternative splicing and causes cardiomyopathy. *Mol Cell Biol* **25**, 6267-6278 (2005).

307. Suzuki, H., Jin, Y., Otani, H., Yasuda, K. & Inoue, K. Regulation of alternative splicing of alpha-actinin transcript by Bruno-like proteins. *Genes Cells* **7**, 133-141 (2002).
308. Philips, A.V., Timchenko, L.T. & Cooper, T.A. Disruption of splicing regulated by a CUG-binding protein in myotonic dystrophy. *Science* **280**, 737-741 (1998).
309. Welm, A.L., Mackey, S.L., Timchenko, L.T., Darlington, G.J. & Timchenko, N.A. Translational induction of liver-enriched transcriptional inhibitory protein during acute phase response leads to repression of CCAAT/enhancer binding protein alpha mRNA. *J Biol Chem* **275**, 27406-27413 (2000).
310. Gromak, N., Matlin, A.J., Cooper, T.A. & Smith, C.W. Antagonistic regulation of alpha-actinin alternative splicing by CELF proteins and polypyrimidine tract binding protein. *RNA* **9**, 443-456 (2003).
311. Timchenko, N.A*., et al.* Overexpression of CUG triplet repeat-binding protein, CUGBP1, in mice inhibits myogenesis. *J Biol Chem* **279**, 13129-13139 (2004).
312. Baldwin, B.R., Timchenko, N.A. & Zahnow, C.A. Epidermal growth factor receptor stimulation activates the RNA binding protein CUG-BP1 and increases expression of C/EBPbeta-LIP in mammary epithelial cells. *Mol Cell Biol* **24**, 3682-3691 (2004).
313. Timchenko, N.A., Wang, G.L. & Timchenko, L.T. RNA CUG-binding protein 1 increases translation of 20-kDa isoform of CCAAT/enhancer-binding protein beta by interacting with the alpha and beta subunits of eukaryotic initiation translation factor 2. *J Biol Chem* **280**, 20549-20557 (2005).
314. Bae, E.J. & Kim, S.G. Enhanced CCAAT/enhancer-binding protein beta-liver-enriched inhibitory protein production by Oltipraz, which accompanies CUG repeat-binding protein-1 (CUGBP1) RNA-binding protein activation, leads to inhibition of preadipocyte differentiation. *Mol Pharmacol* **68**, 660-669 (2005).
315. Mahadevan, M.S*., et al.* Reversible model of RNA toxicity and cardiac conduction defects in myotonic dystrophy. *Nat Genet* **38**, 1066-1070 (2006).
316. Dudaronek, J.M., Barber, S.A. & Clements, J.E. CUGBP1 is required for IFNbeta-mediated induction of dominant-negative CEBPbeta and suppression of SIV replication in macrophages. *J Immunol* **179**, 7262-7269 (2007).
317. Daughters, R.S*., et al.* RNA gain-of-function in spinocerebellar ataxia type 8. *PLoS Genet* **5**, e1000600 (2009).
318. Yu, Z., Wang, A.M., Robins, D.M. & Lieberman, A.P. Altered RNA splicing contributes to skeletal muscle pathology in Kennedy disease knock-in mice. *Dis Model Mech* **2**, 500-507 (2009).
319. Ward, A.J., Rimer, M., Killian, J.M., Dowling, J.J. & Cooper, T.A. CUGBP1 overexpression in mouse skeletal muscle reproduces features of myotonic dystrophy type 1. *Hum Mol Genet* **19**, 3614-3622 (2010).
320. Sureau, A., Sauliere, J., Expert-Bezancon, A. & Marie, J. CELF and PTB proteins modulate the inclusion of the beta-tropomyosin exon 6B during myogenic differentiation. *Exp Cell Res* **317**, 94-106 (2011).
321. Xiao, Q*., et al.* Bcl-x pre-mRNA splicing regulates brain injury after neonatal hypoxia-ischemia. *J Neurosci* **32**, 13587-13596 (2012).
322. Timchenko, N.A., Welm, A.L., Lu, X. & Timchenko, L.T. CUG repeat binding protein (CUGBP1) interacts with the 5' region of C/EBPbeta mRNA and regulates translation of C/EBPbeta isoforms. *Nucleic Acids Res* **27**, 4517-4525 (1999).
323. Iakova, P*., et al.* Competition of CUGBP1 and calreticulin for the regulation of p21 translation determines cell fate. *EMBO J* **23**, 406-417 (2004).
324. Luedde, T*., et al.* C/EBP beta isoforms LIP and LAP modulate progression of the cell cycle in the regenerating mouse liver. *Hepatology* **40**, 356-365 (2004).
325. Fox, J.T. & Stover, P.J. Mechanism of the internal ribosome entry site-mediated translation of serine hydroxymethyltransferase 1. *J Biol Chem* **284**, 31085-31096 (2009).
326. Zheng, Y. & Miskimins, W.K. CUG-binding protein represses translation of p27Kip1 mRNA through its internal ribosomal entry site. *RNA Biol* **8**, 365-371 (2011).

327. Beisang, D., Rattenbacher, B., Vlasova-St Louis, I.A. & Bohjanen, P.R. Regulation of CUG-binding protein 1 (CUGBP1) binding to target transcripts upon T cell activation. *J Biol Chem* **287**, 950-960 (2012).
328. Moraes, K.C., Wilusz, C.J. & Wilusz, J. CUG-BP binds to RNA substrates and recruits PARN deadenylase. *RNA* **12**, 1084-1091 (2006).
329. Katoh, T., Hojo, H. & Suzuki, T. Destabilization of microRNAs in human cells by 3' deadenylation mediated by PARN and CUGBP1. *Nucleic Acids Res* **43**, 7521-7534 (2015).
330. Graindorge, A*., et al.* Identification of CUG-BP1/EDEN-BP target mRNAs in Xenopus tropicalis. *Nucleic Acids Res* **36**, 1861-1870 (2008).
331. An integrated encyclopedia of DNA elements in the human genome. *Nature* **489**, 57-74 (2012).
332. Blech-Hermoni, Y., Dasgupta, T., Coram, R.J. & Ladd, A.N. Identification of Targets of CUG-BP, Elav-Like Family Member 1 (CELF1) Regulation in Embryonic Heart Muscle. *PLoS One* **11**, e0149061 (2016).
333. Wang, E.T*., et al.* Antagonistic regulation of mRNA expression and splicing by CELF and MBNL proteins. *Genome Res* **25**, 858-871 (2015).
334. Blech-Hermoni, Y. & Ladd, A.N. Identification of transcripts regulated by CUG-BP, Elav-like family member 1 (CELF1) in primary embryonic cardiomyocytes by RNA-seq. *Genom Data* **6**, 74-76 (2015).
335. Lee, J.E., Lee, J.Y., Wilusz, J., Tian, B. & Wilusz, C.J. Systematic analysis of cis-elements in unstable mRNAs demonstrates that CUGBP1 is a key regulator of mRNA decay in muscle cells. *PLoS One* **5**, e11201 (2010).
336. Wang, X*., et al.* CUG-binding protein 1 (CUGBP1) expression and prognosis of brain metastases from non-small cell lung cancer. *Thorac Cancer* **7**, 32-38 (2016).
337. Jiao, W*., et al.* CUG-binding protein 1 (CUGBP1) expression and prognosis of non-small cell lung cancer. *Clin Transl Oncol* **15**, 789-795 (2013).
338. Liu, Y*., et al.* Suppression of CUGBP1 inhibits growth of hepatocellular carcinoma cells. *Clin Invest Med* **37**, E10-18 (2014).
339. Wang, X., Wang, H., Ji, F., Zhao, S. & Fang, X. Lentivirus-mediated knockdown of CUGBP1 suppresses gastric cancer cell proliferation in vitro. *Appl Biochem Biotechnol* **173**, 1529-1536 (2014).
340. Chang, E.T*., et al.* The RNA-binding protein CUG-BP1 increases survivin expression in oesophageal cancer cells through enhanced mRNA stability. *Biochem J* **446**, 113-123 (2012).
341. Le Tonqueze, O*., et al.* Chromosome wide analysis of CUGBP1 binding sites identifies the tetraspanin CD9 mRNA as a target for CUGBP1-mediated down-regulation. *Biochem Biophys Res Commun* **394**, 884-889 (2010).
342. Lu, H*., et al.* CUGBP1 promotes cell proliferation and suppresses apoptosis via down-regulating C/EBPalpha in human non-small cell lung cancers. *Med Oncol* **32**, 82 (2015).
343. Fernandez, Y*., et al.* Differential regulation of noxa in normal melanocytes and melanoma cells by proteasome inhibition: therapeutic implications. *Cancer Res* **65**, 6294-6304 (2005).
344. Arnal-Estape, A*., et al.* HER2 silences tumor suppression in breast cancer cells by switching expression of C/EBPss isoforms. *Cancer Res* **70**, 9927-9936 (2010).
345. Gratzner, H.G., Leif, R.C., Ingram, D.J. & Castro, A. The use of antibody specific for bromodeoxyuridine for the immunofluorescent determination of DNA replication in single cells and chromosomes. *Exp Cell Res* **95**, 88-94 (1975).
346. Watson, J.V., Chambers, S.H. & Smith, P.J. A pragmatic approach to the analysis of DNA histograms with a definable G1 peak. *Cytometry* **8**, 1-8 (1987).
347. Alonso-Curbelo, D*., et al.* RAB7 controls melanoma progression by exploiting a lineage-specific wiring of the endolysosomal pathway. *Cancer Cell* **26**, 61-76 (2014).
348. Carro, A., Perez-Martinez, M., Soriano, J., Pisano, D.G. & Megias, D. iMSRC: converting a standard automated microscope into an intelligent screening platform. *Sci Rep* **5**, 10502 (2015).

349. Cock, P.J., Fields, C.J., Goto, N., Heuer, M.L. & Rice, P.M. The Sanger FASTQ file format for sequences with quality scores, and the Solexa/Illumina FASTQ variants. *Nucleic Acids Res* **38**, 1767-1771 (2010).
350. Andrews, S. FASTQC. Vol. 2016 (2016).
351. Trapnell, C*., et al.* Differential gene and transcript expression analysis of RNA-seq experiments with TopHat and Cufflinks. *Nat Protoc* **7**, 562-578 (2012).
352. Langmead, B., Trapnell, C., Pop, M. & Salzberg, S.L. Ultrafast and memory-efficient alignment of short DNA sequences to the human genome. *Genome Biol* **10**, R25 (2009).
353. Li, H*., et al.* The Sequence Alignment/Map format and SAMtools. *Bioinformatics* **25**, 2078-2079 (2009).
354. Uren, P.J*., et al.* Site identification in high-throughput RNA-protein interaction data. *Bioinformatics* **28**, 3013-3020 (2012).
355. Salmon-Divon, M., Dvinge, H., Tammoja, K. & Bertone, P. PeakAnalyzer: genome-wide annotation of chromatin binding and modification loci. *BMC Bioinformatics* **11**, 415 (2010).
356. Chen, Y*., et al.* Ensembl variation resources. *BMC Genomics* **11**, 293 (2010).
357. Quinlan, A.R. BEDTools: The Swiss-Army Tool for Genome Feature Analysis. *Curr Protoc Bioinformatics* **47**, 11 12 11-11 12 34 (2014).
358. Marass, F. & Upton, C. Sequence Searcher: A Java tool to perform regular expression and fuzzy searches of multiple DNA and protein sequences. *BMC Res Notes* **2**, 14 (2009).
359. Bailey, T.L. DREME: motif discovery in transcription factor ChIP-seq data. *Bioinformatics* **27**, 1653-1659 (2011).
360. Dudoit, S., Gentleman, R.C. & Quackenbush, J. Open source software for the analysis of microarray data. *Biotechniques* **Suppl**, 45-51 (2003).
361. Ritchie, M.E*., et al.* limma powers differential expression analyses for RNA-sequencing and microarray studies. *Nucleic Acids Res* **43**, e47 (2015).
362. Ritchie, M.E*., et al.* A comparison of background correction methods for two-colour microarrays. *Bioinformatics* **23**, 2700-2707 (2007).
363. Yang, Y.H*., et al.* Normalization for cDNA microarray data: a robust composite method addressing single and multiple slide systematic variation. *Nucleic Acids Res* **30**, e15 (2002).
364. Wang, E*., et al.* Global profiling of alternative splicing events and gene expression regulated by hnRNPH/F. *PLoS One* **7**, e51266 (2012).
365. Gandoura, S*., et al.* Gene- and exon-expression profiling reveals an extensive LPS-induced response in immune cells in patients with cirrhosis. *J Hepatol* **58**, 936-948 (2013).
366. de la Grange, P., Dutertre, M., Martin, N. & Auboeuf, D. FAST DB: a website resource for the study of the expression regulation of human gene products. *Nucleic Acids Res* **33**, 4276-4284 (2005).
367. de la Grange, P., Dutertre, M., Correa, M. & Auboeuf, D. A new advance in alternative splicing databases: from catalogue to detailed analysis of regulation of expression and function of human alternative splicing variants. *BMC Bioinformatics* **8**, 180 (2007).
368. Shannon, P*., et al.* Cytoscape: a software environment for integrated models of biomolecular interaction networks. *Genome Res* **13**, 2498-2504 (2003).
369. Bindea, G*., et al.* ClueGO: a Cytoscape plug-in to decipher functionally grouped gene ontology and pathway annotation networks. *Bioinformatics* **25**, 1091-1093 (2009).
370. Subramanian, A*., et al.* Gene set enrichment analysis: a knowledge-based approach for interpreting genome-wide expression profiles. *Proc Natl Acad Sci U S A* **102**, 15545-15550 (2005).
371. Jensen, L.J*., et al.* STRING 8--a global view on proteins and their functional interactions in 630 organisms. *Nucleic Acids Res* **37**, D412-416 (2009).
372. Oliveros, J. VENNY: An interactive tool for comparing lists with Venn diagrams., Vol. 2015 (2007-2015).
373. Bardou, P., Mariette, J., Escudie, F., Djemiel, C. & Klopp, C. jvenn: an interactive Venn diagram viewer. *BMC Bioinformatics* **15**, 293 (2014).
374. TCGA. Genomic Classification of Cutaneous Melanoma. *Cell* **161**, 1681-1696 (2015).

375. Relogio, A.*, et al.* Alternative splicing microarrays reveal functional expression of neuron-specific regulators in Hodgkin lymphoma cells. *J Biol Chem* **280**, 4779-4784 (2005).
376. Soengas, M.S.*, et al.* Apaf-1 and caspase-9 in p53-dependent apoptosis and tumor inhibition. *Science* **284**, 156-159 (1999).
377. Gupta, P.B.*, et al.* The melanocyte differentiation program predisposes to metastasis after neoplastic transformation. *Nat Genet* **37**, 1047-1054 (2005).
378. Raj, D., Liu, T., Samadashwily, G., Li, F. & Grossman, D. Survivin repression by p53, Rb and E2F2 in normal human melanocytes. *Carcinogenesis* **29**, 194-201 (2008).
379. Stacey, D. & Kazlauskas, A. Regulation of Ras signaling by the cell cycle. *Curr Opin Genet Dev* **12**, 44-46 (2002).
380. Prakash, M., Kale, S., Ghosh, I., Kundu, G.C. & Datta, K. Hyaluronan-binding protein 1 (HABP1/p32/gC1qR) induces melanoma cell migration and tumor growth by NF-kappa B dependent MMP-2 activation through integrin alpha(v)beta(3) interaction. *Cell Signal* **23**, 1563-1577 (2011).
381. de Wit, N.J., Burtscher, H.J., Weidle, U.H., Ruiter, D.J. & van Muijen, G.N. Differentially expressed genes identified in human melanoma cell lines with different metastatic behaviour using high density oligonucleotide arrays. *Melanoma Res* **12**, 57-69 (2002).
382. Pinzaglia, M.*, et al.* EIF6 over-expression increases the motility and invasiveness of cancer cells by modulating the expression of a critical subset of membrane-bound proteins. *BMC Cancer* **15**, 131 (2015).
383. Silver, D.L., Leeds, K.E., Hwang, H.W., Miller, E.E. & Pavan, W.J. The EJC component Magoh regulates proliferation and expansion of neural crest-derived melanocytes. *Dev Biol* **375**, 172-181 (2013).
384. Marzese, D.M.*, et al.* Brain metastasis is predetermined in early stages of cutaneous melanoma by CD44v6 expression through epigenetic regulation of the spliceosome. *Pigment Cell Melanoma Res* **28**, 82-93 (2015).
385. Quidville, V.*, et al.* Targeting the deregulated spliceosome core machinery in cancer cells triggers mTOR blockade and autophagy. *Cancer Res* **73**, 2247-2258 (2013).
386. Dewaele, M.*, et al.* Antisense oligonucleotide-mediated MDM4 exon 6 skipping impairs tumor growth. *J Clin Invest* **126**, 68-84 (2016).
387. Lianoglou, S., Garg, V., Yang, J.L., Leslie, C.S. & Mayr, C. Ubiquitously transcribed genes use alternative polyadenylation to achieve tissue-specific expression. *Genes Dev* **27**, 2380-2396 (2013).
388. Wang, E.T.*, et al.* Alternative isoform regulation in human tissue transcriptomes. *Nature* **456**, 470-476 (2008).
389. Fu, X.D. & Ares, M., Jr. Context-dependent control of alternative splicing by RNA-binding proteins. *Nat Rev Genet* **15**, 689-701 (2014).
390. Gardiner, A.S., Twiss, J.L. & Perrone-Bizzozero, N.I. Competing Interactions of RNA-Binding Proteins, MicroRNAs, and Their Targets Control Neuronal Development and Function. *Biomolecules* **5**, 2903-2918 (2015).
391. Ho, J.J. & Marsden, P.A. Competition and collaboration between RNA-binding proteins and microRNAs. *Wiley Interdiscip Rev RNA* **5**, 69-86 (2014).
392. Liu, L.*, et al.* Competition between RNA-binding proteins CELF1 and HuR modulates MYC translation and intestinal epithelium renewal. *Mol Biol Cell* **26**, 1797-1810 (2015).
393. Huichalaf, C.*, et al.* Expansion of CUG RNA repeats causes stress and inhibition of translation in myotonic dystrophy 1 (DM1) cells. *FASEB J* **24**, 3706-3719 (2010).
394. Macheret, M. & Halazonetis, T.D. DNA replication stress as a hallmark of cancer. *Annu Rev Pathol* **10**, 425-448 (2015).
395. Deutzmann, A.*, et al.* The human oncoprotein and chromatin architectural factor DEK counteracts DNA replication stress. *Oncogene* **34**, 4270-4277 (2015).

X.

APPENDICES

APÉNDICES

1. SUPPLEMENTARY TABLES

Supplementary Table 1: List of mRNA binding proteins (n=692), their domains and counts of the domains in the protein structure are indicated. %: Percentage of melanoma patients with mutations or copy number variations (n=478, data retrieved from TCGA).

GENE	DOMAIN [COUNT]	%
A1CF	RRM_1[2],DND1_DSRM[1],RRM_6[1]	7.32
ABCF1	ABC_tran_2[1],ABC_tran[2]	4.81
ABT1	RRM_6[1]	4.18
ACIN1	SAP[1],RRM_5[1]	2.51
ACO1	Aconitase_C[1],Aconitase[1]	2.51
ADAD1	A_deamin[1],dsrm[1]	3.13
ADAD2	A_deamin[1],dsrm[1]	2.51
ADAR	A_deamin[1],z-alpha[2],dsrm[3]	4.18
ADARB1	A_deamin[1],dsrm[2]	2.51
ADARB2	A_deamin[1],dsrm[2]	4.39
AFF1	AF-4[1]	3.55
AFF2	AF-4[1]	5.64
AFF3	AF-4[1]	5.23
AFF4	AF-4[1]	5.02
AGFG1	ArfGap[1]	1.67
AKAP1	TUDOR[1],KH_1[1],DUF3552[1]	5.23
AKAP17A	.	1.04
AKAP8	AKAP95[1]	1.67
AKAP8L	AKAP95[1]	1.25
ALKBH1	2OG-FeII_Oxy_2[1]	1.46
ALKBH5	2OG-FeII_Oxy_2[1]	1.04
ALYREF	FoP_duplication[1],RRM_1[1],FYTT[1]	4.18
ANGEL1	Exo_endo_phos[1]	2.71
ANGEL2	Exo_endo_phos[1]	3.13
APEX1	Exo_endo_phos[1]	0.62
API5	API5[1]	0.83
APOBEC1	APOBEC_N[1]	1.88
APOBEC2	APOBEC_N[1]	3.97
APOBEC3F	APOBEC_N[2]	1.88
APOBEC3G	APOBEC_N[2]	2.3
APOBEC4	APOBEC_N[1]	2.92
AQR	AAA_11[1],AAA_12[1]	4.6
ARHGEF28	PH[1],RhoGEF[1],C1_1[1]	3.97
ARL6IP4	SR-25[1]	1.04
ATXN1	ATXN-1_C[1],AXH[1]	8.78
ATXN1L	AXH[1]	0.41
ATXN2	PAM2[1],LsmAD[1],SM-ATX[1]	2.09
ATXN2L	PAM2[1],LsmAD[1],SM-ATX[1]	2.3
AUH	ECH[1]	0.2
BCLAF1	THRAP3_BCLAF1[1]	12.55
BICC1	SAM_1[1],KH_1[3]	3.97
BOLL	RRM_1[1]	0.83
BUD13	Bud13[1]	4.18
BZW1	W2[1]	0.41
BZW2	W2[1]	2.92
C12orf65	RF-1[1]	0.62
C1QBP	MAM33[1]	1.04
CACTIN	CactinC_cactus[1],Cactin_mid[1]	1.46
CALR	Calreticulin[1]	0.83
CAPRIN1	Caprin-1_C[1]	1.67

GENE	DOMAIN [COUNT]	%
CAPRIN2	C1q[1],Caprin-1_C[1]	3.13
CARHSP1	CSD[1]	0.41
CASC3	Btz[1]	2.51
CCAR1	SAP[1],DBC1[1],MIP-T3[1],S1-like[1]	1.25
CCAR2	DBC1[1],S1-like[1]	3.13
CDC40	WD40[5]	3.55
CDC5L	Myb_Cef[1],Myb_DNA-bind_6[1]	3.97
CELF1	RRM_1[3]	1.04
CELF2	RRM_1[3]	0.62
CELF3	RRM_1[3]	3.34
CELF4	RRM_5[1],RRM_1[2]	3.13
CELF5	RRM_1[3]	1.67
CELF6	RRM_1[3]	1.67
CHERP	G-patch[1],Surp[1],CTD_bind[1]	2.71
CHTOP	FoP_duplication[1]	3.55
CIRBP	RRM_1[1]	0.62
CLASRP	DRY_EERY[1]	1.25
CLK1	Pkinase[1]	1.04
CLK2	Pkinase[1]	4.39
CLK3	Pkinase[1]	1.88
CLK4	Pkinase[1]	1.25
CLP1	MobB[1],Clp1[1]	1.04
CMTR1	G-patch[1],FtsJ[1]	5.02
CMTR2	FtsJ[1]	2.51
CNBP	zf-CCHC[7]	0.62
CNOT1	DUF3819[1],Not1[1]	4.81
CNOT10	TPR_1[2],BLOC1_2[1]	2.51
CNOT11	DUF2363[1]	0.2
CNOT2	NOT2_3_5[1]	3.76
CNOT3	Not3[1],NOT2_3_5[1]	1.25
CNOT4	RRM_5[1],zf-RING_4[1]	6.06
CNOT6	LRR_8[1],Exo_endo_phos[1]	2.3
CNOT6L	LRR_8[1],Exo_endo_phos[1]	1.67
CNOT7	CAF1[1]	2.3
CNOT8	CAF1[1]	1.04
CNP	CNPase[1],AAA_33[1]	0.2
CPEB1	RRM_1[1],RRM_6[1]	2.71
CPEB2	RRM_1[1]	1.88
CPEB3	RRM_1[1]	1.04
CPEB4	RRM_1[1]	2.3
CPSF1	MMS1_N[1],CPSF_A[1]	7.53
CPSF2	RMMBL[1],Beta-Casp[1],Lactamase_B[1],CPSF100_C[1]	0.83
CPSF3	RMMBL[1],Beta-Casp[1],Lactamase_B[1],CPSF73-100_C[1]	1.04
CPSF3L	RMMBL[1],Beta-Casp[1],Lactamase_B[1]	2.71
CPSF4	zf-CCHC[1],zf-CCCH[3]	1.67
CPSF4L	zf-CCCH[3]	3.55
CPSF6	RRM_6[1]	4.81
CPSF7	RRM_1[1]	0.83
CRNKL1	HAT[4]	3.97
CRYZ	ADH_N[1],ADH_zinc_N[1]	1.67
CSDC2	CSD[1]	2.92
CSDE1	SUZ-C[1],CSD[5]	4.18
CSTF1	WD40[4]	2.71
CSTF2	RRM_1[1],CSTF2_hinge[1],CSTF_C[1]	1.25
CSTF2T	RRM_1[1],CSTF2_hinge[1],CSTF_C[1]	2.09

GENE	DOMAIN [COUNT]	%
CSTF3	Suf[1],TPR_16[1]	1.46
CTIF	MIF4G[1]	3.13
CWC15	Cwf_Cwc_15[1]	2.92
CWC22	MIF4G[1],MA3[1],CAF-1_p150[1]	1.04
CWC25	Cir_N[1],CWC25[1]	1.46
CWC27	Pro_isomerase[1]	1.88
CWF19L1	Metallophos_3[1],CwfJ_C_1[1],CwfJ_C_2[1]	0.62
CWF19L2	CwfJ_C_1[1],CwfJ_C_2[1]	4.18
CXorf23	THRAP3_BCLAF1[1]	2.09
DAZ1	RRM_1[3]	0
DAZ2	RRM_1[1]	0.2
DAZ3	RRM_1[1]	0
DAZ4	RRM_1[2]	0
DAZAP1	RRM_1[2]	1.67
DAZL	RRM_1[1]	2.3
DBR1	Metallophos[1],DBR1[1]	1.67
DCP1A	DCP1[1]	0.83
DCP1B	DCP1[1]	2.51
DCP2	DCP2[1],NUDIX[1]	2.51
DCPS	DcpS[1],DcpS_C[1]	2.92
DDX1	Helicase_C[1],DEAD[1]	0.62
DDX17	Helicase_C[1],DEAD[1]	4.39
DDX19A	Helicase_C[1],DEAD[1]	0.41
DDX19B	DEAD[1]	0.62
DDX25	Helicase_C[1],DEAD[1]	3.76
DDX26B	VWA_2[1],INT_SG_DDX_CT_C[1]	1.46
DDX39A	Helicase_C[1],DEAD[1]	1.25
DDX39B	Helicase_C[1],DEAD[1]	4.81
DDX3X	Helicase_C[1],DEAD[1]	4.81
DDX3Y	Helicase_C[1],DEAD[1]	0.62
DDX4	Helicase_C[1],DEAD[1]	2.92
DDX41	Helicase_C[1],DEAD[1]	2.92
DDX42	Helicase_C[1],DEAD[1]	5.43
DDX43	Helicase_C[1],DEAD[1],KH_1[1]	4.81
DDX5	P68HR[2],Helicase_C[1],DEAD[1]	4.81
DDX53	Helicase_C[1],DEAD[1],KH_1[1]	3.34
DDX59	zf-HIT[1],Helicase_C[1],DEAD[1]	5.64
DDX6	Helicase_C[1],DEAD[1]	2.92
DEK	SAP[1],DEK_C[1]	5.23
DENR	SUI1[1]	0.41
DGCR14	Es2[1]	3.97
DHX15	OB_NTP_bind[1],DUF1777[1],HA2[1],Helicase_C[1],DEAD[1]	2.71
DHX29	OB_NTP_bind[1],HA2[1],Helicase_C[1],DEAD[1]	3.13
DHX30	OB_NTP_bind[1],HA2[1],Helicase_C[1],dsrm[1],DEAD[1]	1.67
DHX32	OB_NTP_bind[1],HA2[1]	1.88
DHX33	OB_NTP_bind[1],HA2[1],Helicase_C[1],DEAD[1]	1.67
DHX34	OB_NTP_bind[1],HA2[1],Helicase_C[1],DEAD[1]	2.92
DHX35	OB_NTP_bind[1],HA2[1],Helicase_C[1],DEAD[1]	2.3
DHX36	OB_NTP_bind[1],HA2[1],Helicase_C[1],DEAD[1]	2.51
DHX38	OB_NTP_bind[1],HA2[1],Helicase_C[1],DEAD[1]	2.51
DHX40	OB_NTP_bind[1],HA2[1],Helicase_C[1],DEAD[1]	4.81
DHX57	OB_NTP_bind[1],HA2[1],Helicase_C[1],DEAD[1],RWD[1]	1.88
DHX8	OB_NTP_bind[1],S1[1],Helicase_C[1],DEAD[1]	2.92
DND1	RRM_1[1],DND1_DSRM[1]	1.04
DQX1	OB_NTP_bind[1],HA2[1],AAA_22[1]	2.51

GENE	DOMAIN [COUNT]	%
DRG1	MMR_HSR1[1],TGS[1]	0.41
DRG2	MMR_HSR1[1],TGS[1]	1.25
DUSP11	DSPc[1]	0.41
DYNC1H1	Dynein_heavy[1],AAA_9[1],DHC_N1[1],DHC_N2[1],MT[1],AAA_6[1],AAA_5[1],AAA_7[1],AAA_8[1]	5.02
DYNLL1	Dynein_light[1]	0.41
DZIP1	Dzip-like_N[1],zf-C2H2[1]	5.43
DZIP1L	Dzip-like_N[1]	1.67
DZIP3	zf-RING_2[1]	2.51
EDC3	LSM14[1],YjeF_N[1]	2.3
EDC4	WD40[1]	3.55
EEF2K	Alpha_kinase[1]	2.09
EIF1	SUI1[1]	0.2
EIF1AD	eIF-1a[1]	1.67
EIF1AX	eIF-1a[1]	1.25
EIF1AY	eIF-1a[1]	0
EIF1B	SUI1[1]	1.04
EIF2AK1	Pkinase[2]	3.76
EIF2AK3	PQQ_2[1],Pkinase[2]	4.6
EIF2B1	IF-2B[1]	0.83
EIF2B2	IF-2B[1]	0.83
EIF2B3	NTP_transferase[1]	1.46
EIF2B4	IF-2B[1]	0.41
EIF2B5	Hexapep[1],NTP_transferase[1],W2[1]	1.46
EIF3A	PCI[1]	2.3
EIF3B	eIF2A[2],RRM_1[1]	4.18
EIF3C	eIF-3c_N[1],PCI[1]	0.2
EIF3CL	eIF-3c_N[1],PCI[1]	0
EIF3D	eIF-3_zeta[1]	1.88
EIF3E	eIF3_N[1],PCI[1]	4.18
EIF3G	RRM_1[1],eIF3g[1]	0.62
EIF3H	XkdN[1],JAB[1]	4.81
EIF3I	WD40[4]	1.46
EIF3J	eIF3_subunit[1]	1.88
EIF3K	PCI_Csn8[1]	0.83
EIF3L	Paf67[1]	2.92
EIF3M	PCI[1]	0.2
EIF4A1	Helicase_C[1],DEAD[1]	1.25
EIF4A2	Helicase_C[1],DEAD[1]	1.46
EIF4A3	Helicase_C[1],DEAD[1]	5.02
EIF4B	RRM_1[1]	1.25
EIF4E	IF4E[2]	1.04
EIF4E1B	IF4E[1]	1.88
EIF4E2	IF4E[1]	0.62
EIF4E3	IF4E[1]	3.13
EIF4ENIF1	EIF4E-T[1]	0.83
EIF4G1	MIF4G[1],MA3[1],W2[1]	4.18
EIF4G2	MIF4G[1],MA3[1],W2[1]	1.25
EIF4G3	MIF4G[1],MA3[1],W2[1]	4.81
EIF4H	RRM_1[1]	1.88
EIF5	eIF-5_eIF-2B[1],W2[1]	1.46
EIF5A	KOW[1],eIF-5a[1]	0.41
EIF5A2	KOW[1],eIF-5a[1]	0.83
EIF5AL1	eIF-5a[1]	0.83
EIF6	eIF-6[1]	1.46

GENE	DOMAIN [COUNT]	%
ELAVL1	RRM_1[3]	0.83
ELAVL2	RRM_1[3]	9.41
ELAVL3	RRM_1[3]	1.88
ELAVL4	RRM_1[3]	3.34
ENOX1	RRM_1[1]	1.88
ENOX2	RRM_1[1]	1.67
ERN1	PQQ_2[1],Pkinase[1],Ribonuc_2-5A[1]	6.27
ERN2	PQQ_2[1],Pkinase[1],Ribonuc_2-5A[1]	5.02
ESRP1	RRM_6[3]	7.74
ESRP2	RRM_6[3]	1.88
ETF1	eRF1_1[1],eRF1_2[1],eRF1_3[1]	0.83
EWSR1	zf-RanBP[1],RRM_6[1]	2.71
FAM103A1	RAM[1]	1.04
FAM120A	.	1.46
FAM98A	DUF2465[1]	0.62
FASTK	FAST_1[1],FAST_2[1],RAP[1]	4.6
FASTKD1	FAST_1[1],FAST_2[1],RAP[1]	1.04
FASTKD2	FAST_1[1],FAST_2[1],RAP[1]	0.83
FASTKD3	FAST_1[1],FAST_2[1],RAP[1]	3.13
FASTKD5	FAST_1[1],FAST_2[1],RAP[1]	3.13
FIP1L1	Fip1[1],Pkinase_Tyr[1]	3.55
FMR1	Agenet[1],FXR1P_C[1],KH_1[2]	1.46
FRG1	FRG1[1]	3.55
FRG1BP	FRG1[1]	11.29
FTO	FTO_CTD[1],FTO_NTD[1]	1.04
FUBP1	DUF1897[2],KH_1[4]	1.88
FUBP3	KH_1[4]	1.46
FUS	zf-RanBP[1],RRM_1[1]	0.62
FXR1	Agenet[1],FXR1P_C[1],KH_1[2]	1.88
FXR2	Agenet[1],FXR1P_C[1],KH_1[2]	0.83
FYTTD1	FYTT[1]	1.88
G3BP1	RRM_1[1],NTF2[1]	1.46
G3BP2	RRM_1[1],NTF2[1]	1.04
GAPDH	Gp_dh_C[1],Gp_dh_N[1]	1.67
GCFC2	GCFC[1]	1.46
GFM1	EFG_C[1],GTP_EFTU_D2[1],EFG_IV[1],EFG_II[1],GTP_EFTU[1]	1.46
GFM2	EFG_C[1],GTP_EFTU_D2[1],EFG_IV[1],EFG_II[1],GTP_EFTU[1]	1.67
GLE1	GLE1[1]	0.62
GPATCH1	G-patch[1],Cwf_Cwc_15[1],DUF1604[1]	3.34
GRSF1	RRM_6[3]	0.83
GSPT1	PAM2[1],GTP_EFTU_D3[1],GTP_EFTU[1]	1.46
GSPT2	PAM2[1],GTP_EFTU_D3[1],GTP_EFTU[1]	2.92
GTF2F1	TFIIF_alpha[1]	1.25
GTPBP1	GTP_EFTU_D2[1],GTP_EFTU_D3[1],GTP_EFTU[1]	4.18
GTPBP2	GTP_EFTU_D2[1],GTP_EFTU_D3[1],GTP_EFTU[1]	3.34
GUF1	EFG_C[1],GTP_EFTU_D2[1],LepA_C[1],EFG_II[1],GTP_EFTU[1]	1.88
HABP4	HABP4_PAI-RBP1[1]	0.41
HBS1L	HBS1_N[1],GTP_EFTU_D2[1],GTP_EFTU_D3[1],GTP_EFTU[1]	2.71
HDLBP	KH_1[14]	3.34
HELZ	PAM2[1],AAA_19[1],AAA_11[1],zf-CCCH[1],AAA_12[1]	5.64
HELZ2	AAA_11[2],RNB[1],AAA_12[2]	6.9
HNRNPA0	RRM_1[1],RRM_6[1]	0.62
HNRNPA1	HnRNPA1[1],RRM_1[2]	0.83
HNRNPA1L2	HnRNPA1[1],RRM_1[2]	1.04
HNRNPA2B1	RRM_1[1],RRM_6[1]	2.09

GENE	DOMAIN [COUNT]	%
HNRNPA3	RRM_1[1],RRM_6[1]	0.41
HNRNPAB	RRM_1[2],CBFNT[1]	1.67
HNRNPC	RRM_1[1]	0.62
HNRNPCL1	RRM_1[1]	8.15
HNRNPD	RRM_1[2],CBFNT[1]	0.62
HNRNPDL	RRM_1[2],CBFNT[1]	0.2
HNRNPF	zf-RNPHF[1],RRM_1[1],RRM_6[2]	1.67
HNRNPH1	zf-RNPHF[1],RRM_6[3]	2.09
HNRNPH2	zf-RNPHF[1],RRM_6[3]	0.62
HNRNPH3	RRM_6[2]	0.2
HNRNPK	ROKNT[1],KH_1[3]	1.04
HNRNPL	RRM_5[3]	2.51
HNRNPLL	RRM_5[2],RRM_6[1]	0.62
HNRNPM	HnRNP_M[1],RRM_1[3]	2.71
HNRNPR	RRM_1[3]	3.55
HNRNPU	SAP[1],SPRY[1],AAA_33[1]	4.6
HNRNPUL1	SAP[1],SPRY[1],AAA_33[1]	1.67
HNRNPUL2	SAP[1],SPRY[1],AAA_33[1]	0.83
HTATSF1	RRM_5[1],RRM_1[1]	1.88
IGF2BP1	RRM_1[1],KH_1[4],RRM_6[1]	4.6
IGF2BP2	RRM_1[2],KH_1[4]	1.46
IGF2BP3	RRM_1[1],KH_1[4],RRM_6[1]	3.76
ILF2	DZF[1]	3.76
ILF3	dsrm[2],DZF[1]	2.09
IPO11	IBN_N[1],Xpo1[1]	2.3
IPO13	IBN_N[1],Xpo1[1]	1.88
IPO4	IBN_N[1],HEAT_2[1],HEAT_EZ[1]	2.51
IPO5	IBN_N[1],HEAT_2[1],HEAT[1]	4.39
IPO7	Cse1[1],IBN_N[1]	2.09
IPO9	IBN_N[1],Xpo1[1]	5.64
IREB2	Aconitase_C[1],Aconitase[2]	3.34
ISY1	Isy1[1]	0.41
JAKMIP1	.	6.27
KHDC1	.	4.6
KHDC1L	.	3.34
KHDRBS1	KH_1[1]	2.51
KHDRBS2	KH_1[1]	8.57
KHDRBS3	KH_1[1]	5.85
KHNYN	RNase_Zc3h12a[1]	1.25
KHSRP	DUF1897[2],KH_1[4]	0.62
KPNB1	IBN_N[1],HEAT_EZ[1]	1.25
L1TD1	Transposase_22[2]	5.43
LARP1	La[1]	3.55
LARP1B	La[1]	1.88
LARP4	La[1],RRM_6[1]	2.71
LARP4B	La[1],RRM_5[1]	3.76
LARP6	SUZ-C[1],La[1]	2.09
LIN28A	zf-CCHC[1],CSD[1]	1.46
LIN28B	zf-CCHC[1],CSD[1]	4.18
LRPPRC	PPR_2[2],PPR[1]	3.97
LSM12	AD[1]	0.41
LSM14A	LSM14[1],FDF[1]	2.09
LSM14B	LSM14[1],FDF[1]	2.09
LUC7L	LUC7[1]	1.25
LUC7L2	LUC7[1]	4.81

GENE	DOMAIN [COUNT]	%
LUC7L3	LUC7[1]	2.92
LUZP4	FYTT[1]	1.46
MAGOH	Mago_nashi[1]	0.62
MAGOHB	Mago_nashi[1]	1.46
MATR3	RRM_5[2]	2.09
MBNL1	zf-CCCH[1]	1.46
MBNL2	zf-CCCH[2]	1.25
MBNL3	zf-CCCH[2]	0.62
MECP2	MBD[1]	2.09
METTL14	MT-A70[1]	0.83
METTL3	MT-A70[1]	0.83
MEX3A	KH_1[2],zf-C3HC4_3[1]	2.71
MEX3B	KH_1[2],zf-C3HC4_3[1]	1.04
MEX3C	KH_1[2],zf-C3HC4_3[1]	0.83
MEX3D	KH_1[2],zf-C3HC4_3[1]	0.41
MIF4GD	MIF4G[1]	3.97
MKRN1	zf-C3HC4[1],zf-CCCH[3]	5.02
MKRN2	zf-RING_2[1],zf-CCCH[4]	1.88
MKRN3	zf-C3HC4[1],zf-CCCH[1]	4.39
MOV10	AAA_19[1],AAA_11[1],AAA_12[1]	3.55
MOV10L1	AAA_11[2],AAA_12[1],S1-like[1]	7.11
MRTO4	Ribosomal_L10[1]	1.25
MSI1	RRM_1[2]	1.04
MSI2	RRM_1[2]	3.76
MTHFSD	RRM_1[1],5-FTHF_cyc-lig[1]	1.46
MTIF3	IF3_C[1],IF3_N[1]	0.62
MTPAP	GOLGA2L5[1],PAP_assoc[1]	1.04
MTRF1	PCRF[1],RF-1[1]	0.83
MTRF1L	PCRF[1],RF-1[1]	1.46
MYEF2	RRM_1[3]	1.88
NAA38	LSM[1]	3.34
NANOS1	zf-nanos[1]	0.83
NANOS2	zf-nanos[1]	0.83
NANOS3	zf-nanos[1]	1.25
NCBP1	MIF4G_like_2[1],MIF4G[1],MIF4G_like[1]	0.2
NCBP2	RRM_5[1]	1.25
NCBP2L	RRM_1[1]	0.41
NELFE	RRM_1[1]	5.02
NFX1	R3H[1],zf-NF-X1[7]	2.51
NGDN	Sas10_Utp3[1]	1.46
NMD3	NMD3[1]	1.46
NOCT	Exo_endo_phos[1]	1.04
NOL3	CARD[1]	1.25
NOVA1	KH_1[3]	4.6
NOVA2	KH_1[3]	0.62
NR0B1	Hormone_recep[1],NR_Repeat[4]	1.04
NSRP1	DUF2040[1]	1.46
NUDT21	NUDIX_2[1]	1.25
NUFIP2	NUFIP2[1]	1.67
NUPL2	zf-CCCH[1]	2.51
NUTF2	NTF2[1]	0.2
NXF1	LRR_4[1],Tap-RNA_bind[1],NTF2[1],TAP_C[1]	1.25
NXF2	LRR_4[1],Tap-RNA_bind[1],NTF2[1],TAP_C[1]	1.25
NXF2B	LRR_4[1],Tap-RNA_bind[1],NTF2[1],TAP_C[1]	1.04
NXF3	Tap-RNA_bind[1],NTF2[1]	3.13

GENE	DOMAIN [COUNT]	%
NXF5	LRR_4[1],Tap-RNA_bind[1]	2.09
NXT1	NTF2[1]	0.83
NXT2	NTF2[1]	0.41
PABPC1	RRM_1[4],PABP[1]	4.81
PABPC1L	RRM_1[4],PABP[1]	1.88
PABPC1L2A	RRM_1[2]	1.04
PABPC1L2B	RRM_1[2]	1.04
PABPC3	RRM_1[4],PABP[1]	2.3
PABPC4	RRM_1[4],PABP[1]	2.09
PABPC4L	RRM_1[4]	1.25
PABPC5	RRM_1[4]	1.67
PABPN1	RRM_1[1]	0.83
PABPN1L	RRM_1[1]	0.83
PAIP1	PAM2[1],MIF4G[1]	3.34
PAIP2	PAM2[1]	1.04
PAIP2B	PAM2[1]	0.2
PAN2	RNase_T[1],UCH_1[1]	3.13
PAN3	Pkinase[1],zf-CCCH[1]	1.88
PAPD4	PAP_assoc[1],NTP_transf_2[1]	2.09
PAPOLA	PAP_RNA-bind[1],PAP_central[1]	1.25
PAPOLB	PAP_RNA-bind[1],PAP_central[1]	4.18
PAPOLG	PAP_RNA-bind[1],PAP_central[1]	1.46
PARK7	DJ-1_PfpI[1]	1.67
PARN	CAF1[2],RNA_bind[1]	2.3
PARP1	BRCT[1],WGR[1],PARP_reg[1],zf-PARP[2],PARP[1],PADR1[1]	4.39
PATL1	PAT1[1]	2.51
PATL2	PAT1[1]	2.09
PCBP1	KH_1[3]	0.2
PCBP2	KH_1[3]	1.04
PCBP3	KH_1[3]	1.67
PCBP4	KH_1[3]	0.62
PCF11	CTD_bind[1]	4.6
PDCD4	MA3[2]	1.88
PDE12	Exo_endo_phos[1]	1.46
PELO	eRF1_1[1],eRF1_2[1],eRF1_3[1]	1.04
PHF5A	PHF5[1]	3.34
PHRF1	PHD[1],zf-RING_2[1]	2.92
PLRG1	WD40[6]	2.3
PNLDC1	.	2.71
PNN	Pinin_SDK_N[1],Pinin_SDK_memA[1]	1.25
PNRC2	PNRC[1]	1.46
POLDIP3	RRM_1[1]	3.97
POLR2A	RNA_pol_Rpb1_3[1],RNA_pol_Rpb1_R[1],RNA_pol_Rpb1_2[1],RNA_pol_Rpb1_1[1],RNA_pol_Rpb1_5[1],RNA_pol_Rpb1_4[1]	2.71
POLR2B	RNA_pol_Rpb2_7[1],RNA_pol_Rpb2_4[1],RNA_pol_Rpb2_1[1],RNA_pol_Rpb2_3[1],RNA_pol_Rpb2_5[1],RNA_pol_Rpb2_6[1]	3.97
POLR2D	RNA_pol_Rpb4[1]	0.41
POLR2E	RNA_pol_Rpb5_N[1],RNA_pol_Rpb5_C[1]	0.62
POLR2F	RNA_pol_Rpb6[1]	2.51
POLR2G	S1[1],SHS2_Rpb7-N[1]	0
POLR2H	RNA_pol_Rpb8[1]	1.04
POLR2I	RNA_POL_M_15KD[1],TFIIS_C[1]	1.25
POLR2J	RNA_pol_L_2[1]	1.88
POLR2J2	RNA_pol_L_2[1]	1.67
POLR2J3	.	1.67

GENE	DOMAIN [COUNT]	%
POLR2K	DNA_RNApol_7kD[1]	3.13
POLR2L	RNA_pol_N[1]	0.2
POLRMT	RPOL_N[1],RNA_pol[1]	1.67
PPAN	7tm_1[1],Brix[1]	0.2
PPIE	RRM_1[1],Pro_isomerase[1]	0.62
PPIH	Pro_isomerase[1]	1.04
PPIL3	Pro_isomerase[1]	0.41
PPIL4	RRM_1[1],Pro_isomerase[1]	1.46
PPRC1	RRM_1[1]	3.34
PPWD1	Pro_isomerase[1],WD40[2]	1.25
PQBP1	WW[1]	0.83
PRDX1	AhpC-TSA[1],1-cysPrx_C[1]	1.67
PRKDC	PI3_PI4_kinase[1]	7.74
PRPF18	PRP4[1],Prp18[1]	1.25
PRPF19	Prp19[1],U-box[1],WD40[4]	0.83
PSIP1	LEDGF[1],PWWP[1]	3.13
PTBP1	RRM_5[3],RRM_6[1]	1.25
PTBP2	RRM_5[3],RRM_6[1]	1.67
PTBP3	RRM_5[2],RRM_1[1],RRM_6[1]	0.83
PTCD2	MRP-S27[1]	1.88
PTCD3	PPR_2[1],PPR_3[1]	1.25
PUF60	RRM_5[1],RRM_1[2]	5.85
PUM1	Shadoo[1],PUF[8]	3.55
PUM2	PUF[8]	1.67
PUM3	CPL[1]	2.09
PURA	PurA[1]	1.25
PURB	PurA[1]	0.41
PURG	PurA[1]	2.51
PYM1	Mago-bind[1]	1.25
QKI	KH_1[1]	2.71
RAE1	WD40[3]	1.88
RALY	RRM_1[1]	2.3
RALYL	RRM_1[1]	5.43
RAN	Ras[1]	0.62
RANBP17	IBN_N[1],CRM1_C[1]	5.85
RANBP2	TPR_1[1],IR1-M[2],zf-RanBP[8],Ran_BP1[4],Pro_isomerase[1]	6.69
RANBP6	HEAT_2[2]	3.13
RAVER1	RRM_1[1],RRM_6[2]	2.09
RAVER2	RRM_1[2],RRM_6[1]	1.88
RBBP6	DWNN[1],zf-CCHC[1],zf-C3HC4_2[1]	4.6
RBFOX1	Fox-1_C[1],RRM_1[1]	7.32
RBFOX2	Fox-1_C[1],RRM_1[1]	2.09
RBFOX3	Fox-1_C[1],RRM_1[1]	4.6
RBM10	G-patch[1],zf-RanBP[1],RRM_6[2]	1.88
RBM11	RRM_1[1]	4.39
RBM12	RRM_1[1],RRM_6[4]	3.76
RBM12B	RRM_6[5]	5.02
RBM14	RRM_1[2]	3.13
RBM15	RRM_5[2],RRM_1[1],SPOC[1]	2.3
RBM15B	RRM_5[1],RRM_1[2],SPOC[1]	1.46
RBM17	G-patch[1],RRM_5[1]	0.83
RBM18	RRM_1[1]	0.41
RBM20	RRM_5[1]	0.62
RBM22	FYVE[1],RRM_1[1],zf-CCCH[1]	3.13
RBM23	RRM_1[2],RBM39linker[1]	1.67

GENE	DOMAIN [COUNT]	%
RBM24	RRM_6[1]	5.02
RBM25	RRM_1[1],PWI[1]	2.51
RBM26	RRM_5[1],PWI[1],zf-CCCH[1],RRM_6[1]	2.71
RBM27	RRM_5[1],PWI[1],zf-CCCH[1]	2.92
RBM3	RRM_1[1]	0.62
RBM33	RRM_6[1]	4.81
RBM34	RRM_1[2]	3.76
RBM38	RRM_1[1]	2.09
RBM39	RRM_5[1],RRM_1[2],RBM39linker[1]	1.88
RBM4	RRM_1[2],zf-CCHC[1]	2.09
RBM41	RRM_1[1]	0.62
RBM42	RRM_1[1]	1.46
RBM43	RRM_6[1]	0.62
RBM44	RRM_1[1]	2.3
RBM45	RRM_5[1],RRM_1[3]	1.04
RBM46	RRM_1[3],DND1_DSRM[1]	5.02
RBM47	RRM_1[3]	3.76
RBM48	RRM_5[1]	1.67
RBM4B	RRM_1[2],zf-CCHC[1]	2.09
RBM5	G-patch[1],zf-RanBP[1],RRM_6[2]	2.71
RBM6	G-patch[1],RRM_6[2]	2.51
RBM7	RRM_1[1]	3.55
RBM8A	RRM_1[1]	4.39
RBMS1	RRM_1[2]	1.25
RBMS2	RRM_1[2]	2.3
RBMS3	RRM_1[2]	2.51
RBMX	RBM1CTR[1],RRM_1[1]	1.88
RBMX2	RRM_1[1]	0.62
RBMXL1	RBM1CTR[1],RRM_1[1]	2.3
RBMXL2	RBM1CTR[1],RRM_1[1]	3.13
RBMXL3	RRM_1[1]	0.41
RBMY1A1	RBM1CTR[1],RRM_1[1]	0
RBMY1B	RBM1CTR[1],RRM_1[1]	0
RBMY1D	RBM1CTR[1],RRM_1[1]	0
RBMY1E	RBM1CTR[1],RRM_1[1]	0.2
RBMY1F	RBM1CTR[1],RRM_1[1]	0
RBMY1J	RBM1CTR[1],RRM_1[1]	0
RBPMS	RRM_1[1]	1.67
RBPMS2	RRM_1[1]	0.62
RC3H1	zf-CCCH[1],zf-RING_UBOX[1]	4.81
RC3H2	zf-RING_5[1],zf-CCCH[1]	2.51
RNF17	TUDOR[5]	9.62
RNGTT	mRNA_cap_C[1],mRNA_cap_enzyme[1],DSPc[1]	3.13
RNMT	Pox_MCEL[1]	1.46
RNPS1	RRM_1[1]	0.41
RPUSD3	PseudoU_synth_2[1]	1.04
RPUSD4	PseudoU_synth_2[1]	3.97
RQCD1	Rcd1[1]	2.3
RRBP1	Rib_recp_KP_reg[1],IncA[1]	1.88
RSRC1	THRAP3_BCLAF1[1]	1.88
RTF1	Plus-3[1],SYF2[1]	2.09
RUVBL1	TIP49[1]	0.62
RUVBL2	TIP49[1]	1.25
SAFB	SAP[1],RRM_6[1]	2.09
SAFB2	SAP[1],RRM_1[1]	1.25

GENE	DOMAIN [COUNT]	%
SAMD4A	SAM_1[1]	1.67
SAMD4B	PHAT[1],SAM_1[1]	1.25
SAP18	SAP18[1]	0.83
SARNP	SAP[1]	0.83
SCAF1	.	4.39
SCAF11	zf-RING_2[1]	2.71
SCAF4	RRM_1[1],CTD_bind[1]	2.09
SCAF8	RRM_1[1],CTD_bind[1]	3.76
SECISBP2	Ribosomal_L7Ae[1]	1.46
SECISBP2L	Ribosomal_L7Ae[1]	2.51
SERBP1	HABP4_PAI-RBP1[1]	1.04
SETX	AAA_11[1],AAA_12[1]	3.76
SF1	zf-CCHC[1],KH_1[1]	2.3
SF3B1	HEAT_2[1],SF3b1[1]	3.34
SF3B14	RRM_1[1]	0.62
SF3B2	SAP[1],DUF382[1],PSP[1]	3.76
SF3B3	MMS1_N[1],CPSF_A[1]	2.09
SF3B4	RRM_1[2]	3.34
SF3B5	SF3b10[1]	1.67
SFPQ	RRM_1[2],NOPS[1]	1.46
SFSWAP	Surp[2],DRY_EERY[1]	2.51
SKIV2L	Helicase_C[1],rRNA_proc-arch[2],DSHCT[1],DEAD[1]	7.32
SLBP	SLBP_RNA_bind[1]	1.46
SLTM	SAP[1],RRM_1[1]	2.71
SLU7	Slu7[1]	2.09
SMG1	PI3_PI4_kinase[1],FATC[1]	3.55
SMG5	PIN_4[1],EST1_DNA_bind[2],EST1[1]	3.55
SMG6	PIN_4[1],EST1[1],EST1_DNA_bind[1]	2.51
SMG7	EST1_DNA_bind[1]	5.43
SMG8	DUF2146[2]	4.6
SMG9	DUF2146[1]	0.83
SMNDC1	SMN[1]	0.62
SND1	SNase[5],TUDOR[1]	6.48
SNW1	SKIP_SNW[1]	0.83
SON	G-patch[1],DND1_DSRM[1]	2.71
SPATS2	DUF1387[1]	1.88
SPATS2L	GVQW[1],DUF1387[1]	1.04
SPEN	RRM_5[1],RRM_1[3],SPOC[1]	8.78
SREK1	RRM_1[1],RRM_6[1]	1.67
SRPK2	Pkinase[2]	3.13
SRRM1	PWI[1]	3.76
SRRM2	cwf21[1]	5.85
SRRM3	cwf21[1],SRRM_C[1]	1.67
SRRM4	SRRM_C[1]	2.51
SRSF1	RRM_1[2]	3.55
SRSF10	RRM_1[1]	1.67
SRSF11	RRM_1[1]	1.46
SRSF12	RRM_1[1]	2.71
SRSF2	RRM_1[1]	5.23
SRSF3	RRM_1[1]	3.97
SRSF4	RRM_1[2]	1.67
SRSF5	RRM_1[2]	1.25
SRSF6	RRM_1[2]	2.09
SRSF7	RRM_1[1],zf-CCHC[1]	1.25
SRSF8	RRM_1[1]	2.71

GENE	DOMAIN [COUNT]	%
SRSF9	RRM_1[2]	0.83
SSU72	Ssu72[1]	2.51
STAU1	dsrm[3]	3.97
STAU2	dsrm[4]	4.18
STRAP	WD40[5]	1.25
STRBP	dsrm[2],DZF[1]	1.04
SUB1	PC4[1]	3.34
SUGP1	G-patch[1],Surp[2]	2.51
SUGP2	G-patch[1],Surp[2]	3.97
SUPT4H1	Spt4[1]	3.34
SUPT5H	KOW[3],CTD[1],Spt5-NGN[1],Spt5_N[1]	2.09
SUPT6H	S1[1],DLD[1],SH2_2[1],YqgF[1],HTH_44[1],Tex_N[1],HHH_7[1],SPT6_acidic[1]	4.39
SUPV3L1	Helicase_C[1],SUV3_C[1]	1.25
SWT1	PIN_4[1]	4.6
SYF2	SYF2[1]	1.46
SYMPK	DUF3453[1],Cohesin_HEAT[1],Symplekin_C[1]	2.09
SYNCRIP	RRM_1[3]	3.34
TAF15	zf-RanBP[1],RRM_1[1]	1.67
TARBP1	SpoU_methylase[1]	6.9
TARBP2	dsrm[2]	0
TARDBP	RRM_1[2]	2.3
TBRG4	FAST_1[1],FAST_2[1],RAP[1]	1.46
TCERG1	FF[6],WW[3]	3.55
TDRD3	TUDOR[1],DUF1767[1],UBA[1]	2.09
TDRD7	TUDOR[3],OST-HTH[1]	2.09
TEFM	HHH_3[1]	0.62
TEX13A	zf-RanBP[1],TEX13[1]	3.76
TFAM	HMG_box[1],HMG_box_2[1]	1.88
TFIP11	G-patch[1],TIP_N[1],GCFC[1]	2.71
THOC1	efThoc1[1],Death[1]	1.25
THOC2	Tho2[1],Thoc2[1]	5.02
THOC3	WD40[4]	1.67
THOC5	FimP[1]	1.67
THOC6	WD40[1]	0.62
THOC7	THOC7[1]	2.09
THRAP3	THRAP3_BCLAF1[1]	3.97
TIA1	RRM_1[3]	0.2
TIAL1	RRM_1[3]	1.04
TNPO1	IBN_N[1],HEAT_2[1],HEAT_EZ[1],HEAT[1]	2.3
TNPO2	IBN_N[1],HEAT_2[1],Arm[1],HEAT_EZ[1],HEAT[1]	0.83
TNPO3	Xpo1[1]	6.06
TNRC6A	RRM_5[1],Ago_hook[1]	2.92
TNRC6B	RRM_5[1],Ago_hook[1]	7.32
TNRC6C	RRM_5[1],M_domain[1],Ago_hook[1]	8.15
TOP3B	Topoisom_bac[1],Toprim[1]	2.92
TPR	TPR_MLP1_2[2]	4.39
TRA2A	RRM_1[1]	1.67
TRA2B	RRM_1[1]	1.67
TRIM25	SPRY[1],PRY[1],zf-C3HC4_4[1],zf-B_box[1]	3.55
TSFM	EF_TS[1],UBA[1]	3.13
TTF2	zf-GRF[1],Helicase_C[1],SNF2_N[1]	3.97
TUFM	GTP_EFTU_D2[1],GTP_EFTU_D3[1],GTP_EFTU[1]	1.67
U2AF1	RRM_5[1],zf-CCCH[2]	0.41
U2AF1L4	RRM_5[1],zf-CCCH[2]	1.25
U2AF2	RRM_1[2],Transformer[1],RRM_6[1]	1.25

GENE	DOMAIN [COUNT]	%
UBA1	UBACT[2],UBA_e1_C[1],UBA_e1_thiolCys[1],ThiF[2]	0.83
UBAP2	DUF3697[1],UBA[1]	2.51
UBAP2L	DUF3697[1],UBA[1]	5.23
UHMK1	RRM_5[1],Pkinase[1]	3.34
UPF1	AAA_11[1],AAA_12[1],UPF1_Zn_bind[1]	3.13
UPF2	MIF4G[3],Upf2[1]	4.6
UPF3A	Smg4_UPF3[1]	1.88
UPF3B	Smg4_UPF3[1]	2.3
USP10	PAM2[1],UCH[1]	2.71
WBP4	WW[2],zf-U1[1]	1.04
WDR61	WD40[6]	1.04
WDR83	WD40[3]	0.62
XAB2	TPR_2[1],TPR_12[1]	1.67
XPO1	IBN_N[1],Xpo1[1],CRM1_C[1]	1.04
XPO4	CRM1_C[1]	2.3
XPO6	IBN_N[1],Xpo1[1]	1.88
XPO7	IBN_N[1],CRM1_C[1]	3.34
XRCC6	SAP[1],Ku[1],Ku_C[1],Ku_N[1]	3.13
YBX1	CSD[1]	1.67
YBX2	CSD[1]	2.3
YBX3	CSD[1]	2.09
YTHDC1	YTH[1]	2.71
YTHDC2	OB_NTP_bind[1],Ank_2[1],HA2[1],Helicase_C[1],YTH[1],R3H[1],DEAD[1]	3.97
YTHDF1	YTH[1]	5.23
YTHDF2	YTH[1]	2.3
YTHDF3	YTH[1]	2.51
ZC3H14	zf-CCCH_2[3]	1.88
ZC3H3	zf-CCCH[3]	9.2
ZCCHC13	zf-CCHC[4]	2.09
ZCCHC8	zf-CCHC[1],PSP[1]	1.04
ZFP36	zf-CCCH[2]	0.83
ZFP36L1	Tis11B_N[1],zf-CCCH[2]	0.83
ZFP36L2	Tis11B_N[1],zf-CCCH[2]	1.67
ZNF326	AKAP95[1]	1.67
ZNF385A	GVQW[1],zf-met[2]	1.04
ZNF598	.	2.3
ZNF638	RRM_5[2],zf-C2H2_jaz[1],RRM_6[1]	4.6
ZRANB2	zf-RanBP[2]	0.83
ZRSR1	RRM_5[1],zf-CCCH[2]	2.71
ZRSR2	RRM_5[1],zf-CCCH[2]	0.83

Supplementary Table 2: List of RNA binding proteins (and their RNA binding domains) included in the melanoma cell lines vs. melanocytes microarray. Pink: upregulated genes, green: downregulated genes (for regulation levels, see Table S3). N/A: not available. Data extracted from ref[218].

GENE	FAMILY	# DOMAINS	DOMAINS
ACIN1	mRNA	2	SAP[1],RRM_5[1]
AFF2	mRNA	1	AF-4[1]
BUB3	mRNA	N/A	N/A
BUD13	mRNA	1	Bud13[1]
BUD31	snRNA	N/A	N/A
C1QBP	mRNA	1	MAM33[1]
CCNT2	ncRNA	1	Cyclin_N[1]
CDC40	mRNA	5	WD40[5]
CDK9	ncRNA	1	Pkinase[1]
CELF1	mRNA	3	RRM_1[3]
CELF2	mRNA	3	RRM_1[3]
CLASRP	mRNA	1	DRY_EERY[1]
CLK1	mRNA	1	Pkinase[1]
CLK2	mRNA	1	Pkinase[1]
CLK3	mRNA	1	Pkinase[1]
CLK4	mRNA	1	Pkinase[1]
CPSF1	mRNA	2	MMS1_N[1],CPSF_A[1]
CPSF2	mRNA	4	RMMBL[1],Beta-Casp[1],Lactamase_B[1],CPSF100_C[1]
CPSF4	mRNA	4	zf-CCHC[1],zf-CCCH[3]
CRNKL1	mRNA	4	HAT[4]
DDX11	mRNA	N/A	N/A
DDX23	mRNA	2	Helicase_C[1],DEAD[1]
DDX39B	mRNA	2	Helicase_C[1],DEAD[1]
DDX46	mRNA	2	Helicase_C[1],DEAD[1]
DDX5	mRNA	4	P68HR[2],Helicase_C[1],DEAD[1]
DEK	mRNA	2	SAP[1],DEK_C[1]
DHX15	mRNA	5	OB_NTP_bind[1],DUF1777[1],HA2[1],Helicase_C[1],DEAD[1]
DHX9	mRNA	6	OB_NTP_bind[1],HA2[1],Helicase_C[1],dsrm[2],DEAD[1]
DNAJC8	snRNA	N/A	N/A
DUSP11	mRNA	1	DSPc[1]
DYRK1A	diverse	N/A	N/A
EFTUD2	tRNA	5	EFG_C[1],GTP_EFTU_D2[1],EFG_IV[1],EFG_II[1],GTP_EFTU[1]
EIF6	mRNA	1	eIF-6[1]
ELAVL1	mRNA	3	RRM_1[3]
ELAVL2	mRNA	3	RRM_1[3]
ELAVL4	mRNA	3	RRM_1[3]
ERG	diverse	N/A	N/A
EWSR1	mRNA	2	zf-RanBP[1],RRM_6[1]
FMR1	mRNA	4	Agenet[1],FXR1P_C[1],KH_1[2]
FNBP1	mRNA	N/A	N/A
FRG1	mRNA	1	FRG1[1]
FUBP1	mRNA	6	DUF1897[2],KH_1[4]
FUS	mRNA	2	zf-RanBP[1],RRM_1[1]
FXR1	mRNA	4	Agenet[1],FXR1P_C[1],KH_1[2]
FXR2	mRNA	4	Agenet[1],FXR1P_C[1],KH_1[2]
GEMIN2	snRNA	1	SIP1[1]
HNRNPA1	mRNA	3	HnRNPA1[1],RRM_1[2]
HNRNPA2B1	mRNA	2	RRM_1[1],RRM_6[1]
HNRNPDL	mRNA	3	RRM_1[2],CBFNT[1]
HNRNPF	mRNA	4	zf-RNPHF[1],RRM_1[1],RRM_6[2]
HNRNPH3	mRNA	2	RRM_6[2]
HNRNPK	mRNA	4	ROKNT[1],KH_1[3]

GENE	FAMILY	# DOMAINS	DOMAINS
HNRNPM	mRNA	4	HnRNP_M[1],RRM_1[3]
HNRNPR	mRNA	3	RRM_1[3]
ISY1	mRNA	1	Isy1[1]
KHDRBS1	mRNA	1	KH_1[1]
KHDRBS3	mRNA	1	KH_1[1]
KHSRP	mRNA	6	DUF1897[2],KH_1[4]
LSM1	snRNA	1	LSM[1]
LSM4	snRNA	1	LSM[1]
LSM7	snRNA	1	LSM[1]
LUC7L	mRNA	1	LUC7[1]
LUC7L3	mRNA	1	LUC7[1]
MAGOH	mRNA	1	Mago_nashi[1]
MBNL1	mRNA	1	zf-CCCH[1]
MBNL2	mRNA	2	zf-CCCH[2]
NAA38	snoRNA	1	LSM[1]
NCBP1	mRNA	3	MIF4G_like_2[1],MIF4G[1],MIF4G_like[1]
NCBP2	mRNA	1	RRM_5[1]
NHP2L1	snRNA	1	Ribosomal_L7Ae[1]
NOL4	mRNA	N/A	N/A
NONO	mRNA	3	RRM_1[2],NOPS[1]
NOP56	snoRNA	3	NOP5NT[1],Nop[1],NOSIC[1]
NOSIP	mRNA	N/A	N/A
NOVA1	mRNA	3	KH_1[3]
NOVA2	mRNA	3	KH_1[3]
NUDT21	mRNA	1	NUDIX_2[1]
NUMA1	mRNA	N/A	N/A
PABPC1	mRNA	5	RRM_1[4],PABP[1]
PABPC4	mRNA	5	RRM_1[4],PABP[1]
PCBP2	mRNA	3	KH_1[3]
PPIE	mRNA	2	RRM_1[1],Pro_isomerase[1]
PPIL2	mRNA	N/A	N/A
PPIL3	mRNA	1	Pro_isomerase[1]
PPP1R8	diverse	1	FHA[1]
PRPF18	mRNA	2	PRP4[1],Prp18[1]
PRPF19	mRNA	6	Prp19[1],U-box[1],WD40[4]
PRPF3	snRNA	3	DUF1115[1],PRP3[1],PWI[1]
PRPF31	snRNA	3	Nop[1],Prp31_C[1],NOSIC[1]
PRPF4B	mRNA	1	Pkinase[1]
PRPF8	snRNA	8	PROCN[1],RRM_4[1],U6-snRNA_bdg[1],PROCT[1],PRO8NT[1],PRP8_domainIV[1],U5_2-snRNA_bdg[1],JAB[1]
PSIP1	mRNA	2	LEDGF[1],PWWP[1]
PTBP1	mRNA	4	RRM_5[3],RRM_6[1]
PTBP2	mRNA	4	RRM_5[3],RRM_6[1]
PTK6	diverse	N/A	N/A
PUF60	mRNA	3	RRM_5[1],RRM_1[2]
QKI	mRNA	1	KH_1[1]
RALY	mRNA	1	RRM_1[1]
RAVER1	mRNA	3	RRM_1[1],RRM_6[2]
RBFOX2	mRNA	2	Fox-1_C[1],RRM_1[1]
RBM10	mRNA	4	G-patch[1],zf-RanBP[1],RRM_6[2]
RBM15	mRNA	4	RRM_5[2],RRM_1[1],SPOC[1]
RBM17	mRNA	2	G-patch[1],RRM_5[1]
RBM39	mRNA	4	RRM_5[1],RRM_1[2],RBM39linker[1]
RBM5	mRNA	4	G-patch[1],zf-RanBP[1],RRM_6[2]

GENE	FAMILY	# DOMAINS	DOMAINS
RBM6	mRNA	3	G-patch[1],RRM_6[2]
RBM7	mRNA	1	RRM_1[1]
RBM8A	mRNA	1	RRM_1[1]
RBMS1	mRNA	2	RRM_1[2]
RNPS1	mRNA	1	RRM_1[1]
SAFB	mRNA	2	SAP[1],RRM_6[1]
SF1	mRNA	2	zf-CCHC[1],KH_1[1]
SF3A1	snRNA	4	ubiquitin[1],PRP21_like_P[1],Surp[2]
SF3A2	snRNA	2	CactinC_cactus[1],zf-met[1]
SF3A3	snRNA	3	Telomere_Sde2_2[1],SF3a60_bindingd[1],DUF3449[1]
SF3B1	mRNA	2	HEAT_2[1],SF3b1[1]
SF3B14	mRNA	1	RRM_1[1]
SF3B3	mRNA	2	MMS1_N[1],CPSF_A[1]
SF3B4	mRNA	2	RRM_1[2]
SLU7	mRNA	1	Slu7[1]
SMN1	snRNA	1	SMN[1]
SMN2	snRNA	1	SMN[1]
SMNDC1	mRNA	1	SMN[1]
SNRNP200	snRNA	6	Helicase_C[2],Sec63[2],DEAD[2]
SNRNP40	mRNA	7	WD40[7]
SNRNP70	snRNA	2	RRM_1[1],U1snRNP70_N[1]
SNRPA	snRNA	2	RRM_1[2]
SNRPA1	snRNA	1	LRR_9[1]
SNRPB	snRNA	1	LSM[1]
SNRPC	snRNA	1	zf-U1[1]
SNRPD1	snRNA	1	LSM[1]
SNRPD2	snRNA	1	LSM[1]
SNRPD3	snRNA	1	LSM[1]
SNRPE	snRNA	1	LSM[1]
SNRPN	snRNA	1	LSM[1]
SNW1	mRNA	1	SKIP_SNW[1]
SRC	mRNA	N/A	N/A
SRP54	ncRNA	3	SRP_SPB[1],SRP54[1],SRP54_N[1]
SRP9	ncRNA	1	SRP9-21[1]
SRPK2	mRNA	2	Pkinase[2]
SRRM1	mRNA	1	PWI[1]
SRRM2	mRNA	1	cwf21[1]
SRSF1	mRNA	2	RRM_1[2]
SRSF10	mRNA	1	RRM_1[1]
SRSF11	mRNA	1	RRM_1[1]
SRSF12	mRNA	1	RRM_1[1]
SRSF14	mRNA	N/A	N/A
SRSF2	mRNA	1	RRM_1[1]
SRSF3	mRNA	1	RRM_1[1]
SRSF4	mRNA	2	RRM_1[2]
SRSF5	mRNA	2	RRM_1[2]
SRSF6	mRNA	2	RRM_1[2]
SRSF7	mRNA	2	RRM_1[1],zf-CCHC[1]
SRSF8	mRNA	1	RRM_1[1]
SRSF9	mRNA	2	RRM_1[2]
SSRP1	mRNA	N/A	N/A
STAU1	mRNA	3	dsrm[3]
SUGP1	mRNA	3	G-patch[1],Surp[2]
SUPT16H	mRNA	N/A	N/A
SYNJ1	mRNA	N/A	N/A

GENE	FAMILY	# DOMAINS	DOMAINS
TAF15	mRNA	2	zf-RanBP[1],RRM_1[1]
TCERG1	mRNA	9	FF[6],WW[3]
THOC1	mRNA	2	efThoc1[1],Death[1]
THOC3	mRNA	4	WD40[4]
TIA1	mRNA	3	RRM_1[3]
TIAL1	mRNA	3	RRM_1[3]
TOPORS	diverse	N/A	N/A
TRA2A	mRNA	1	RRM_1[1]
TRA2B	mRNA	1	RRM_1[1]
U2AF1	mRNA	3	RRM_5[1],zf-CCCH[2]
U2AF2	mRNA	4	RRM_1[2],Transformer[1],RRM_6[1]
U2SURP	snRNA	4	cwf21[1],RRM_1[1],Surp[1],CTK3[1]
UPF1	mRNA	3	AAA_11[1],AAA_12[1],UPF1_Zn_bind[1]
UPF2	mRNA	4	MIF4G[3],Upf2[1]
USP39	snRNA	2	UCH[1],zf-UBP[1]
WT1	mRNA	N/A	N/A
YTHDC1	mRNA	1	YTH[1]
ZBP1	mRNA	N/A	N/A
ZNF207	mRNA	N/A	N/A
ZRSR2	mRNA	3	RRM_5[1],zf-CCCH[2]

Supplementary Table 3: List of genes regulated in melanoma cell lines vs. melanocyte microarray (at least in one cell line) with fold change values**.** FC: Fold change.

UPREGULATED GENES				DOWNREGULATED GENES	
GENE	**FC**	**Gene**	**FC**	**Gene**	**FC**
TGFBI	4.100	RBM17	1.489	CASP1	0.164
SNRPE	3.417	EFTUD2	1.482	CDH1	0.421
CDKN2A	2.477	E2F4	1.471	CTNNB1	0.458
EIF6	2.278	U2AF1	1.470	TFDP2	0.465
NME1	2.188	TRA2B	1.469	CUGBP2	0.472
SNRPD1	2.167	SRSF2	1.468	FOS	0.476
DDX39B	2.152	HNRNPDL	1.462	FN1	0.484
SF3B14	2.057	STAU1	1.457	FAP	0.491
SNRPA1	2.017	LSM7	1.435	MYH10	0.532
MAGOH	1.991	PSIP1	1.411	MYC	0.573
NOP56	1.903	LSM1	1.411	POLB	0.586
GADD45A	1.820	MAPK6	1.406	ATM	0.589
CCNA2	1.818	MAP3K7	1.406	CASP4	0.599
C1QBP	1.806	NUDT21	1.406	FGFR1	0.630
SNRPD2	1.795	PLK1	1.388	CTSL2	0.674
SSRP1	1.788	PTBP1	1.379	MAPK3	0.678
NHP2L1	1.781	KHDRBS1	1.371	MYD88	0.685
SRSF7	1.757	MCL1	1.371	KAI1	0.692
HNRNPA1	1.707	DDX46	1.363	MAP3K6	0.695
SF3A3	1.696	HNRNPK	1.361	CD164	0.697
BUB3	1.696	PRPF4B	1.356	ETS1	0.705
SNRPB	1.693	BUB1B	1.355	FNBP1	0.711
DEK	1.684	FAF1	1.350	LMNA	0.714
PLK2	1.682	SRRM1	1.338	PDCD8	0.726
LMNB1	1.671	CCNC	1.337	C21orf33	0.731
SRSF3	1.661	HIF1A	1.331	CCND3	0.735
MBNL1	1.648	DHX15	1.330	PTEN	0.736
SMN2	1.630	SNRNP200	1.328	PTGS2	0.741
CDC2	1.605	CELF1	1.326	ENAH	0.743
TFPI2	1.594	VEGFA	1.322	DYRK1A	0.744
MSH6	1.585	ABL1	1.317	APBB1	0.750
SUPT16H	1.573	PABPC4	1.311	ZNF198	0.750
MYBL2	1.564	FUBP1	1.309	SCUBE2	0.755
SRSF9	1.543	RBM7	1.286	NME5	0.759
AATF	1.543	CDK9	1.276	SPTAN1	0.765
MSH2	1.495	SKP2	1.275	PTK2	0.774
PDCD2	1.491				

Supplementary Table 4: List of genes regulated in each Gene Ontology Terms found to be significantly enriched in melanoma melanocyte microarray.

NODE	GENE ONTOLOGY TERM	GENE ONTOLOGY	# GENES	P-VALUE	REGULATED GENES
1	Spliceosomal Complex Assembly	GO:0000245	11	3.89E-14	**CUGBP1**, CUGBP2, DDX39B, MBNL1, PSIP1, SF3A3, SNRNP200, SNRPD1, SNRPD2, SNRPE, SRSF9
2	Ribonucleoprotein Complex Biogenesis	GO:0022613	19	2.37E-12	AATF, C1QBP, CDKN2A, **CUGBP1,** CUGBP2, DDX39B, EIF6, MBNL1, NHP2L1, NOP56, PSIP1, PTEN, SF3A3, SNRNP200, SNRPB, SNRPD1, SNRPD2, SNRPE, SRSF9
3	mRNA Splice Site Selection	GO:0006376	6	2.69E-08	**CUGBP1,** CUGBP2, MBNL1, PSIP1, SF3A3, SRSF9
4	Ribonucleoprotein Complex Assembly	GO:0022618	14	3.14E-11	C1QBP, **CUGBP1,** CUGBP2, DDX39B, EIF6, MBNL1, PSIP1, SF3A3, SNRNP200, SNRPB, SNRPD1, SNRPD2, SNRPE, SRSF9
5	mRNA Splicing, via Spliceosome	GO:0000398	33	2.76E-34	C1QBP, **CUGBP1,** CUGBP2, DDX39B, DDX46, DYRK1A, EFTUD2, HNRNPA1, HNRNPK, LSM7, MAGOH, MBNL1, NHP2L1, NUDT21, PRPF4B, PSIP1, PTBP1, RBM17, SF3A3, SF3B6, SNRNP200, SNRPA1, SNRPB, SNRPD1, SNRPD2, SNRPE, SRRM1, SRSF2, SRSF3, SRSF7, SRSF9, TRA2B, U2AF1
6	RNA Splicing	GO:0008380	35	1.31E-31	C1QBP, **CUGBP1,** CUGBP2, DDX39B, DDX46, DHX15, DYRK1A, EFTUD2, HNRNPA1, HNRNPK, LSM1, LSM7, MAGOH, MBNL1, NHP2L1, NUDT21, PRPF4B, PSIP1, PTBP1, RBM17, SF3A3, SF3B6, SNRNP200, SNRPA1, SNRPB, SNRPD1, SNRPD2, SNRPE, SRRM1, SRSF2, SRSF3, SRSF7, SRSF9, TRA2B, U2AF1
7	RNA Processing	GO:0006396	42	2.23E-28	C1QBP, CDK9, CDKN2A, **CUGBP1,** CUGBP2, DDX39B, DDX46, DHX15, DYRK1A, EFTUD2, HNRNPA1, HNRNPDL, HNRNPK, KHDRBS1, LSM1, LSM7, MAGOH, MBNL1, NHP2L1, NOP56, NUDT21, PABPC4, PRPF4B, PSIP1, PTBP1, RBM17, SF3A3, SF3B6, SMN2, SNRNP200, SNRPA1, SNRPB, SNRPD1, SNRPD2, SNRPE, SRRM1, SRSF2, SRSF3, SRSF7, SRSF9, TRA2B, U2AF1

NODE	GENE ONTOLOGY TERM	GENE ONTOLOGY	# GENES	P-VALUE	REGULATED GENES
8	mRNA Metabolic Process	GO:0016071	39	8.12E-29	ATM, C1QBP, CDK9, **CUGBP1,** CUGBP2, DDX39B, DDX46, DHX15, DYRK1A, EFTUD2, HNRNPA1, HNRNPK, KHDRBS1, LSM1, LSM7, MAGOH, MBNL1, NHP2L1, NUDT21, PRPF4B, PSIP1, PTBP1, RBM17, SF3A3, SF3B6, SMN2, SNRNP200, SNRPA1, SNRPB, SNRPD1, SNRPD2, SNRPE, SRRM1, SRSF2, SRSF3, SRSF7, SRSF9, TRA2B, U2AF1
9	Spliceosomal snRNP Assembly	GO:0000387	4	1.34E-04	SNRPB, SNRPD1, SNRPD2, SNRPE
10	Histone mRNA Metabolic Process	GO:0008334	4	2.61E-05	ATM, LSM1, SNRPB, SNRPE
11	Alternative mRNA Splicing, via Spliceosome	GO:0000380	8	7.38E-11	DYRK1A, HNRNPA1, MAGOH, MBNL1, PTBP1, RBM17, SRSF2, TRA2B
12	Negative Regulation of mRNA Processing	GO:0050686	6	3.32E-08	C1QBP, CDK9, DYRK1A, PTBP1, SRSF7, SRSF9
13	Regulation of RNA Splicing	GO:0043484	10	3.79E-10	C1QBP, **CUGBP1,** DYRK1A, MAGOH, MBNL1, PTBP1, SRSF2, SRSF7, SRSF9, TRA2B
14	Regulation of Alternative mRNA Splicing, via Spliceosome	GO:0000381	6	2.17E-08	DYRK1A, MAGOH, MBNL1, PTBP1, SRSF2, TRA2B
15	Regulation of mRNA Processing	GO:0050684	10	3.79E-10	C1QBP, CDK9, DYRK1A, MAGOH, MBNL1, PTBP1, SRSF2, SRSF7, SRSF9, TRA2B
16	mRNA 3'-End Processing	GO:0031124	11	4.20E-12	CDK9, MAGOH, NUDT21, SNRPB, SNRPE, SRRM1, SRSF2, SRSF3, SRSF7, SRSF9, U2AF1
17	RNA Export from Nucleus	GO:0006405	10	2.75E-10	DDX39B, HNRNPA1, KHDRBS1, MAGOH, SRRM1, SRSF2, SRSF3, SRSF7, SRSF9, U2AF1
18	Nucleocytoplasmic Transport	GO:0006913	18	2.02E-10	C21orf33, CDH1, CDKN2A, DDX39B, EIF6, FAF1, HNRNPA1, KHDRBS1, LMNA, MAGOH, MAPK3, PTGS2, SRRM1, SRSF2, SRSF3, SRSF7, SRSF9, U2AF1
19	Termination of RNA Polymerase II Transcription	GO:0006369	10	3.91E-13	MAGOH, NUDT21, SNRPB, SNRPE, SRRM1, SRSF2, SRSF3, SRSF7, SRSF9, U2AF1
20	Nuclear Export	GO:0051168	12	2.13E-10	CDKN2A, DDX39B, EIF6, HNRNPA1, KHDRBS1, MAGOH, SRRM1, SRSF2, SRSF3, SRSF7, SRSF9, U2AF1
21	RNA Localization	GO:0006403	11	1.72E-08	DDX39B, HNRNPA1, KHDRBS1, MAGOH, SRRM1, SRSF2, SRSF3, SRSF7, SRSF9, STAU1, U2AF1
22	Ribonucleoprotein Complex Export from Nucleus	GO:0071426	9	5.22E-09	DDX39B, EIF6, MAGOH, SRRM1, SRSF2, SRSF3, SRSF7, SRSF9, U2AF1

NODE	GENE ONTOLOGY TERM	GENE ONTOLOGY	# GENES	P-VALUE	REGULATED GENES
23	Negative Regulation of Cell Cycle	GO:0045786	21	5.77E-12	ABL1, APBB1, ATM, BUB1B, BUB3, CCNA2, CDK1, CDK9, CDKN2A, CTNNB1, DDX39B, ETS1, FAP, GADD45A, KHDRBS1, MSH2, MYC, PLK1, PLK2, PTEN, PTGS2
24	Anaphase-Promoting Complex-Dependent Proteasomal Ubiquitin-Dependent Protein Catabolic Process	GO:0031145	7	1.01E-05	ATM, BUB1B, BUB3, CDK1, PLK1, PTEN, SKP2
25	Negative Regulation of Mitotic Cell Cycle Phase Transition	GO:1901991	7	1.13E-04	ATM, BUB1B, BUB3, CCNA2, CDK1, PLK1, PTEN
26	Regulation of Cyclin-Dependent Protein Serine/Threonine Kinase Activity	GO:0000079	7	2.81E-06	CCNA2, CCNC, CCND3, CDKN2A, GADD45A, PLK1, PTEN
27	G2/M Transition of Mitotic Cell Cycle	GO:0000086	9	4.47E-06	ATM, CCNA2, CDK1, CDKN2A, GADD45A, KHDRBS1, MYBL2, PLK1, SKP2
28	Mitochondrial Depolarization	GO:0051882	3	3.34E-04	ABL1, CASP1, CDKN2A
29	Regulation of DNA Damage Response, Signal Transduction By P53 Class Mediator	GO:0043516	3	1.34E-03	ATM, CDKN2A, DYRK1A
30	Regulation of Response to DNA Damage Stimulus	GO:2001020	9	4.82E-07	ABL1, ATM, CDK9, CDKN2A, DDX39B, DEK, DYRK1A, MCL1, MYC
31	Regulation of G2/M Transition of Mitotic Cell Cycle	GO:0010389	4	4.10E-04	ATM, CCNA2, CDK1, CDKN2A
32	Regulation of Ubiquitin-Protein Transferase Activity	GO:0051438	8	2.03E-06	ABL1, ATM, BUB1B, BUB3, CDK1, CDKN2A, PLK1, PTEN
33	Negative Regulation of Mitotic Cell Cycle	GO:0045930	11	3.75E-07	ABL1, ATM, BUB1B, BUB3, CCNA2, CDK1, CTNNB1, MSH2, PLK1, PLK2, PTEN
34	Centrosome Organization	GO:0051297	5	4.24E-04	CDK1, CTNNB1, GADD45A, PLK1, PLK2
35	Mitotic Nuclear Envelope Disassembly	GO:0007077	3	2.43E-03	CDK1, LMNA, PLK1
36	Regulation of Ubiquitin-Protein Ligase Activity Involved in Mitotic Cell Cycle	GO:0051439	6	4.25E-05	ATM, BUB1B, BUB3, CDK1, PLK1, PTEN
37	Negative Regulation of Protein Modification By Small Protein Conjugation or Removal	GO:1903321	7	4.46E-05	ABL1, ATM, BUB1B, BUB3, CDKN2A, CTNNB1, PLK1
38	Regulation of Protein Modification By Small Protein Conjugation or Removal	GO:1903320	12	2.07E-07	ABL1, ATM, BUB1B, BUB3, CDK1, CDK9, CDKN2A, CTNNB1, PLK1, PTEN, PTK2, SKP2
39	Negative Regulation of Ubiquitin-Protein Transferase Activity	GO:0051444	6	3.80E-05	ABL1, ATM, BUB1B, BUB3, CDKN2A, PLK1
40	Regulation of Fibroblast Proliferation	GO:0048145	4	2.06E-03	CCNA2, CTNNB1, FN1, MYC

NODE	GENE ONTOLOGY TERM	GENE ONTOLOGY	# GENES	P-VALUE	REGULATED GENES
41	Ureteric Bud Development	GO:0001657	5	5.77E-04	C21orf33, CTNNB1, FGFR1, MYC, VEGFA
42	Positive Regulation of Stem Cell Proliferation	GO:2000648	6	6.22E-06	CTNNB1, FGFR1, HIF1A, MYC, PDCD2, VEGFA
43	Neuroblast Proliferation	GO:0007405	4	4.69E-04	CTNNB1, FGFR1, HIF1A, VEGFA
44	Organ Formation	GO:0048645	4	8.59E-04	C21orf33, CTNNB1, FGFR1, MAPK3
45	Positive Regulation of Mesenchymal Cell Proliferation	GO:0002053	4	6.47E-05	CTNNB1, FGFR1, MYC, VEGFA
46	Telomere Maintenance	GO:0000723	4	2.06E-03	ATM, CTNNB1, MYC, PTEN
47	Adherens Junction Assembly	GO:0034333	4	1.73E-03	CTNNB1, PTEN, PTK2, VEGFA
48	Cell-Substrate Junction Assembly	GO:0007044	4	2.43E-03	FN1, PTEN, PTK2, VEGFA
49	Regulation of Protein Ubiquitination Involved in Ubiquitin-Dependent Protein Catabolic Process	GO:2000058	5	3.52E-04	CDK1, CDKN2A, PLK1, PTEN, PTK2
50	Positive Regulation of Chromosome Organization	GO:2001252	6	3.20E-05	CDK9, CTNNB1, MAPK3, PLK1, PTEN, VEGFA
51	Regulation of Chromosome Segregation	GO:0051983	6	1.72E-05	ATM, BUB1B, BUB3, CTNNB1, PLK1, PTEN
52	Negative Regulation of Cyclin-Dependent Protein Serine/Threonine Kinase Activity	GO:0045736	3	1.03E-03	CDKN2A, PLK1, PTEN
53	Cell Aging	GO:0007569	5	4.44E-04	ABL1, ATM, CDKN2A, LMNA, PTEN
54	Regulation of Cell-Matrix Adhesion	GO:0001952	4	3.07E-03	CDKN2A, PTEN, PTK2, VEGFA
55	Regulation of Chromosome Organization	GO:0033044	10	2.29E-06	ATM, BUB1B, BUB3, CDK9, CTNNB1, MAPK3, MYC, PLK1, PTEN, VEGFA
56	Positive Regulation of Histone Modification	GO:0031058	4	1.01E-03	CDK9, CTNNB1, MAPK3, VEGFA
57	Positive Regulation of Response to DNA Damage Stimulus	GO:2001022	3	8.13E-03	ATM, CDKN2A, MYC
58	Cellular Component Disassembly Involved in Execution Phase of Apoptosis	GO:0006921	8	1.89E-08	AIFM1, CDH1, CDKN2A, CTNNB1, LMNA, LMNB1, PTK2, SPTAN1
59	Execution Phase of Apoptosis	GO:0097194	11	9.31E-11	AIFM1, CASP1, CASP4, CDH1, CDKN2A, CTNNB1, FAP, LMNA, LMNB1, PTK2, SPTAN1
60	Regulation of Mitotic Metaphase/Anaphase Transition	GO:0030071	5	2.79E-05	ATM, BUB1B, BUB3, PLK1, PTEN
61	Multicellular Organismal Aging	GO:0010259	4	5.10E-05	ATM, CTSV, MSH2, MSH6
62	Somatic Diversification of Immune Receptors via Germline Recombination within a Single Locus	GO:0002562	4	6.05E-04	ATM, MSH2, MSH6, POLB
63	Somatic Hypermutation of Immunoglobulin Genes	GO:0016446	3	1.02E-04	MSH2, MSH6, POLB

NODE	GENE ONTOLOGY TERM	GENE ONTOLOGY	# GENES	P-VALUE	REGULATED GENES
64	Mitotic Spindle Assembly Checkpoint	GO:0007094	4	1.75E-04	ATM, BUB1B, BUB3, PLK1
65	Mitotic Cell Cycle Checkpoint	GO:0007093	8	1.91E-05	ATM, BUB1B, BUB3, CCNA2, CDK1, MSH2, PLK1, PLK2
66	Negative Regulation of Proteolysis Involved in Cellular Protein Catabolic Process	GO:1903051	5	1.70E-04	ATM, BUB1B, BUB3, CDKN2A, PLK1
67	Negative Regulation of Cell Division	GO:0051782	6	2.09E-05	ATM, BUB1B, BUB3, MSH2, MYC, PLK1
68	Meiosis I	GO:0007127	4	2.63E-03	ATM, MSH2, MSH6, PLK1
69	G2 DNA Damage Checkpoint	GO:0031572	4	9.96E-05	ATM, CCNA2, CDK1, PLK1
70	Regulation of Execution Phase of Apoptosis	GO:1900117	3	6.91E-04	AIFM1, CDKN2A, FAP
71	Cardiac Muscle Cell Development	GO:0055013	3	5.41E-03	LMNA, MYH10, VEGFA
72	Regulation of Oxidative Stress-induced Intrinsic Apoptotic Signaling Pathway	GO:1902175	3	1.03E-03	HIF1A, MCL1, NME5
73	TRIF-Dependent Toll-Like Receptor Signaling Pathway	GO:0035666	4	1.65E-03	CDK1, FOS, MAP3K7, MAPK3
74	Positive Regulation of Viral Life Cycle	GO:1903902	4	2.06E-03	CDK9, SSRP1, STAU1, SUPT16H
75	Regulation of Smooth Muscle Cell Proliferation	GO:0048660	4	2.73E-03	CTNNB1, MYD88, PTGS2, SKP2

Supplementary Table 5: Differential regulation levels of genes identified in CUGBP1 regulated networks upon DEK downregulation by short hairpin RNA in SK-Mel-103 cells at day 4.5 (unpublished data). FC: Fold change. FDR<0.05.

GENE	FC	LOG2FC
UBE2C	0.13	-2.93
DHFR	0.16	-2.60
CDC20	0.20	-2.31
PRKDC	0.21	-2.28
CCNB1	0.29	-1.80
RPA3	0.35	-1.51
MCM4	0.37	-1.45
MCM6	0.38	-1.38
FANCA	0.40	-1.34
FANCD2	0.45	-1.16
RFC4	0.47	-1.08
RFC5	0.52	-0.93
RFC5	0.52	-0.93
POLA1	0.57	-0.80

Supplementary Table 6: List of genes identified by RIP-Seq in melanoma cell lines SKMEL-103 and UACC. Sorted by identified region of binding. Gray highlights mark novel targets and blue genes indicate genes with CUG repeats in the indicated region.

3' UNTRANSLATED REGION					
AAK1	CISD2	GNG12	MSN	RAP2A	SRSF7
AASDHPPT	CIT	GNG2	MTAP	RAP2B	SRSF9
ABCC9	CKAP4	GNPDA1	MTCH2	RAPH1	SS18
ABHD2	CKS1B	GNPNAT1	MTDH	RASA2	SSB
ABL2	CKS2	GOLIM4	MTHFD2	RASSF3	SSFA2
AC006465.3	CLASP2	GOLT1B	MTMR4	RBBP4	SSH2
AC015987.2	CLIC1	GPCPD1	MTMR6	RBBP7	SSR1
AC073346.2	CLIC4	GPD2	MTMR9	RBFOX2	SSR2
AC104841.2	CLINT1	GPI	MTPN	RBM15	SSR3
AC119673.1	CLIP4	GPR56	MTRNR2L1	RBM22	ST13
AC120194.1	CLN6	GPS2	MTRNR2L10	RBM25	STAG2
ACAT2	CLNS1A	GPX1	MYL12A	RBM27	STARD4
ACBD3	CLPTM1L	GRSF1	MYL12B	RBM3	STARD7
ACBD7	CLTA	GRWD1	MYL6	RBM39	STAT3
ACLY	CLTC	GSK3B	MYLK	RBM5	STAT5B
ACOT13	CMAS	GSTP1	MYO1B	RBM8A	STAU1
ACSL3	CMIP	GTF2A1	MZT2B	RBMS1	STK17A
ACSL4	CMPK1	GTF2E2	NAA20	RBMX	STK4
ACTB	CMTM4	GTPBP3	NAA50	RBMXL1	STMN1
ACTG1	CMTM6	GULP1	NAB1	RBPJ	STRAP
ACTR2	CMTM7	H2AFV	NACA	RBX1	STX3
ACTR3	CNBP	H2AFY	NACA2	RC3H1	STX6
ADAM10	CNIH	H2AFZ	NACC1	RC3H2	STYX
ADAM9	CNN3	H3F3A	NACC2	RCAN1	SUB1
ADAR	CNOT6	H3F3B	NAMPT	RCC2	SUCO
ADH5	CNOT6L	HAUS2	NAP1L1	RCCD1	SUDS3
ADPGK	CNPY2	HCFC1	NAPB	RCN1	SUMO1
ADSS	COLGALT1	HDAC1	NAPG	RCN2	SUMO2
AFF1	COMMD10	HDAC2	NBN	RCOR1	SUMO3
AFF4	COPA	HDDC2	NBPF16	RDX	SUPT16H
AGBL5	COPB1	HDGF	NCAPD2	REEP3	SUSD5
AGFG1	COPB2	HDLBP	NCKAP1	REST	SYAP1
AGPAT5	COPRS	HEATR3	NCL	REXO1L1	SYNC
AGPAT9	COPS7A	HELLS	NCOA3	REXO2	SYNCRIP
AHCY	COPS8	HERPUD1	NDNL2	RFK	SYPL1
AHNAK	COPZ1	HIATL1	NDRG3	RFWD3	TACC1
AK2	CORO1C	HIF1A	NDUFA1	RFX7	TAF1
AK4	COTL1	HIF1AN	NDUFA13	RHEB	TAF13
AKAP11	COX4I1	HIGD1A	NDUFA4	RHOA	TAF1L
AKAP12	COX5B	HIGD2A	NDUFB2	RIF1	TAF5
AKAP2	COX6A1	HINT1	NDUFB3	RLIM	TAF7
AKIRIN1	COX6B1	HINT3	NDUFB4	RMND5A	TAGLN2
AKR1B1	COX7A2	HIPK1	NDUFB9	RNASEH1	TANC2
AKT2	COX7A2L	HIPK2	NDUFC2	RND3	TAOK1
ALDH9A1	COX7B	HIST1H1B	NDUFS2	RNF11	TARDBP
ALDOA	COX7C	HIST1H1C	NDUFS5	RNF114	TAX1BP1
ALKBH5	COX8A	HIST1H2AB	NECAP1	RNF139	TBC1D13
ALS2CR8	CPM	HIST1H2AM	NEDD8	RNF144A	TBCA
AMD1	CPNE3	HIST1H2BC	NEK4	RNF219	TBL1XR1
AMOTL1	CPNE8	HIST1H2BL	NEK7	RNF38	TBPL1
ANAPC13	CPOX	HIST1H3B	NF2	RNPS1	TCEA1
ANKFY1	CPSF6	HIST1H3F	NFAT5	ROMO1	TCEAL8
ANKRD52	CREB3L2	HIST1H3J	NFIB	RP11-762I7.5	TCF7L2

ANLN	CREB5	HIST1H4B	NFYC	RP5-1165K10.1	TCP1
ANP32A	CREBL2	HIST1H4D	NGFRAP1	RPAIN	TEAD1
ANXA1	CRIM1	HIST1H4H	NGRN	RPL12	TERF2IP
ANXA2	CRIP2	HIST1H4K	NHP2L1	RPL13A	TET3
ANXA5	CRK	HIST2H2AA3	NMD3	RPL14	TFCP2
AP000350.10	CRKL	HIST2H2AA4	NME1	RPL15	TFDP1
AP000350.4	CRTAP	HIST2H2AB	NME1-NME2	RPL17	TFRC
AP1G1	CSDE1	HIST2H3C	NME2	RPL17-C18orf32	TGFBR1
AP1M1	CSE1L	HIST2H4B	NME7	RPL18	TGFBR2
AP1S1	CSNK1A1	HIST4H4	NOC2L	RPL18A	TGOLN2
AP1S2	CSNK1E	HK2	NOL9	RPL22	THBS1
AP2M1	CSNK2A2	HLA-B	NOLC1	RPL23	THOC3
AP2S1	CTBP1	HLTF	NONO	RPL23A	THRAP3
AP3B1	CTBP2	HMG20A	NOP56	RPL24	THUMPD1
AP3M1	CTDSP2	HMGA1	NOP58	RPL26	TIMM17A
AP3S1	CTDSPL2	HMGA2	NOTCH2	RPL27A	TIMP2
APH1A	CTGF	HMGB1	NOTCH2NL	RPL29	TM4SF1
API5	CTNNA1	HMGB2	NPAS2	RPL3	TM9SF3
APLP2	CTNNB1	HMGCR	NPC2	RPL30	TMA7
APMAP	CTSB	HMGN1	NPM1	RPL31	TMBIM6
APP	CTSC	HMGN2	NPTN	RPL32	TMCO1
APTX	CUL4B	HMGN3	NQO1	RPL35	TMED10
ARCN1	CXorf57	HMGN4	NR3C1	RPL35A	TMED2
ARF1	CYCS	HMOX1	NRAS	RPL36	TMED7
ARF3	DAD1	HN1	NREP	RPL36AL	TMED8
ARF4	DAP3	HN1L	NSF	RPL37	TMEM107
ARF6	DAZAP2	HNRNPA0	NT5DC3	RPL37A	TMEM109
ARFGEF2	DBI	HNRNPA1	NUCKS1	RPL39	TMEM123
ARHGAP12	DCAF12	HNRNPA1L2	NUDC	RPL39L	TMEM164
ARID5B	DCAF16	HNRNPA2B1	NUDCD3	RPL4	TMEM167A
ARIH1	DCAF17	HNRNPA3	NUDT19	RPL41	TMEM19
ARL1	DCAF7	HNRNPAB	NUDT21	RPL7	TMEM2
ARL2BP	DCBLD2	HNRNPC	NUDT3	RPL9	TMEM212
ARL5A	DCK	HNRNPD	NUFIP2	RPLP0	TMEM237
ARL6IP1	DCP2	HNRNPF	NUP153	RPN1	TMEM248
ARL8B	DCTN4	HNRNPH1	NUP62	RPN2	TMEM30A
ARMCX6	DCUN1D4	HNRNPH2	NUP93	RPP14	TMEM33
ARPC2	DDB1	HNRNPK	NUPL1	RPRD1B	TMEM47
ARPC4	DDX1	HNRNPL	NXPE3	RPS10	TMEM48
ARPC5	DDX17	HNRNPM	OAZ1	RPS11	TMEM59
ARPP19	DDX21	HNRNPR	OAZ2	RPS13	TMEM64
ARRDC3	DDX24	HNRNPU	ODC1	RPS14	TMEM66
ASAP1	DDX3X	HNRPDL	ODF2L	RPS15	TMEM9B
ASH1L	DDX3Y	HOOK3	OPA1	RPS15A	TMPO
ASPH	DDX5	HOXB7	OPHN1	RPS17	TMSB10
ASTN2	DDX56	HP1BP3	OSBP	RPS17L	TMX1
ATAD1	DEK	HPCAL1	OSBPL10	RPS2	TMX2
ATF1	DENND6A	HPRT1	OSBPL3	RPS20	TMX3
ATF2	DENR	HSBP1	OSBPL8	RPS21	TNC
ATF4	DEPDC1	HSD17B12	OST4	RPS23	TNFRSF21
ATF7IP	DESI2	HSP90AA1	OSTC	RPS24	TNKS
ATG7	DGCR2	HSP90AB1	OTUD4	RPS27	TNKS2
ATL3	DGUOK	HSP90B1	OTUD6B	RPS27L	TNPO1
ATM	DHX15	HSPA13	P2RY11	RPS28	TNPO2
ATMIN	DHX36	HSPA1A	P4HB	RPS29	TNRC6A
ATOX1	DHX40	HSPA1B	PABPC1	RPS3	TNRC6B
ATP13A3	DHX9	HSPA8	PABPN1	RPS3A	TOM1L2
ATP1B1	DIABLO	HSPA9	PACS2	RPS4X	TOMM20

ATP1B3	DICER1	HSPD1	PAFAH1B1	RPS5	TOMM22
ATP2A2	DIP2B	HSPE1	PAFAH1B2	RPS6	TOMM34
ATP5A1	DKC1	HSPH1	PAGR1	RPS6KA3	TOMM5
ATP5B	DLG1	IDS	PAK2	RPS8	TOMM6
ATP5C1	DLX1	IER2	PALM2-AKAP2	RPS9	TOMM7
ATP5E	DMXL1	IER3IP1	PANK3	RPSA	TOMM70A
ATP5EP2	DNAJA1	IER5	PAPD5	RQCD1	TOP1
ATP5F1	DNAJA2	IFI16	PAPOLA	RRAGA	TOP2A
ATP5G2	DNAJB1	IL1RAP	PAPOLG	RRM2	TOP2B
ATP5G3	DNAJB11	IL6ST	PARK7	RRP15	TOR1AIP2
ATP5I	DNAJC5	ILF2	PARN	RSF1	TP53RK
ATP6AP1	DNER	ILF3	PARP1	RSL24D1	TPGS2
ATP6AP2	DPY19L1	IMMT	PCBP1	RTN4	TPI1
ATP6V0B	DPY19L3	IMP3	PCBP2	RUNX1	TPM1
ATP6V0D1	DPY19L4	IMP4	PCGF3	RWDD1	TPM3
ATP6V0E1	DPYSL2	IMPAD1	PCNA	RYBP	TPM4
ATP6V1A	DR1	INCENP	PCNP	RYK	TPT1
ATP6V1B2	DSTN	INHBA	PCYT1A	S100A10	TRA2A
ATP6V1C1	DTX3L	INIP	PDAP1	S100A13	TRA2B
ATP6V1C2	DTYMK	INO80D	PDCD10	S100A6	TRAM1
ATP6V1E1	DUSP11	INPP5A	PDCD5	SAE1	TRAPPC10
ATP6V1F	DUSP5	IPO7	PDCD6	SAMD1	TRIB1
ATP6V1G1	DUSP6	IQGAP1	PDE12	SAMD11	TRIM28
ATP8B2	DUSP7	IRAK1	PDGFA	SAMD4A	TRIM4
ATP9A	DUT	IRF2BP2	PDIA6	SAP18	TRIM58
ATPIF1	DYNC1H1	IRF2BPL	PDLIM5	SARNP	TRIP12
ATRX	DYNC1I2	ISCA1	PDS5A	SART3	TRIP6
ATXN7	DYNC1LI2	IST1	PDZD8	SATB2	TRMT112
ATXN7L3B	DYNLL1	ITGA6	PEA15	SBNO1	TROVE2
AUP1	DYNLL2	ITGAV	PEBP1	SCD	TRPS1
AURKB	DYRK2	ITGB1	PEG10	SCD5	TSC22D1
AZIN1	E2F3	ITGB8	PERP	SCOC	TSN
B2M	EDARADD	ITM2B	PEX11B	SDC4	TSPAN3
B3GNT4	EEF1A1	JKAMP	PEX26	SDCBP	TSPAN31
B4GALT1	EEF1E1	JUND	PFDN2	SDE2	TSR1
B4GALT5	EEF1G	KBTBD2	PFDN5	SDHB	TTC3
B4GALT6	EEF2	KCMF1	PFKFB3	SEC23B	TUBA1A
BACH1	EEF2K	KCNJ5	PFN1	SEC24A	TUBA1B
BAG4	EFCAB14	KCTD10	PFN2	SEC61A1	TUBA1C
BAG5	EFHD2	KCTD20	PGAM1	SEC61B	TUBB
BAX	EFNA5	KDELR2	PGAM4	SEC61G	TUBB3
BAZ2A	EFR3A	KDM5A	PGK1	SEH1L	TUBB4B
BCAP31	EI24	KDM6B	PGM2	SEL1L	TUFM
BCL2L2-PABPN1	EID1	KHDRBS1	PGRMC1	SELT	TULP4
BCLAF1	EIF1	KIAA0101	PHACTR4	SEPT11	TVP23B
BEST1	EIF1AD	KIAA0355	PHC1	SEPT15	TWF1
BIRC2	EIF1AX	KIAA1456	PHC3	SEPT2	TWISTNB
BIRC5	EIF1B	KIAA1715	PHF6	SEPT7	TWSG1
BLCAP	EIF2AK2	KIF13A	PHF8	SEPT8	TXLNA
BLMH	EIF2S1	KIF18B	PHLDA1	SEPT9	TXN
BLOC1S5-	EIF2S2	KIF1C	PHTF2	SEPW1	TXNDC17
BLOC1S6	EIF2S3	KIF2C	PIGS	SERBP1	TXNDC5
BMPR2	EIF3A	KIF5B	PIK3R1	SERF2	TXNRD1
BNIP2	EIF3B	KIFAP3	PIKFYVE	SERINC1	TYMS
BNIP3	EIF3D	KLHDC10	PIP4K2B	SERP1	U2AF2
BRD4	EIF3E	KLHDC7A	PITHD1	SERPINE2	U2SURP
BRI3	EIF3F	KLHL8	PJA2	SERTAD2	UBA2
BRI3BP	EIF3G	KLHL9	PKM	SET	UBA52

BRK1	EIF3I	KPNA2	PLEKHA2	SETD7	UBAP2L
BRWD1	EIF3L	KPNB1	PLEKHA3	SF1	UBB
BTBD1	EIF4A1	KTN1	PLEKHA5	SF3A3	UBC
BTBD7	EIF4A2	LAMP2	PLEKHB2	SF3B1	UBE2A
BTF3	EIF4A3	LAMTOR1	PLS3	SF3B14	UBE2C
BTF3L4	EIF4B	LAMTOR3	PMEPA1	SFPQ	UBE2E1
BTG1	EIF4E	LAMTOR5	PMP22	SFT2D1	UBE2E3
BUB3	EIF4E2	LAPTM4A	PNN	SFT2D2	UBE2G1
BZW1	EIF4EBP2	LAPTM4B	PNPO	SGK1	UBE2K
BZW2	EIF4G1	LARP1	POLDIP3	SGK196	UBE2M
C11orf31	EIF4G2	LARP4	POLE3	SGPL1	UBE2N
C11orf58	EIF4H	LARS	POLR2M	SHISA5	UBE2W
C12orf23	EIF5	LASP1	POLR3K	SHISA9	UBE2Z
C14orf166	EIF5A	LBR	POMP	SHOC2	UBE3A
C14orf2	EIF5AL1	LDHA	POTEE	SHQ1	UBL5
C16orf52	EIF6	LDHB	POU2F1	SIAE	UBLCP1
C17orf103	ELAVL1	LDLRAD3	PPAT	SIAH1	UBN2
C18orf25	ELK3	LDOC1L	PPIA	SIAH2	UBQLN1
C1orf216	ELK4	LEF1	PPIB	SKA2	UBXN7
C1orf43	ELL2	LEPROT	PPIC	SKIL	UGCG
C1orf56	ELOF1	LETM1	PPIL4	SKP1	UGDH
C1QBP	ELOVL5	LGALS1	PPIP5K2	SLA2	UGGT1
C20orf24	EMC1	LHFPL2	PPM1A	SLC16A1	UGT8
C21orf91	ENAH	LIMA1	PPP1CB	SLC1A5	UHMK1
C2orf15	ENC1	LIMS1	PPP1CC	SLC20A1	UPF3B
C4orf46	ENO1	LIN52	PPP1R12A	SLC25A1	UQCR10
C5orf15	ENSA	LIN7C	PPP1R14B	SLC25A12	UQCR11
C5orf22	EOGT	LMNB1	PPP1R15B	SLC25A24	UQCRH
C5orf24	EPB41L3	LMO4	PPP1R2	SLC25A3	UQCRQ
C5orf45	EPDR1	LNPEP	PPP2CA	SLC25A39	USMG5
C5orf51	EPPIN	LONP2	PPP2CB	SLC25A44	USP22
C6orf62	EPT1	LPP	PPP2R1A	SLC25A46	USP34
C7orf73	ERGIC3	LRPPRC	PPP2R4	SLC25A5	USP37
CADM1	ERH	LRRC58	PPP3CB	SLC26A2	UTP11L
CALD1	ERLEC1	LRRC59	PPP3R1	SLC29A1	VAMP3
CALM1	ERO1L	LRRC8A	PPP4R2	SLC30A5	VAPA
CALM2	ETF1	LSM14A	PPP6C	SLC30A7	VAPB
CALR	ETFA	LSM14B	PPP6R3	SLC35B4	VAT1
CALU	ETNK1	LSM4	PRDX1	SLC35E1	VAV2
CAMK2D	ETS1	LSM5	PRDX3	SLC35F2	VDAC1
CAMSAP2	ETV5	LYPLA1	PRDX4	SLC38A2	VDAC2
CAND1	EVI5	LYPLA2	PRDX6	SLC39A10	VEZF1
CANX	EZR	LZIC	PREPL	SLC39A14	VGLL4
CAP1	FABP5	M6PR	PRKAA1	SLC39A9	VHL
CAPN2	FAM105B	MAB21L3	PRKAR1A	SLC44A1	VIM
CAPRIN1	FAM120A	MAFG	PRKD3	SLC4A5	VMA21
CAPZA1	FAM122B	MAGEA12	PRKDC	SLC4A7	VPS26A
CAPZA2	FAM126A	MAGEA3	PRMT1	SLC5A3	VPS29
CARD8	FAM129B	MAGEA4	PRMT5	SLC6A6	VPS35
CASC3	FAM134A	MAGEA6	PRNP	SLC9A6	VPS36
CASD1	FAM160B1	MAGEB10	PRPF4B	SLIRP	WBP5
CASP2	FAM166A	MAGT1	PRPF8	SLMO2	WDR1
CAV1	FAM178A	MANF	PRPS1	SMAD2	WDR3
CAV2	FAM199X	MAP1LC3B	PRR14L	SMAD5	WDR36
CBFB	FAM219A	MAP3K13	PRR3	SMAP2	WDR37
CBL	FAM3C	MAP4	PRRC2B	SMARCAD1	WDR77
CBX1	FAM49B	MAPK1	PRRG4	SMARCC1	WDR82
CBX3	FAM60A	MAPK14	PRSS23	SMARCE1	WEE1

CBX5	FAM83D	MAPK6	PSAP	SMC1A	WIPF2
CBX6	FAM91A1	MAPKAPK2	PSAT1	SMC5	WNK1
CCDC50	FAM96A	MAPRE1	PSD3	SMCR7L	WSB2
CCDC73	FAR1	MARCH5	PSMA2	SMG1	WTAP
CCDC90B	FAT1	MARCH6	PSMA3	SMG7	WWTR1
CCNB1	FAU	MARCH7	PSMA4	SMIM13	XIAP
CCND1	FBXL17	MARCKS	PSMA5	SMIM15	XPO1
CCNI	FBXO21	MARCKSL1	PSMA6	SMIM7	XPO4
CCNT1	FBXO5	MAT2A	PSMA7	SMNDC1	XPOT
CCT2	FBXW11	MAT2B	PSMB1	SMS	XRCC2
CCT3	FCF1	MATR3	PSMB4	SNAP23	XRCC5
CCT4	FEM1C	MAX	PSMB5	SNRK	XRCC6
CCT5	FERMT2	MAZ	PSMC1	SNRPB	XRN1
CCT6A	FGF13	MBNL1	PSMD1	SNRPB2	YAP1
CCT7	FHL2	MCAM	PSMD10	SNRPD1	YBX1
CCT8	FKBP1A	MCL1	PSMD11	SNRPD2	YBX3
CD151	FKBP4	MCM2	PSMD12	SNRPD3	YOD1
CD164	FMNL2	MCM3	PSMD13	SNRPE	YTHDF2
CD2AP	FNBP1L	MCM7	PSMD2	SNRPG	YWHAB
CD44	FNBP4	MCMDC2	PSMD3	SNTB2	YWHAE
CD46	FNDC3B	MDH1	PSME3	SNX12	YWHAG
CD47	FOXJ3	MDH2	PTAR1	SNX22	YWHAQ
CD59	FOXK1	MDM2	PTBP1	SNX27	YWHAZ
CD63	FOXK2	MEAF6	PTBP3	SNX3	YY1
CD9	FRMD6	MECOM	PTCH2	SNX30	ZBTB33
CDC25B	FRS2	MED28	PTGES3	SNX4	ZC3H11A
CDC27	FTH1	MED29	PTMA	SNX5	ZC3H13
CDC34	FTL	MELK	PTP4A1	SOCS5	ZC3H15
CDC42	FUBP1	MESDC2	PTP4A2	SOD1	ZCCHC3
CDC42SE1	FUS	METAP2	PTPN1	SOD2	ZFAND5
CDC42SE2	FXR1	METTL21A	PTPN11	SOX10	ZFAND6
CDC73	FYTTD1	METTL5	PTPN12	SOX13	ZFHX3
CDCA3	G2E3	METTL9	PUM1	SOX4	ZFP36L1
CDCA4	G3BP1	MFSD1	PURA	SP1	ZFP91
CDK1	G3BP2	MGAT5	PURB	SP3	ZFR
CDK14	GABARAP	MIA	PXN	SPARC	ZFX
CDK17	GABARAPL2	MIB1	PYGB	SPATS2L	ZMAT2
CDK2	GAPDH	MIDN	PYGO2	SPCS1	ZMAT3
CDK2AP1	GBE1	MIF	PYURF	SPCS3	ZMPSTE24
CDK4	GCN1L1	MINOS1	QDPR	SPECC1L	ZNF146
CDK5R1	GCOM1	MKRN1	QKI	SPG21	ZNF346
CDK6	GDI1	MLEC	QSER1	SPIN1	ZNF37A
CDKN1A	GEMIN6	MLLT6	RAB10	SPIN4	ZNF451
CDS2	GFM1	MMADHC	RAB11A	SPOPL	ZNF460
CDV3	GFPT1	MMGT1	RAB12	SPRED1	ZNF471
CEACAM8	GGPS1	MMP14	RAB14	SPRYD7	ZNF532
CEBPB	GHITM	MMS22L	RAB18	SPTSSA	ZNF611
CEBPG	GID8	MOB1A	RAB1A	SQSTM1	ZNF623
CELF1	GINS1	MOB4	RAB23	SRD5A1	ZNF652
CELF2	GIT2	MORF4L1	RAB2A	SREK1	ZNF655
CENPI	GLO1	MORF4L2	RAB2B	SRGAP1	ZNF664
CERS2	GLRX3	MPRIP	RAB5C	SRI	ZNF697
CERS5	GLS	MRFAP1	RAB7A	SRP14	ZNF703
CERS6	GLTP	MRFAP1L1	RABL2B	SRP72	ZNF706
CFL1	GMFB	MRPL19	RAC1	SRP9	ZNF770
CGGBP1	GNA13	MRPL3	RACGAP1	SRPK1	ZNF772
CHCHD2	GNAI3	MRPL30	RAD21	SRR	ZNF793
CHD9	GNAQ	MRPL42	RAD23B	SRRM2	ZNF805

CHORDC1	GNAS	MRPL51	RAN	SRSF1	ZRANB2
CHP1	GNB1	MRPS24	RANBP1	SRSF2	ZWINT
CHSY1	GNB2L1	MSI2	RANBP6	SRSF3	
CHTOP	GNB4	MSL2	RAP1B	SRSF6	

INTRON					
AAK1	CHD3	GNB2L1	MYEOV2	RACGAP1	SMIM7
ABHD12	CLASP1	GNG2	MYL6	RAD23B	SMS
ABR	CLIP4	GNPDA1	MYO1D	RAPH1	SNAP23
AC004076.9	CLTC	GOSR2	NAP1L1	RBBP4	SNRPD3
AC007401.2	CMTM4	GPATCH2L	NAPEPLD	RBBP7	SOD2
AC024592.12	CNGA4	GPM6A	NBL1	RBM15	SOX10
AC073610.5	CNGB3	GPR75-ASB3	NCAPD2	RBMX	SPAG17
AC087645.1	CNPY2	GPS2	NCSTN	RCC1	SPARC
ACSM3	CNRIP1	GYG2	NDUFA11	RCCD1	SPECC1
ACTN4	COL6A2	H2AFV	NDUFA13	RDX	SPRY1
AGXT2L2	COPB2	HDDC2	NDUFB2	RFX7	SQRDL
AHNAK	CORO1C	HDGF	NDUFB9	RNF14	SRSF1
AHRR	COX7A2	HELLS	NDUFC2-	RNF144A	SSR1
AK2	COX7A2L	HES6	NEDD8-MDP1	RP11-	SSR2
AKIRIN1	CPM	HFM1	NHSL2	RP11-159D12.5	STMN1
AL162431.1	CRTAP	HHAT	NKIRAS1	RP11-315D16.2	SUMF1
ALDOA	CSDE1	HIBADH	NMD3	RP11-318A15.7	SUMO2
AMY2B	CSGALNACT1	HIST1H2BC	NME2	RP11-343C2.3	SUPT20H
ANXA2	CSNK2A2	HIST1H2BJ	NONO	RP11-618P17.4	TAF1
ANXA5	CTBP2	HIST1H2BK	NOTCH2	RP1-164F3.9	TARDBP
AP1M1	CTC-203F4.1	HN1	NOTCH2NL	RP11-664D7.4	TCEB1
AP2S1	CTD-2510F5.6	HN1L	NPC2	RP11-81K2.1	TCP1
APH1A	CTNNA1	HNRNPA1	NPM1	RP1-187N21.4	TEAD1
ARF3	CTNNA3	HNRNPC	NQO1	RP13-512J5.1	TERF2IP
ARF4	CTNNB1	HNRNPH1	NR3C1	RPL10	TFRC
ARHGDIA	CTSB	HOOK3	NREP	RPL12	THOC3
ARIH2	CTSC	HOXA3	NUFIP2	RPL15	THUMPD1
ARL10	CYB5D2	HSBP1	ODF2L	RPL17-C18orf32	TICAM2
ARL2BP	DAGLB	HSP90AA1	OR2W3	RPL18	TMED7-TICAM2
ARL6IP1	DAZAP2	HSP90B1	ORAOV1	RPL18A	TMEM19
ARMC2	DCBLD2	HSPA8	OTUD7A	RPL22	TMEM222
ARPC4-TTLL3	DDX3X	HSPD1	P4HB	RPL23	TMEM33
ARPC5	DHFR	IGF2R	PABPC1	RPL27A	TMEM64
ARSI	DIDO1	IL1RAP	PABPC1L	RPL30	TMPO
ASB3	DLG2	IL4I1	PAFAH1B2	RPL31	TMTC4
ASPH	DMD	IMPAD1	PANK4	RPL37	TNC
ASTN2	DNAJB11	IPO7	PCYT1A	RPL37A	TNPO1
ATG16L1	DNMT1	IQCG	PDCD6	RPL4	TNRC6A
ATP1B3	DOLPP1	JUP	PDE3A	RPL6	TOP2A
ATP2A2	DPP6	KAT8	PDS5A	RPL7A	TOR1AIP2
ATP5A1	DPYSL2	KCNH8	PEX1	RPL8	TPGS2
ATP5B	DTWD2	KCNK15	PEX11B	RPL9	TPM4
ATP5E	E2F3	KCNMA1	PFDN5	RPLP0	TRIM4
ATP5L	ECH1	KCTD2	PFN2	RPS11	TROVE2
ATP6V0E1	EEF1E1	KIAA1456	PGK1	RPS2	TRRAP
ATP7A	EEF2	KPNA4	PHB	RPS20	TSHZ1
ATPIF1	EFCAB11	KTN1	PHB2	RPS23	TTC3
AVL9	EFCAB14	LAMP2	PHC1	RPS24	TTC39C
B4GALT1	EI24	LAMTOR1	PHC3	RPS29	TUBA1B
BACH1	EIF1	LARP4	PHKB	RPS3	TUBB
BAG6	EIF2B5	LDHA	PID1	RPS3A	TUBB3
BCL2L14	EIF2S2	LEPR	PIP5K1C	RPS5	UBA2

BMI1	EIF3E	LMNA	PKM	RPS9	UBA52
BOLA2B	EIF4A1	LONP2	PLEKHA2	RUVBL1	UBAP2L
BRI3	EIF4A2	LPIN2	PLEKHB2	SAMSN1	UBB
BRWD1	EIF4G2	LRRC59	PLXDC1	SARNP	UBC
BTF3L4	ELAVL1	LRRTM3	PMEL	SARS	UBE2C
BTRC	ENO2	LRTOMT	PMF1	SCD5	UBE2W
BUB3	ENOSF1	LSM14A	PMF1-BGLAP	SDK2	UGT8
BZW1	ENSA	LYPLA2	POLDIP3	SEC14L1	UHMK1
C11orf65	EPPIN	LZIC	POLR2F	SEH1L	UNC45B
C16orf52	EPPIN-	M6PR	POLR2M	SEPT11	UNC5D
C16orf72	ERCC1	MAD1L1	POLR3G	SEPT2	USP13
C1orf228	ERO1LB	MAP2K5	PPARG	SEPT8	USP33
CALR	EYA4	MAP3K13	PPEF2	SEPT9	USP7
CALU	EYS	MATR3	PPP1CC	SERF2	UTP23
CAND2	FAM122B	MAX	PPP1R8	SETD7	VSX2
CANX	FAM160B1	MAZ	PPP2CB	SEZ6	WDFY4
CARD8	FAM189A1	MBNL1	PPP3CB	SFRP4	WDR4
CBFB	FAM20B	MDH1	PPP6R3	SGOL1	WEE1
CBX3	FAM219A	MDM2	PRDX1	SHANK3	XRCC6
CCBL2	FASTKD2	MEAF6	PRKAR1A	SHC4	YJEFN3
CCNB1IP1	FBLN2	MED28	PRR14L	SHOC2	YPEL1
CCND1	FBRSL1	METTL21A	PRRX2	SKP1	YWHAE
CCT2	FBXO10	METTL5	PRSS23	SLC18A2	YWHAZ
CCT3	FGF13	MIB2	PSMA1	SLC20A2	ZC3H11A
CCT8	FICD	MLEC	PSMA4	SLC25A3	ZMIZ1
CD164	FKBP4	MLPH	PSMB5	SLC25A53	ZNF114
CD44	FLJ27365	MME	PSMD8	SLC26A2	ZNF280D
CD46	FNDC3B	MOB4	PSME3	SLC30A5	ZNF346
CD59	FNTA	MORF4L2	PTGR1	SLC39A14	ZNF417
CDC42SE2	FRK	MPRIP	PTMA	SLC39A9	ZNF451
CDCA3	FTH1	MRPL19	PTP4A1	SLC3A1	ZNF483
CDCA4	FUT5	MRPL3	PTPN6	SLC44A1	ZNF565
CDH8	FXR1	MRPS6	PVRL3	SLC51A	ZNF587B
CDK1	GATC	MSTO1	QDPR	SLC9B1	ZNF706
CDV3	GCOM1	MTAP	QSER1	SLCO5A1	ZNF772
CELF1	GLB1	MTHFD2	RAB1A	SLIRP	ZNF793
CERS2	GLRX3	MTMR6	RAB5C	SMCR7L	
CFTR	GLS	MUM1	RABEP2	SMEK2	

5' UNTRANSLATED REGION					
AC015987.2	FTL	MTRNR2L8	RBBP4	RPS19	TUBA1A
AC114546.1	G3BP1	MYL6	RND3	RPS20	TUBA1B
AC119673.1	GAPDH	NACA	RP11-159D12.5	RPS3	TUBB
AC120194.1	GPM6A	NAP1L1	RPL10	RPS3A	TXNRD1
ANXA2	HES6	NELFB	RPL23A	RRAGC	UGT8
ARSI	HN1	NKD2	RPL27	RYK	USP33
BEND3	HNRPLL	NME2	RPL36A	SLC25A1	WDR74
CALR	HSP90AA1	NPM1	RPL37A	SNRPD2	XRCC6
CANX	HSPA8	NPTX1	RPL4	SPARC	YWHAZ
CRIPAK	KPNB1	PAPOLA	RPL5	SSH3	ZC3H11A
CSDE1	MAPK6	PPARG	RPL6	TARDBP	ZNF146
EIF3E	MBNL1	PTP4A1	RPL7A	TCP1	
EIF4A1	MORF4L2	PTP4A2	RPN1	TFDP1	
ERO1L	MTHFD2	RABEP2	RPS11	TFRC	
FBLN2	MTRNR2L2	RAN	RPS18	TPI1	

CODING SEQUENCE					
AC015987.2	CNOT6	HIST1H3F	NQO1	RPL22	SPRED1
AC087645.1	COPRS	HIST1H3H	NR3C1	RPL23	SRP9
AC119673.1	COPS7A	HIST1H4C	NUCKS1	RPL23A	SRSF1
AC120194.1	CORO1C	HIST1H4D	NUFIP2	RPL24	SRSF3
ACLY	COX4I1	HIST1H4E	NUP62	RPL26	SRSF9
ACSL3	COX6C	HIST1H4H	NUP93	RPL27	SSB
ACSL4	COX7A2	HIST1H4I	OAZ1	RPL27A	SSR1
ACTB	COX7B	HIST1H4J	ODC1	RPL29	SSR2
ACTG1	COX7C	HIST1H4K	ORAOV1	RPL3	SSR3
ACTR2	CPM	HIST2H2AA3	OSBPL8	RPL30	STARD7
ACTR3	CREBL2	HIST2H2AA4	P4HB	RPL31	STK4
ADPRHL1	CRTAP	HIST2H2AC	PABPC1	RPL32	STRAP
AHNAK	CSDE1	HIST2H3A	PABPC3	RPL34	STX16
AKIRIN1	CSK	HIST2H3C	PABPN1	RPL35	SUB1
ALDOA	CSNK1A1	HIST2H3D	PAFAH1B1	RPL35A	SUMO2
AMD1	CSNK2A2	HIST2H4A	PAFAH1B2	RPL36	SUMO3
ANLN	CTNNA1	HIST2H4B	PAPOLA	RPL36A	SYNCRIP
ANXA1	CTNNB1	HMGA1	PARP1	RPL37	TARDBP
ANXA2	CYCS	HMGB1	PCBP1	RPL37A	TBL1XR1
ANXA5	DAZAP2	HNRNPA1	PCBP2	RPL38	TCEB1
AP000350.10	DCBLD2	HNRNPA1L2	PCNA	RPL4	TCP1
AP000350.4	DDOST	HNRNPA2B1	PDGFA	RPL41	TEAD1
AP1M1	DDX17	HNRNPC	PDIA3	RPL5	TFDP1
AP2S1	DDX3X	HNRNPH1	PDIA6	RPL6	TFRC
APH1A	DDX5	HNRNPK	PDZD8	RPL7	THOC3
ARF4	DNAJA1	HNRNPU	PEA15	RPL7A	TM4SF1
ARHGDIA	DNAJB1	HNRPDL	PFDN5	RPL8	TM9SF3
ARL2BP	DSTN	HOXA4	PFN1	RPL9	TMBIM6
ARL6IP1	DYNLL2	HSP90AA1	PFN2	RPLP0	TMCO1
ARPC2	EEF1A1	HSP90AB1	PGAM1	RPLP1	TMED10
ARPC5	EEF1B2	HSP90B1	PGK1	RPLP2	TMED2
ARPP19	EEF1G	HSPA4	PHB	RPN1	TMEM123
ATAD1	EEF2	HSPA5	PIGY	RPS10	TMEM167A
ATF4	EI24	HSPA8	PITHD1	RPS11	TMEM19
ATP13A3	EIF1	HSPA9	PKM	RPS12	TMEM30A
ATP1B3	EIF1AD	HSPD1	PLS3	RPS13	TMEM33
ATP2A2	EIF2S2	HSPE1	POLR2M	RPS14	TMEM48
ATP5A1	EIF2S3	IFRG15	POTEE	RPS15	TMEM64
ATP5B	EIF3E	IMPAD1	PPIA	RPS15A	TMPO
ATP5E	EIF3G	ITGA6	PPIAL4G	RPS17	TMSB10
ATP5F1	EIF3I	ITGB1	PPIB	RPS17L	TMTC4
ATP5G3	EIF3K	ITGB8	PPP1CB	RPS18	TMX1
ATP5L	EIF3L	JUND	PPP1CC	RPS19	TNC
ATP6V0B	EIF3M	KDELR2	PPP2R1A	RPS2	TNPO1
ATP6V1A	EIF4A1	KIF5B	PPP3CB	RPS20	TOP2A
ATP6V1G1	EIF4A2	KLF16	PPP4R2	RPS23	TPI1
AUP1	EIF4B	KPNA2	PRDX1	RPS24	TPT1
AZIN1	EIF4E2	KPNB1	PRDX6	RPS25	TRA2B
B2M	EIF4G1	LAMP2	PRKAR1A	RPS26	TRAM1
B4GALT5	EIF4G2	LAPTM4B	PRKDC	RPS27	TRIM28
BAG6	EIF4H	LARP1	PRPF8	RPS27A	TRIM58
BCL2L2-PABPN1	EIF5A	LDHA	PRSS23	RPS27L	TSN
BIRC5	EIF5AL1	LDHB	PSAP	RPS28	TUBA1A
BSG	ELAVL1	LGALS1	PSMA4	RPS29	TUBA1B
BTF3	ENO1	LIMS1	PSMA7	RPS3	TUBA1C
BTF3L4	ENO2	LMNA	PSMB1	RPS3A	TUBB

BUB3	ERH	LONP2	PSMB3	RPS4X	TUBB4B
BZW1	ERO1L	LSM14A	PSMB4	RPS5	TXN
C16orf72	ETF1	LUZP6	PSMD2	RPS6	TXNRD1
C1QBP	FAM91A1	LYPLA2	PSMD8	RPS7	UBA1
CALM2	FASN	MAPK6	PSME3	RPS8	UBA2
CALR	FAU	MAPKAPK2	PTAR1	RPS9	UBA52
CANX	FBXW11	MAPRE1	PTMA	RPSA	UBB
CAPZA1	FERMT2	MARCH6	PTP4A1	RPSAP58	UBC
CBFB	FGF13	MAT2A	PTP4A2	RRM2	UBE2C
CBX3	FKBP1A	MATR3	PTTG1	RTN4	UBE2E3
CCDC50	FNDC3B	MAZ	RAB10	RYK	UBL5
CCNB1	FRMD6	MBNL1	RAB1A	S100A6	UHMK1
CCND1	FTH1	MDH1	RAC1	SAP18	UQCRFS1
CCNI	FTL	MDM2	RAD21	SBNO1	UQCRH
CCT2	FUS	MEAF6	RAN	SEC23B	UQCRQ
CCT3	G3BP1	METTL24	RANBP1	SEH1L	USP22
CCT4	GAPDH	MFSD1	RAP2A	SELT	USP33
CCT5	GBE1	MIF	RAP2B	SEPT2	USP34
CCT6A	GCOM1	MLEC	RBBP4	SEPT7	UVSSA
CCT7	GLS	MMADHC	RBBP7	SEPT9	VDAC1
CCT8	GNA13	MOB1A	RBX1	SERBP1	VDAC2
CD44	GNAS	MORF4L1	RCC2	SERF2	VHL
CD59	GNB1	MORF4L2	RCN2	SERINC1	VIM
CD63	GNB2L1	MRPL19	RFK	SERPINE2	VMA21
CDC42	GNPDA1	MRPL3	RHEB	SET	VPS35
CDC42EP5	GPI	MSN	RNASEH1	SFPQ	WDR82
CDK1	GSTP1	MTCH2	RND3	SGK196	WTAP
CDK2AP1	H2AFV	MTHFD2	RNF139	SHISA5	XPO1
CDK6	H2AFZ	MTPN	RP11-1035H13.3	SIAH1	XPO4
CELF1	H3F3A	MYL12B	RP1-164F3.9	SLC16A1	XRCC5
CFL1	HDDC2	MYL6	RP1-187N21.4	SLC1A5	XRCC6
CGGBP1	HDGF	MZT2B	RPL10	SLC20A1	YBX1
CHCHD2	HDLBP	NACA	RPL10A	SLC25A1	YWHAB
CHSY1	HEATR3	NAMPT	RPL11	SLC25A3	YWHAE
CISD2	HIF1A	NAP1L1	RPL12	SLC25A5	YWHAQ
CLASP2	HIF1AN	NCL	RPL13	SLC9B1	YWHAZ
CLIC1	HINT1	NDUFC2	RPL13A	SLIRP	ZC3H11A
CLIC4	HIST1H1B	NEK7	RPL14	SMS	ZFAND5
CLTA	HIST1H1C	NGFRAP1	RPL15	SNRPB	ZFAND6
CLTC	HIST1H2AG	NHP2L1	RPL17	SNRPB2	ZFP91
CMAS	HIST1H2AH	NME1	RPL17-C18orf32	SNRPD2	ZFR
CMTM4	HIST1H2AI	NME1-NME2	RPL18	SNX4	ZNF460
CNBP	HIST1H2BC	NME2	RPL18A	SNX5	
CNGA4	HIST1H2BO	NONO	RPL19	SOD1	
CNN3	HIST1H3B	NPM1	RPL21	SPARC	

2. ORAL PRESENTATIONS

2nd International Meeting on RNA Biology in Cancer and other Diseases, Barcelona, Spain, November 2015: New oncogenic networks controlled by the RNA binding factor CUGBP1 in melanoma identified by an integrated transcriptomic and proteomic analysis

3rd International Congress of the Molecular Biology Association of Turkey, Izmir, Turkey, September 2014: Transcriptomic and proteomic analyses identify DEK oncogene as a target of the RNA binding factor CUGBP1 in melanoma

3. POSTER PRESENTATIONS

6th European Melanoma Workshop, Las Palmas de Gran Canaria, Spain, June 2014: New roles of the RNA-binding factor CUGBP1 in Melanoma Proliferation and Maintenance

Society for Melanoma Research 2013 International Congress, Philadelphia, USA, November 2013: Alternative splicing regulators in melanoma

Society for Melanoma Research 2012 International Congress, Los Angeles, USA, November 2012: Alternative splicing regulators in melanoma

4. PUBLICATIONS

New oncogenic networks controlled by the RNA binding factor CUGBP1 in melanoma. Cifdaloz M, Osterloh L, Graña O, Riveiro-Falkenbach E, Peralta JM, Calvo TG, Karras P, Olmeda D, Belén BM, Gómez-López G, Rodríguez-Peralto JL, Valcarcel J and Soengas MS. *In preparation.*

DEK overexpression in melanoma progression: a biomarker of malignancy and poor prognosis. Riveiro-Falkenbach E, Ruano Y, García-Martín RM, Lora D, Acquadro F, Ballestin C, Cifdaloz M, Soengas MS, Ortiz-Romero PL, and Rodríguez-Peralto JL. *Submitted.*

Lineage-specific control of melanoma cell proliferation by the cytoplasmic polydenylation factor CPEB4. Pérez-Guijarro E, Karras P, Cifdaloz M, Cañon E, Alonso-Curbelo D, Martínez-Herranz R, Graña O, Horcajadas C, Calvo TG, Osterloh L, Colmenar A, Riveiro-Falkenbach E, Eyras E, Pisano DG, Rodríguez-Peralto JL, Megías D, Méndez R, and Soengas MS. *Submitted.*

Metastatic risk and resistance to BRAF inhibitors in melanoma defined by selective allelic loss of ATG5. García-Fernández M, Karras P, Checinska A, Cañón E, Calvo TG, Gómez-López G, Cifdaloz M, Colmenar A, Espinosa L, Olmeda D, and Soengas MS. Autophagy. *In press*.

RAB7 controls melanoma progression by exploiting a lineage-specific wiring of the endolysosomal pathway. Alonso-Curbelo D, Riveiro-Falkenbach E, Pérez-Guijarro E, Cifdaloz M, Osterloh L, Megías D, Olmeda D, Cañon E, Karras P, Calvo TG, Gómez-López G, Graña O, Checinska A, Wang HW, Pisano DG, Pastor J, Ortiz-Romero P, Tormo D, Hoek K, Rodríguez-Peralto JL, Joyce JA, and Soengas MS. Cancer Cell. 2014 Jul 14;26(1):61-76.

5. CERTIFICATES

Hands-on Introduction to R, CNIO, July 2014.

Access to ENCODE data through the UCSC Genome Browser, CNIO, June 2014.

Survival Skills for Young Investigators by Henry Sun, Complutense University, Madrid, June 2013.

Introduction to Microarray Gene Expression Analysis, CNIO, May 2013.

Introduction to Sequence Analysis, CNIO, March 2013.

Access to Genes and Genomes with Ensembl, CNIO, October 2012.